Aus dem
Adlolf-Butenandt-Institut
Lehrstuhl für Stoffwechselbiochemie
der
Universität München
Vorstand: Prof. Dr. rer. nat. Christian Haass

---

# Identification of a BACE dimer and characterization of its biochemical and enzymatic properties

---

Dissertation
zum Erwerb des Doktorgrades der Medizin
an der Medizinischen Fakultät der
Ludwig-Maximilians-Universität München

vorgelegt von
Gil Gregor Westmeyer
aus Essen
2006

Mit Genehmigung der Medizinischen Fakultät
der Universität München

Berichterstatter: Prof. Dr. C. Haass
2. Berichterstatter: Prof. Dr. Th. Heinzeller

Mitberichterstatter: Prof. Dr. Dr. h.c. Th. Brandt
Mitberichterstatter: Prof. Dr. H. A. Kretschmar

Mitbetreuung durch den
promovierten Mitarbeiter: Dr. Michael Willem

Dekan: Prof. Dr. med. D. Reinhardt

Tag der mündlichen Prüfung: 20.7.2006

# 1 Contents

**1 CONTENTS ..... 3**

**1.1 Index of Figures ..... 8**

**2 ZUSAMMENFASSUNG ..... 9**

**3 SUMMARY ..... 10**

**4 LIST OF ABBREVIATIONS ..... 11**

**5 INTRODUCTION ..... 14**

**5.1 Epidemiology of Dementia and Alzheimer´s Disease ..... 14**

**5.2 Definition of Alzheimer`s Dementia ..... 14**

**5.3 Morphology ..... 15**

**5.4 Pathogenesis ..... 17**
5.4.1 β-Amyloid Precursor Protein (APP) ..... 17
5.4.2 Proteolytic Processing of APP ..... 17
5.4.2.1 Amyloid-β as the necessary pathogen of AD ..... 18
5.4.2.2 Toxicity of Amyloid-β ..... 18
5.4.3 The *Tau* pathology as a consequence of Aβ formation ..... 20

**5.5 Risk factors ..... 21**
5.5.1 Environmental risk Factors ..... 21
5.5.2 Genetic risk factors ..... 21
5.5.2.1 Missense mutations in APP and overexpression of APP ..... 22
5.5.2.2 Missense mutations in the Presenilins ..... 23
5.5.2.3 Apolipoprotein E4 Allele ..... 23

**5.6 Proteolytic processing of APP ..... 23**
5.6.1 The α-Secretase ..... 23
5.6.2 BACE2 has a non-amyloidogenic effect ..... 24
5.6.2.1 Sequence Structure of BACE2 ..... 25
5.6.2.2 Tissue Expression of BACE2 ..... 26
5.6.2.3 Localization of BACE2 ..... 26
5.6.2.4 Cleavage Site of BACE2 ..... 26
5.6.2.5 3D Structure of BACE2 ..... 27

**5.7 The amyloidogenic pathway ..... 27**
5.7.1 The Presenilin Complex ..... 27

5.7.1.1 Role of the Presenilin complex in signal transduction ..... 29
5.7.2 The β-Secretase ..... 30
5.7.2.1 Identification of β-Secretase (BACE) ..... 30
5.7.2.2 Domain Structure of BACE ..... 31
5.7.2.3 Mouse Models studying BACE ..... 32
5.7.2.3.1 BACE Knock-out Mice ..... 32
5.7.2.3.2 Transgenic Mice overexpressing BACE ..... 32
5.7.2.4 Posttranslational Maturation of BACE ..... 33
5.7.2.4.1 The role of the pro-domain of BACE ..... 33
5.7.2.4.2 Posttranslational Modifications of BACE ..... 33
5.7.2.4.3 Dissulfide Bonds in BACE ..... 34
5.7.2.5 Localization and Trafficking of BACE ..... 34
5.7.2.5.1.1 Cellular localization of BACE ..... 34
5.7.2.5.1.2 Cellular localization of β-secretase activity ..... 34
5.7.2.5.1.3 Trafficking through the Exocytotic Pathway ..... 34
5.7.2.5.1.4 Role of the TM domain of BACE ..... 36
5.7.2.5.1.5 Polarized Sorting of BACE ..... 36
5.7.2.5.1.6 Lipid Rafts and BACE ..... 36
5.7.2.6 Tissue Expression and Tissue localization of β-secretase activity ..... 38
5.7.2.6.1 BACE mRNA – distribution ..... 38
5.7.2.6.2 Tissue Expression of the BACE protein ..... 38
5.7.2.6.3 Altered protein expression of BACE in AD patients ..... 39
5.7.2.6.4 Mechanisms regulating BACE expression ..... 39
5.7.2.7 Crystallographic Structure of BACE ..... 40
5.7.2.8 Subsite Specificity of BACE ..... 41
5.7.2.8.1 Cleavage at Asp 1 and the “swedish mutation” ..... 41
5.7.2.8.2 Alternative cleavage at Glu11 by BACE ..... 42
5.7.2.8.3 Sequence of alternative cleavages of BACE ..... 43
5.7.2.8.4 The ideal substrate sequence of BACE ..... 44
5.7.2.9 Known substrates for BACE ..... 45
5.7.2.10 Enzyme Kinetics of BACE ..... 47
5.7.2.10.1 Comparison of BACE ectodomain and full length BACE ..... 47
5.7.2.10.2 Kinetic parameters of the pro-domain ..... 47
5.7.3 Interaction partners of BACE ..... 47

**6 GOALS OF THE CURRENT WORK ..... 50**

**7 MATERIAL AND METHODS ..... 52**

**7.1 Cloning ..... 52**
7.1.1 Existing constructs used ..... 52
7.1.2 Cloning Vectors ..... 52
7.1.2.1 Maps of the Vectors ..... 52
7.1.3 Summary of Cloning of BACE expression constructs ..... 52
7.1.4 Generation of myc-tagged BACE variants ..... 53

7.1.4.1 Primers used for cloning ..... 53
7.1.4.1.1 BACE-pA: ..... 53
7.1.4.1.2 BACE-GPI ..... 53
7.1.4.1.3 BACE-KKXX ..... 53
7.1.5 PCR ..... 53
7.1.5.1 PCR reaction solution ..... 54
7.1.5.2 PCR Program ..... 54
7.1.6 Gel electrophoresis ..... 54
7.1.7 Restriction Digest and Ligation of DNA ..... 54
7.1.8 Transformation of E. Coli preparation of plasmids ..... 54
7.1.9 Screening of positive clones and sequencing of the constructs ..... 55

**7.2 Cell lines and cell culture ..... 55**
7.2.1 Existing Cell lines ..... 55
7.2.2 Newly Generated cell lines ..... 55
7.2.2.1 Standard medium ..... 56
7.2.2.2 Media for Selection ..... 56
7.2.3 Transient and stable transfection of cells ..... 56
7.2.4 Splitting and Freezing ..... 56
7.2.5 Mouse lines and tissue preparation ..... 56

**7.3 Immunocytochemistry and fluorescence microscopy ..... 56**
7.3.1 Antibodies ..... 56
7.3.1.1 Primary antibodies ..... 56
7.3.1.2 Cell markers ..... 56
7.3.1.3 Secondary antibodies ..... 57
7.3.2 Preparation of Cells for Immunofluorescence ..... 57
7.3.3 Microscopy ..... 57

**7.4 Protein Biochemistry ..... 57**
7.4.1 Production of Protein extracts ..... 57
7.4.1.1 Total Cell lysates for SDS PAGE and CoIP ..... 57
7.4.1.2 Membrane Preparations ..... 58
7.4.2 Assessment of total protein amount ..... 58
7.4.3 Immunoprecipitation of proteins ..... 58
7.4.4 Antibodies for immunoprecipitation/ immunoblotting ..... 58
7.4.5 PAGE and Western Blotting of proteins ..... 59
7.4.6 Blue Native PAGE (BN-PAGE) ..... 59
7.4.7 Detection of proteins with antibodies ..... 59
7.4.8 Stripping of Western Blot membranes ..... 60
7.4.9 Radiolabeling of cellular proteins ..... 60
7.4.10 FPLC purification of His-tagged soluble and membrane bound BACE ..... 60

**7.5 Enzymatic assays ..... 60**

**7.6 Machines/Devices used ..... 61**

**8 RESULTS ..... 62**

**8.1 Molecular Size of Native BACE ..... 62**

**8.2 Identification of the BACE dimer ..... 63**

**8.3 Conditions for Dimerization ..... 65**
8.3.1 The native conformation of the BACE-ectodomain ..... 65
8.3.2 Essential Domains for Dimerization ..... 66
8.3.3 Membrane Association ..... 69
8.3.4 Cellular assembly of the BACE Dimer ..... 71

**8.4 Kinetic Properties of dimeric BACE ..... 72**

**9 DISCUSSION ..... 76**

**9.1 Evidence for a BACE-Dimer ..... 76**

**9.2 Methods to identify a Dimer ..... 77**

**9.3 BN gels to study native proteins ..... 79**

**9.4 Co-Immunoprecipitation to detect Dimers ..... 81**

**9.5 Domain deletion analysis ..... 81**
9.5.1 Functionality of the BACE constructs ..... 82
9.5.2 The role of the transmembrane domain ..... 82

**9.6 Rafts and membrane attachment of BACE ..... 82**
9.6.1 The effect of attaching a GPI anchor to BACE ..... 83

**9.7 Kinetic Properties of monomeric and dimeric BACE ..... 84**

**9.8 Physiological function of Dimers in general ..... 86**

**9.9 Physiological function of the BACE dimer in particular ..... 87**
9.9.1 Stability ..... 87
9.9.2 Dimerization and Raft association ..... 88
9.9.3 Cooperative active sites ..... 88
9.9.3.1 Cooperation of active sites in the BACE Dimer ..... 88
9.9.4 Interference with the dimer interface as a therapeutic strategy ..... 89
9.9.4.1 Prediction of the dimer interface of BACE ..... 90

**10 CONCLUSIONS ..... 94**

**11 ACKNOWLEDGEMENTS ..... 95**

**12 BIBLIOGRAPHY ..... 96**

**13 LEBENSLAUF ..... 101**

## 1.1 Index of Figures

Figure 1: Histopathology of AD ..... 16
Figure 2: Proteolytic Processing of APP by secretases ..... 18
Figure 3: Hypothetical sequence of pathogenic events in the “amyloid cascade” ..... 19
Figure 4: The tau hypothesis and putative relations to amyloid ..... 20
Figure 5: βAPP mutations linked to familial Alzheimer´s disease ..... 22
Figure 6: Homology between BACE and BACE2 ..... 25
Figure 7: Stepwise assembly and activation of the γ-secretase complex ..... 28
Figure 8: Notch- Signal Transduction Pathway in comparison to APP-processing ..... 30
Figure 9: Amino Acid sequence of BACE and Domain structure ..... 31
Figure 10: 3D- structure of BACE ..... 41
Figure 11: Cleavage sites of BACE in APP ..... 42
Figure 12: Comparison of the cleavage sites of the known substrates for BACE ..... 46
Figure 13: Overview of kinetic parameters of BACE from the literature ..... 49
Figure 14: Endogenous and transgenic BACE migrates at 140 kDa on a BN gel. ..... 63
Figure 15: Co-immunoprecipitation of differentially tagged BACE ..... 64
Figure 16: BACE-NT is a monomer on BN-PAGE ..... 65
Figure 17: Differently tagged BACE-NT does not co-immunoprecipitate ..... 66
Figure 18: Schematic representation of BACE constructs ..... 67
Figure 19: Plasma membrane expression of BACE variants ..... 68
Figure 20: Intracelllular enzymatic activity of BACE variants ..... 68
Figure 21: Analysis of BACE variants on BN-PAGE in comparison to SDS-PAGE ..... 69
Figure 22: Membrane preparations compared to native lysates on BN-PAGE ..... 70
Figure 23: Subsite specificity of BACE in distinct subcellular compartments. ..... 71
Figure 24: Purification of native dimeric BACE-FL and monomeric BACE-NT ..... 73
Figure 25: Michaelis-Menten kinetics of BACE-FL compared to BACE-NT ..... 74
Figure 26: Effect of the pro-domain of BACE on its enzymatic efficiency ..... 75
Figure 27: Table showing the kinetic properties of BACE-FL compared to BACE-NT ..... 75
Figure 28: Matrix of Docking Simulations performed with ClusPro ..... 92
Figure 29: Residues predicted by ClusPro to be in the dimer interface ..... 92

# 2 Zusammenfassung

Die Ablagerung von Amyloid-β Peptid in den Gehirnen von Patienten ist ein Charakteristikum der Alzheimer Erkrankung und spielt höchstwahrscheinlich eine entscheidende pathogenetische Rolle in der Entwicklung der dementiellen Symptome dieser schweren Krankheit. Amyloid-β Peptid ensteht aus dem Amyloid-β Vorläuferprotein (APP) durch den proteolytischen Schnitt der „APP schneidenden β-Sekretase“ (BACE), gefolgt von einem Schnitt der „γ-Sekretase“. Während kürzlich entdeckt wurde, dass die γ-Sekretase ein Multi-Protein Komplex ist, wurde bisher noch nicht untersucht, ob BACE unter nativen Bedingungen in Assoziation mit anderen Proteinen enyzmatisch aktiv ist. In der vorliegenden Arbeit konnte mittels nativer Gelelektrophorese gezeigt werden, dass natives BACE ein molekulares Gewicht von 140 kDa besitzt, während BACE unter denaturierenden Bedingungen mit 70 kDa nur halb so gross ist. Co-Immunopräzipitationsexperimente, bei denen BACE-Konstrukte mit unterschiedlichen Epitopmarkierungen untersucht wurden, konnten im Nachfolgenden demonstrieren, dass es sich bei der höhermolekularen BACE Spezies um ein BACE Homodimer handelt. Im Gegensatz dazu ist die lösliche BACE Ektodomäne, der sowohl der C-terminus als auch die Transmembrandomäne fehlen, ein Monomer. Eine anschliessend durchgeführte Domänenanalyse ergab, dass weder der C-terminus noch die Transmembrandomäne notwendig für die Dimerisierung sind. Im Einklang damit zeigte sich, dass die BACE Ektodomäne dimerisieren kann, wenn sie durch einen GPI-Anker mit der Membran verbunden wird. In Bezug auf die zelluläre Lokalisierung des Dimerisierungsprozesses wurde ermittelt, dass ein Zurückhalten von BACE im ER durch Anfügen eines KKXX Motives die Dimerisierung nicht verhindert. Dies legt nahe, dass die Dimerisierung stattfindet, bevor BACE im Golgi Apparat voll maturiert. Darüberhinaus ergaben enzymkinetische Analysen des gereinigten nativen BACE Dimers eine höhere Affinität und maximale Umsatzrate für ein APP-ähnliches Substrat im Vergleich zu der löslichen, monomeren BACE Ektodomäne. Dies lässt vermuten, dass eine mögliche Funktion der Dimerisierung in der Verbesserung der enzymatischen Effizienz besteht. Die sich daraus ergebenden Implikationen für unser Verständnis der Amyloid-β Synthese, sowie für eine möglicherweise alternative therapeutische Strategie werden diskutiert.

# 3 Summary

The deposition amyloid-β peptide in the brains of patients is a hallmark of Alzheimer's disease and is thought to play a major pathogenetic role in the development of the demential symptoms of this severe illness. The amyloid-β peptide is generated from the β-amyloid precursor protein (APP) by cleavage of the "β-site APP-cleaving enzyme" (BACE) followed by "cleavage of the γ-secretase". Whereas it has recently been discovered that the γ-secretase is a multi-protein complex, it has not yet been investigated whether under native conditions, BACE functions in association with other proteins. The present work thus studied BACE by means of blue native gel electrophoresis and found that native BACE has a molecular weight of 140 kDa, whereas BACE under denaturing conditions has a molecular weight of 70 kDa which is only half of its native mass. Co-immunoprecipitation experiments with differently tagged full-length BACE constructs subsequently showed that this higher molecular weight species of BACE corresponds to a BACE homodimer. In contrast, a BACE ectodomain, lacking the C-terminus and the transmembrane domain, is a monomer. A consecutive domain analysis revealed that both the C-terminus and the transmembrane domain of BACE are dispensable for dimerization. In line with this, it could be shown that the ectodomain of BACE can dimerize if it is attached to the membrane by a GPI anchor. In terms of the cellular localization of the dimerization process, it could furthermore be demonstrated that retention of BACE in the ER by addition of a KKXX-motif does not prevent dimerization. This suggests that dimerization can occur prior to full maturation of BACE which takes place in the Golgi apparatus. In addition, kinetic analyses of the purified native BACE dimer revealed a higher affinity and turnover rate for an APP-like substrate in comparison to the monomeric soluble BACE ectodomain. This suggests a putative function of dimerization in improving enzymatic efficiency. The implication of these findings for our understanding of the Amyloid-β synthesis as well as for a putatively alternative therapeutic strategy are discussed.

# 4 List of abbreviations

| | |
|---|---|
| AD | Alzheimer`s Disease |
| AICD | APP intracellular domain |
| APP | ß-Amyloid Precursor Protein |
| APP CTFß (C99) | 99 amino acids long C-terminal fragment of APP generated by β-secretase |
| APP CTFα (C83) | 83 amino acids long C-terminal fragment of APP generated by α-secretase |
| APPsα or sAPPα | Soluble APP α, the ectodomain of APP released after α-secretase cleavage |
| APPsβ or sAPPβ | Soluble APP β, the ectodomain of APP released after β-secretase cleavage |
| Amyloid-ß or Aß (40 or 42) | Amyloid ß-peptide (40 or 42 amino-acids long) |
| BACE | β-secretase |
| BACE-FL | full length BACE |
| BBB | Blood-brain-barrier |
| BME | β–mercaptoethanol |
| C. elegans | Caenorhabditis elegans |
| CFP | cyan fluorescent protein |
| Co-IP | Co-immunoprecipitation |
| DRMs | Detergent resistant membranes |
| E. coli | Escherichia coli |
| ELISA | Enzyme-Linked Immunosorbent Assay |
| ER | Endoplasmic reticulum |
| FAD | Familial Alzheimer’s disease |
| FRET | Fluorescence Resonance Energy Transfer |

| | |
|---|---|
| GFP | Green Fluorescent Protein |
| HEK | Hyman Embryonic Kidney Cells |
| IP | Immunoprecipitation |
| Nct | Nicastrin |
| NICD | Notch intracellular domain |
| PCR | Polymerase chain reaction |
| Pen2 | Presenilin enhancer, component of the Presenilin complex |
| PET | positron emission tomography |
| Pro-BACE | Pro-peptide containing immature form of BACE |
| PS 1 | Presenilin 1 |
| PS 2 | Presenilin 2 |
| PS CTF | C-terminal fragment of Presenilin |
| PS NTF | N-terminal fragment of Presenilin |
| RIP | regulated intramembrane proteolysis |
| RNAi | RNA interference |
| RR | relative risk (epidemiological parameter) |
| sAPPα (APPsα) | Soluble APP α, the ectodomain of APP released after α-secretase cleavage |
| sAPPβ (APPsβ) | Soluble APP β, the ectodomain of APP released after β-secretase cleavage |
| siRNAs | small interfering RNAs |
| Sporadic Alzheimer's disease | As opposed to FAD, AD which does not cumulatively occur in certain families and which does not (yet) have identifiable genetic causes |
| Swe cells | HEK (human embryonic kidney) cells stably expressing APPSwe |

| | |
|---|---|
| Tg2576 mice | swAPP overexpressing mice |
| TGN | Trans Golgi Network |
| TM | Transmembrane Domain |
| wtBACE | Wild-type BACE |
| YFP | yellow fluorescent protein |
| 293 cells | HEK cells overexpressing wtAPP |

# 5 Introduction

## 5.1 Epidemiology of Dementia and Alzheimer´s Disease

Alzheimer's disease (AD) is a progressive neurological disorder that results in memory loss, personality changes, global cognitive dysfunction, and functional impairments. Loss of short-term memory is most prominent early in the disease process. In the late stages of disease, patients are totally dependent upon others for basic activities of daily living such as feeding and toileting.

AD accounts for 60 to 80 percent of all cases of dementia among the elderly. According to recent calculations* about 6% to 9% of the elderly population in Western industrialized countries suffers from a dementia leading to a devastating decay of cognitive powers such as memory, language, sense of orientation and faculty of judgment. To date, there are about one million people affected with a dementia in Germany, two third of them suffering from AD-dementia. Every year, about 125.000 people are newly diagnosed with AD which will increase the number of patients with AD by 20.000 a year accumulating to about 2 million until the year 2050 if no major breakthrough in therapy will be reached. In the United States, about four million Americans have Alzheimer's disease at the moment, and close to three million Americans are caring for relatives or friends who suffer from it[1].

## 5.2 Definition of Alzheimer`s Dementia

The name of the disease was coined by the German psychiatrist Kraepelin after Alois Alzheimer who at the beginning of the 20th century was the first to describe the clinical symptoms and histopathological features of the disease. In 1906 and 1907 Alzheimer published a short case study entitled “A peculiar disease of the cortex” [2-4] in which he described the intellectual decay of his 51-year-old patient Auguste D. over five years until her death and correlated this to histopathological observations in her brain upon autopsy. He noticed that large portions of the brain were heavily destroyed and described deposits of proteins, filaments and dead neurons without any evidence for atherosclerotic changes. While the publication on this case in 1907 is only a relatively short communication, Alzheimer published a very comprehensive paper in 1911 [5] in which he discussed the concept of the disease in detail. This publication focused on the report of a second patient suffering from Alzheimer's disease (AD), the case of Johann F. Interestingly, the neurohistopathological sections from Johann F. were found in the archives of the Institute of Neuropathology of the University of Munich and could be reinvestigated as presented further below [6, 7].

According to the “Diagnostic and Statistical Manual of Mental Disorders” in its current fourth edition [8], AD is defined by the gradual onset and continuing decline of cognitive function from a previously higher level, resulting in impairment in social or occupational function, impairment of recent memory (inability to learn new information) and at least one of the following: disturbance of language; inability to execute skilled

* http://www.deutsche-alzhei companies mer.de/pdf/FactSheet01.pdf

motor activities in the absence of weakness; disturbances of visual processing; or disturbances of executive function (including abstract reasoning and concentration). The cognitive deficits are not due to other psychiatric, neurologic, or systemic diseases. The deficits do not occur exclusively in the setting of delirium [1].

## 5.3 Morphology

The clinical diagnosis of AD can only be fully verified by its characteristic pathologic morphology. The major abnormalities of AD are atrophy of the brain, neurofibrillary tangles, senile neuritic plaques, and cerebral amyloid angiopathy. All of these may be present to a lesser extent in the brains of elderly non-demented individuals [9].

The macroscopic examination of the brain shows the variable degree of cortical atrophy with widening of the cerebral sulci that is most pronounced in the frontal, temporal, and parietal lobes. With significant atrophy, there is a compensatory ventricular enlargement secondary to loss of parenchyma [9].

Histopathologically, the brains of individuals with Alzheimer's disease are characterized by extracellular deposition of Amyloid-β protein, intracellular neurofibrillary tangles, and loss of neurons. The presence of amyloid plaques and neurofibrillary tangles is associated with neuronal dystrophy [10].

Neurofibrillary tangles are bundles of filaments in the cytoplasm of the neurons that displace or encircle the nucleus. They often have an elongated “flame” shape; in some cells, the basket weave of fibers around the nucleus takes on a rounded shape (“globose tangles”). They are visible as basophilic fibrillary structures with standard staining techniques but are much better demonstrated by silver staining. They are commonly found in cortical neurons, especially in the enthorinal cortex, as well as in other sites such as pyramidal cells of the hippocampus, the amygdala, the basal forebrain, and the raphe nuclei. Neurofibrillary tangles are insoluble and apparently difficult to proteolyze in vivo, thus remaining visible in tissue sections as “ghost” or “tombstone” tangles long after the death of the parent neuron. Ultrastructurally, neurofibrillary tangles are composed predominantly of paired helical filaments along with some straight filaments that appear to have comparable composition. A major component of paired helical filaments is abnormally hyperphosphorylated *tau*, an axonal microtubule-associated protein that can enhance microtubule assembly [11].

Paired helical filaments are also found in the dystrophic neurites that form the outer portions of neuritic plaques and in axons leading through the affected grey matter-neuropil threads. Although Neurofibrillary tangles are characteristic of AD, they are not specific to this condition, being also found in diseases like supranuclear palsy (a subtype of Parkinson syndrome), and postencephalitic Parkinson syndrome. They probably represent the endpoint of a number of different cellular pathophysiological processes. The neurofibrillary tangles and its major components are a manifestation of the abnormal organization of elements of the cytoskeleton in neurons of patients with AD [9].

Neuritic plaques are focal, spherical collections of dilated, tortuous, silver-staining neuritic processes surrounding a central amyloid core, often surrounded by a clear halo. Neuritic plaques range in size from 20 to 200 micrometer in diameter; activated microglial cells and reactive astrocytes are present at their periphery [9]. Plaques can be found in

the hippocampus and amygdala as well as in the neocortex, although there is usually a relative sparing of primary motor and sensory cortices (this also applies for neurofibrillary tangles). Comparable lesions can also be found in the corresponding regions of the brains of aged, nonhuman primates [9]. The dystrophic neurites contain paired helical filaments as well as synaptic vesicles and abnormal mitochondria. The amyloid core, which can be stained by Congo red and silver staining methods, contains several abnormal proteins. The dominant component of the plaque is Amyloid-β, a peptide of predominantly 40 to 42 amino acids [12, 13] derived from a larger molecule termed the "amyloid precursor protein" (APP) [14] in a process which will be described in the following chapters. Other proteins, including components of the complement cascade, α1-antichymotrypsin, and apolipoproteins are present in less abundance. Immunostaining of Amyloid-β demonstrates the existence of amyloid peptide deposits of lesions lacking the surrounding neuritic reaction. These diffuse plaques, are found in superficial portions of the cerebral cortex as well as in basal ganglia and cerebellar cortex [9]. Commonly, when diffuse plaques are found in the cerebral cortex, they appear to be centered on small vessels or on clusters on the neurons. Diffuse plaques may represent an early stage of neuritic plaque development.
Amyloid angiopathy, that is the deposition of Amyloid within the walls of the vasculature, is an almost invariable accompaniment of AD; however, it can also be found in brains of individuals without AD [9]. Vascular amyloid is derived from the same precursor as the amyloid cores of plaques [9].

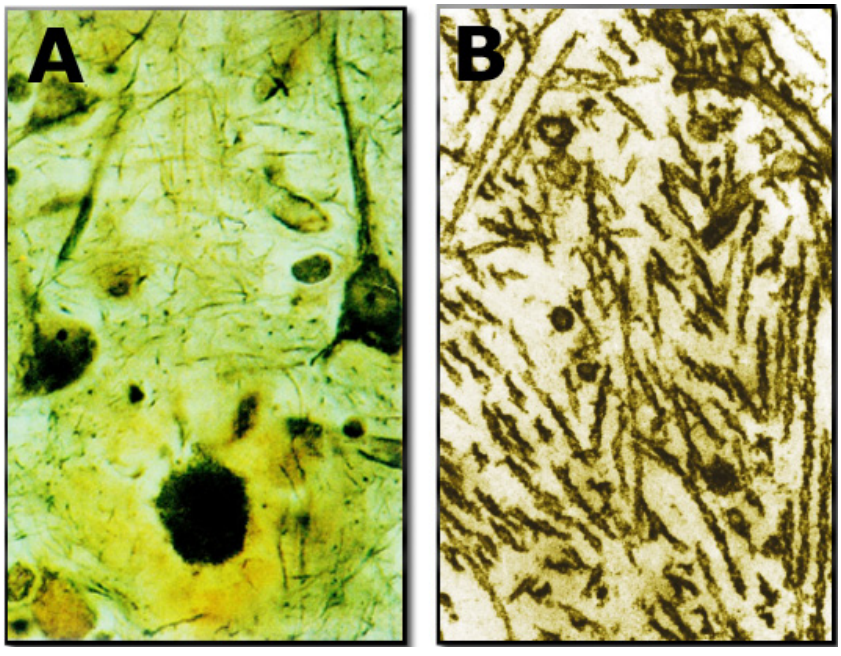


**Figure 1: Histopathology of AD**

A: Original Silver impregnations performed over 2 days in Alzheimer's laboratory using the Bielschowsky method. The figure shows Amyloid plaques in the cerebral cortex of Alzheimer´s patient Johann F. (Magnification x500)
Source: [6].
B: The Illustration shows an electron-microscopic picture of a neurofibrillary tangle
Source: [15]

## 5.4 Pathogenesis

### 5.4.1 β-Amyloid Precursor Protein (APP)

Amyloid-β is cleaved out of the membrane bound amyloid precursor protein (APP). APP is a type 1 integral membrane protein which is expressed in various tissues as alternatively spliced isoforms and with different post-translational modifications. The predominant form of neurons is the 695-residue form [16, 17]. The protein matures through the secretory pathway and is transported to the plasma membrane. The mature protein then can be taken up by endocytotic vesicles which move through the endosomal recycling pathway back to the plasma membrane [18-20].

The physiological functions of the different isoforms of APP are not clear. Studies in vitro suggested various possible functions of APP: cell-cell interactions, inhibition of a factor of the clotting cascade, neurite outgrowth and signal transduction. In vivo, those putative functions could not be clearly confirmed, because APP knockout mice only show very subtle phenotypes including decreased locomotion, minor gliosis in aged brains and reduced viability of cultured neurons at birth [15, 17]. There has been no evidence to date that the pathology of AD might be related to a functional loss of APP. Instead, the series of endoproteolytic cleavages of APP is likely to cause the toxic consequences which lead to neuronal decay.

### 5.4.2 Proteolytic Processing of APP

The regulated cascade of proteolytic events in APP relies on at least three different proteolytic activities along two main pathways, the non-amyloidogenic α-secretase and the amyloid producing β-secretase pathway (shown in Figure 2). The majority of the APP molecules is cleaved by the α-secretase [candidate genes are the Metalloprotease ADAM10 [21] and ADAM17 [22-24], see separate section 5.6.1 below] in the middle of the Amyloid-β region thus preventing Amyloid-β production and leading to an N-terminal soluble fragment (sAPPα). The C-terminal fragment C83 remains in the membrane and is subsequently cleaved by the γ-secretase to yield $p3_{40}$ and $p3_{42}$ which are truncated forms of Amyloid-β.

A smaller portion of APP is cleaved by the β-secretase or BACE (short for beta-site beta-amyloid precursor protein-cleaving enzyme) at the Aspartate 1 (Asp+1), producing the soluble (sAPPβ) and the membrane bound C99 peptide. If this C99 peptide is subsequently cleaved by γ-secretase, two isoforms of Amyloid-β are generated with a length of 40 and 42 amino acids respectively as well as a C-terminal fragment known as AICD (γ-secretase derived intracellular fragment of APP) whose putative function in signal transduction is discussed in a separate section below.

The β-secretase can also cleave 10 residues behind the Aspartate, at Glutamate 11 thus yielding the shorter C89 and a truncated Amyloid-β 11-40 or 11-42, which are also found in Amyloid plaques. The significance of this alternative cleavage will be discussed in the section “subsite specificity” (5.7.2.8) below.

It is important to mention that soluble Amyloid-β is produced during normal cellular metabolism and that the pathogenesis must be understood as the consequence of subtle deregulations of the process described above [25].

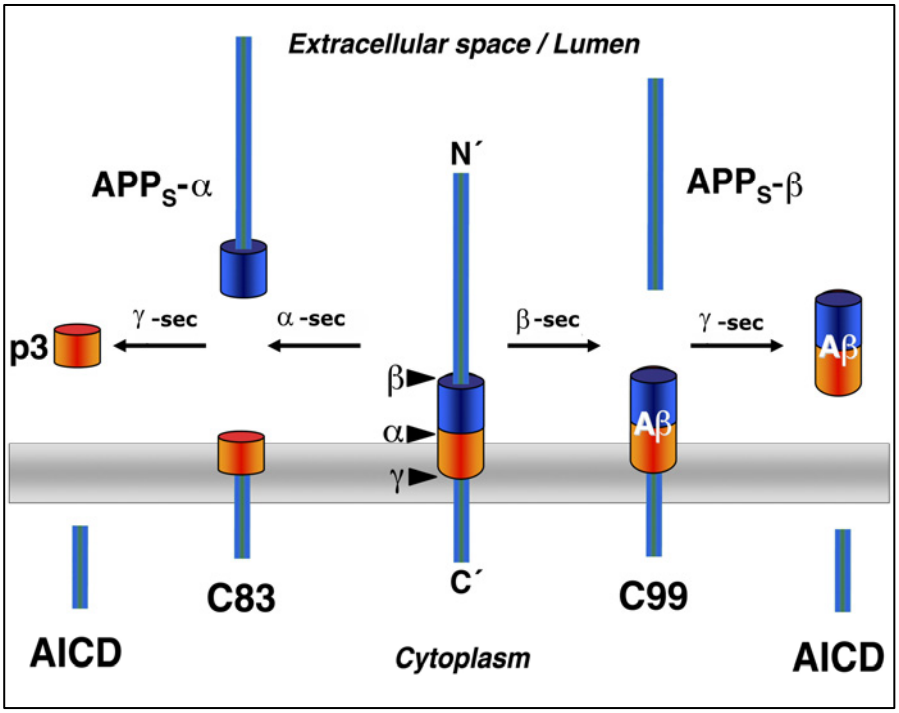


**Figure 2: Proteolytic Processing of APP by secretases**

α-Secretase cleavage occurs within the Aβ domain and prevents amyloidogenesis. A small peptide (p3) is generated by the subsequent cleavage of the C83 fragment by γ-secretase. Besides p3, the large ectodomain (APPs-α) is secreted. A shorter APPs species is secreted upon cleavage by BACE (APPs-β). The resulting C99 fragment is cleaved by γ-secretase to produce Aβ. The γ-secretase cut releases the APP intracellular domain (AICD), which may be involved in nuclear signalling – Source: [26].

### 5.4.2.1 Amyloid-β as the necessary pathogen of AD

It can by hypothesized that the formation of Amyloid-β 42, as described above, induces all the subsequent pathologic steps including *tau* aggregation to neurofibrillary tangles which finally lead to neuronal death and clinical dementia. According to Mudher et al., there are indeed several lines of evidence in support of this hypothesis. First, there are mutations in APP and PS responsible for the rare cause of early-onset familial Alzheimer's disease (FAD) displaying the full pathological features, including neurofibrillary tangles, all of which can be replicated in cell and animal models. Thus genetically caused alterations of Amyloid-β generation also seem to lead to *tau* aggregation. Second, some studies showed that Amyloid-β is neurotoxic to cultured cells and is able to induce *tau* phosphorylation under experimental conditions [27]. Third, it was shown that mutations of *tau* on the other hand, lead to various forms of fronto-temporal degeneration disorders without any increased Amyloid-β plaque formation [28]. This point is also stressed by Hardy and Selkoe who take it that *tau* alteration is not sufficient to induce the amyloid plaques characteristics of AD [29].

### 5.4.2.2 Toxicity of Amyloid-β

The exact mechanism by which Amyloid-β induces the neurotoxic effect is not utterly clear. It is conceivable that the extracellular insoluble aggregations of Amyloid-β to plaques can rather be seen as an end point since they seem to be largely inert [29]. The soluble oligomeric and even intracellular Amyloid-β peptides, a preliminary stage prior to

formation of plaques, may be more toxic. As fleshed out by Hardy and Selkoe, those effects might include subtle effects on synapses (Figure 3), immune responses, disturbance of homeostasis and oxidative stress as well as tangle formation, whose net effect is neuronal dysfunction and cell death [29]. As Selkoe suggests, impairment of higher cortical functions in AD patients could be understood as "synaptic failure" long before morphologic alterations are identified [30]. Studies in mice transgenic for mutations in APP revealed smaller excitatory postsynaptic potentials and rapid decay of "Long Term Potentiation" (LTP) as a correlate for neuronal plasticity and formation of memory traces. These inhibitions of hippocampal LTP in vivo could be attributed specifically to soluble oligomers of Amyloid-β and appeared to be due to a significant reduction in synaptic number, but not synaptic strength [31, 32].

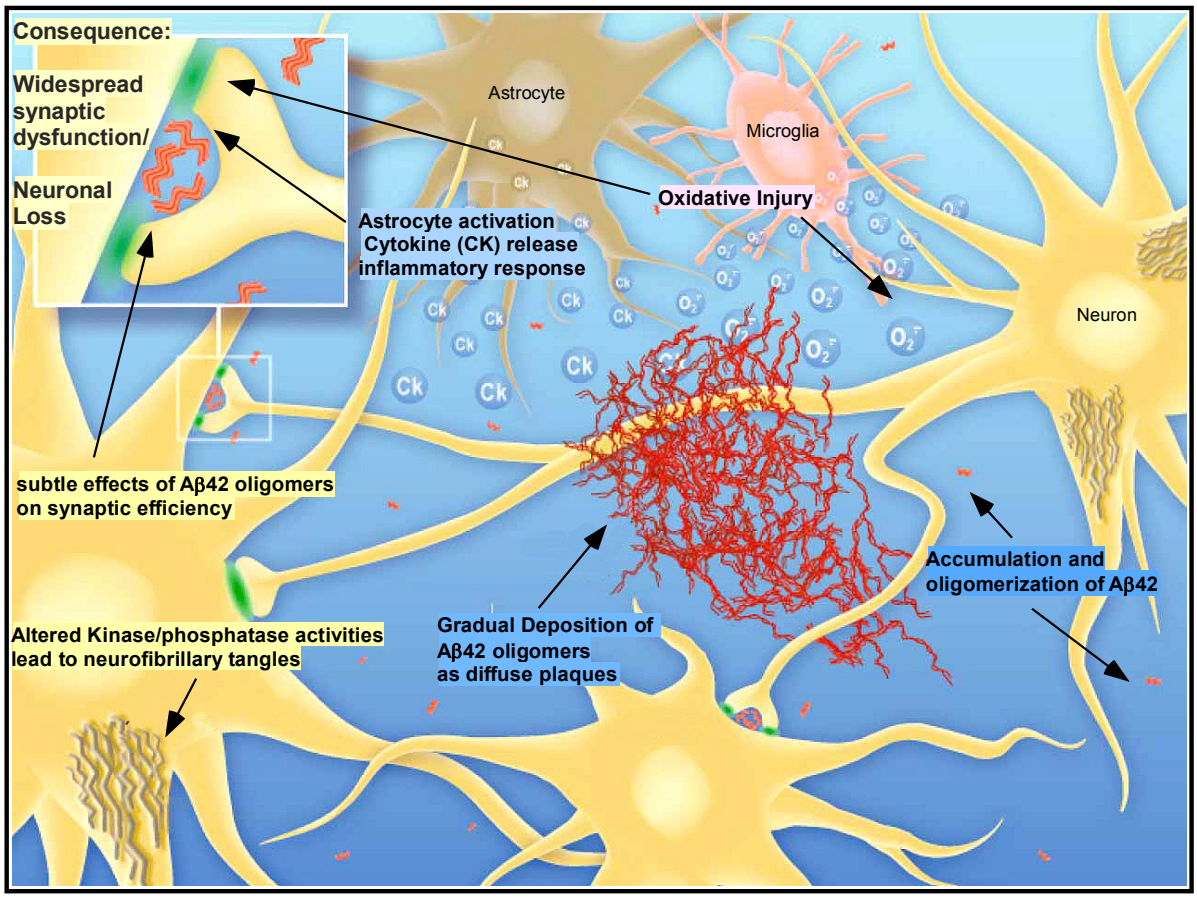


**Figure 3: Hypothetical sequence of pathogenic events in the "amyloid cascade"**

A hypothetical sequence of the pathogenetic steps of AD resulting in synaptic dysfunction and neuronal loss – Several Different Pathogenic Events May Contribute to Synaptic Dysfunction in Alzheimer's Disease. Different Aβ assembly forms may mediate diverse cytotoxic effects, including decreased synaptic efficacy, distortion of axonal pathways, shrinkage of dendritic arbors, activation of microglia, free radical release, and inflammatory changes. The figure shows the distortion of axonal trajectories observed within amyloid plaques and the activation of astrocytes in the proximity to amyloid plaques, resulting in the release of various cytokines (Ck), and microglia, resulting in the generation of superoxide radicals ($O2^-$). Disruption of synaptic efficacy by diffusible, smaller oligomers of Aβ is depicted as a decrease in normal transmission at synapses (green cloud) due to the presence of Aβ dimers and trimers in the cleft that can contact synaptic plasma membranes. All Aβ species are shown in red, with amyloid plaques shown as an interwoven mass of fibrils and soluble Aβ dimers and trimers depicted as stacked W-shaped structures (suggesting their β sheet-rich structure).
Source: Figure adapted from [30] and [32]

### 5.4.3 The *Tau* pathology as a consequence of Aβ formation

As Mudher et. al. suggested, the novel immunization approach, which attempts to specifically remove amyloid plaques from human brains by using antibodies against Amyloid-β [33, 34], might be able to prove that *tau* pathology is consequential to Aβ formation: if specifically removing amyloid plaques also reverses tangle pathology, it is probable that *tau* pathology significantly depends on the amyloid cascade. If removing amyloid does not effect tangle formation but it reverses clinical dementia, than *tau* formation is shown to be largely epiphenomenological [28]. Indeed, using a triple transgenic mouse model (3xTg-AD) that develops Amyloid-β as well as *tau* pathology, Oddo et. al. could recently show that immunization therapy leads to the clearance of Amyloid-β and as well as early *tau* pathology [35]. Hyperphosphorylated *tau*, which forms the fibrillary tangles, however is not effectively cleared. Those fibrillary tangles are composed of microtubules associated protein *tau*, which becomes highly phosphorylated and aggregates into the abnormal filaments in the cell body. The stabilization of microtubules is consequently impaired and microtubules in affected neurons are gradually replaced by tangles which finally leads to neuronal death. As stated above, *tau* pathology is sufficient for dementia in fronto-temporal degeneration disorders but it does not give rise to amyloid plaque formation. As Mudher et al. point out, amyloid pathology on the other hand seems to be related to *tau* pathology. Double mutant mice overexpressing APP as well as *tau* have more widely distributed tangles then mutant-*tau* mice alone [36]. Furthermore, injection of amyloid into the brain of mutant *tau* transgenic mice aggravate tangle pathology in brain regions from were neurons project to the injection site [27, 37].

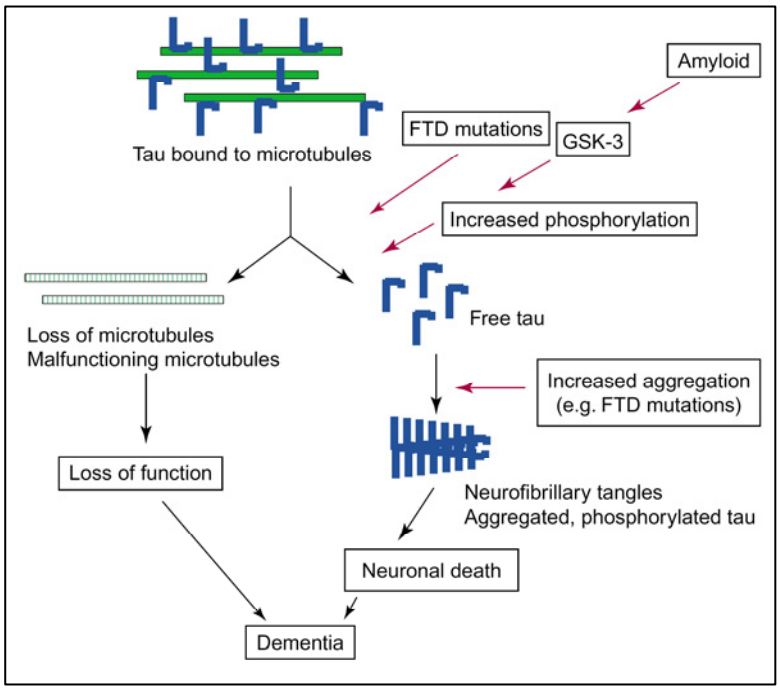


**Figure 4: The tau hypothesis and putative relations to amyloid**

*Tau* binding to microtubules is disturbed by phosphorylation directly by mutations that alter function, and by mutations that alter isoform expression. Decreased *tau* binding to microtubules might result in increased free *tau* which, under the appropriate conditions, will self-aggregate to form insoluble paired helical filaments. Loss of *tau* binding is predicted to result in loss of microtubule function. The process of *tau* aggregation in the absence of

mutations is not known but might result from increased phosphorylation, protease action or exposure to polyanions, such as glycosaminoglycans. Abbreviations: GSK-3, glycogen synthase kinase 3; FTD, fronto–temporal degeneration – Source: Figure adapted from [28].

## 5.5 Risk factors

### 5.5.1 Environmental risk Factors

Age is still the strongest risk factor for dementia, particularly for Alzheimer's disease . In a community-based study, for example, the estimated annual incidence of AD was 0.6 percent for individuals ages 65 to 69 years, 1.0 percent for those 70 to 74 years, 2.0 percent for those 75 to 79 years, 3.3 percent for those 80 to 84 years, and 8.4 percent for those 85 years and older [38]. Dementia is estimated to be present in one-half to two-thirds of nursing home residents [39].

Family history is a risk factor for the development of Alzheimer's disease (AD); patients who have a first-degree relative with dementia have a 10 to 30 percent increased risk of developing the disorder. One study found that the increased risk in first-degree relatives was lower if the patient developed AD late in life (age 85 or older) and similar to the risk in a control group [40].

Weaker risk factors include a history of head trauma associated with loss of consciousness, history of depression, low educational attainment, and possibly organic solvent exposure [1]. AD is more common in women; approximately 16 percent of women surviving to an average life expectancy will develop AD compared with 6 percent of men [1].

Limited data suggest that a diet high in saturated or unsaturated fat or low in non hydrogenated unsaturated fats, may be associated with an increased risk of developing Alzheimer's disease or cognitive decline. However, the evidence is debated [1].

A cohort study found no association between total cholesterol level and AD in a multivariate model [41]. There is furthermore conflicting evidence on whether high dietary intake of fatty fish and marine omega-3 polyunsaturated fatty acid may decrease the risk of cognitive impairment and Alzheimer's disease, whereas intake of cholesterol and saturated fat may increase the risk [42]. Another prospective cohort study however, found no such association [43].

### 5.5.2 Genetic risk factors

Alzheimer's disease can cluster in families in an autosomal dominant manner. The estimates for those genetically caused familial AD (FAD) however vary significantly from 5% to 10% to sometimes even up to 50% [17].

Mutations in APP, Presenilin1 (PS1) and Presenilin2 (PS2) have been identified in FAD patients and are nicely documented in a web-based mutation databank (please see webpage † for references).

In addition to those familial autosomal dominant cases, some geneticists believe that in the future, large percentages of the sporadic cases will also be explainable on the basis

† http://www.molgen.ua.ac.be/ADMutations/default.cfm?MT=0&ML=1&Page=AD

of polymorphic alleles that predispose to the condition in a multicausal fashion. The fact that numerous families cannot be matched to one of the genetic risk factors described above, makes it probable that further risk factors will be identified. Importantly, the clinical presentation and the histopathology of FAD are indistinguishable from sporadic AD cases, suggesting, that the study of FAD generates valid information about the general pathogenesis of the disease [1]. Moreover, since APP is encoded on chromosome 21, an elevated gene dose in patients with trisomy 21 leads to an overexpression of APP [22]. The increased amount of substrate is believed to contribute to the premature AD pathology with early appearance of Amyloid-β 42 in patients who are in their 20s or 30s and consequently develop an AD syndrome, although additional factors might be influential.

### 5.5.2.1 Missense mutations in APP and overexpression of APP

There are so far nine known missense mutations in FAD which are located in APP around the critical cleavage sites of the three involved secretases [22]. Those mutations have been analyzed and are known to alter the proteolytic secretases in different manner. A mutation that is extensively used in the laboratories around the world is the so-called Swedish mutation (APPSwe) in which two amino acids are replaced (K670N/M671L numbering according to the β-APP770 isoform) which leads to a higher affinity of β-secretase and consequently more β-cleavage products which are turned over to Amyloid-β [44, 45].

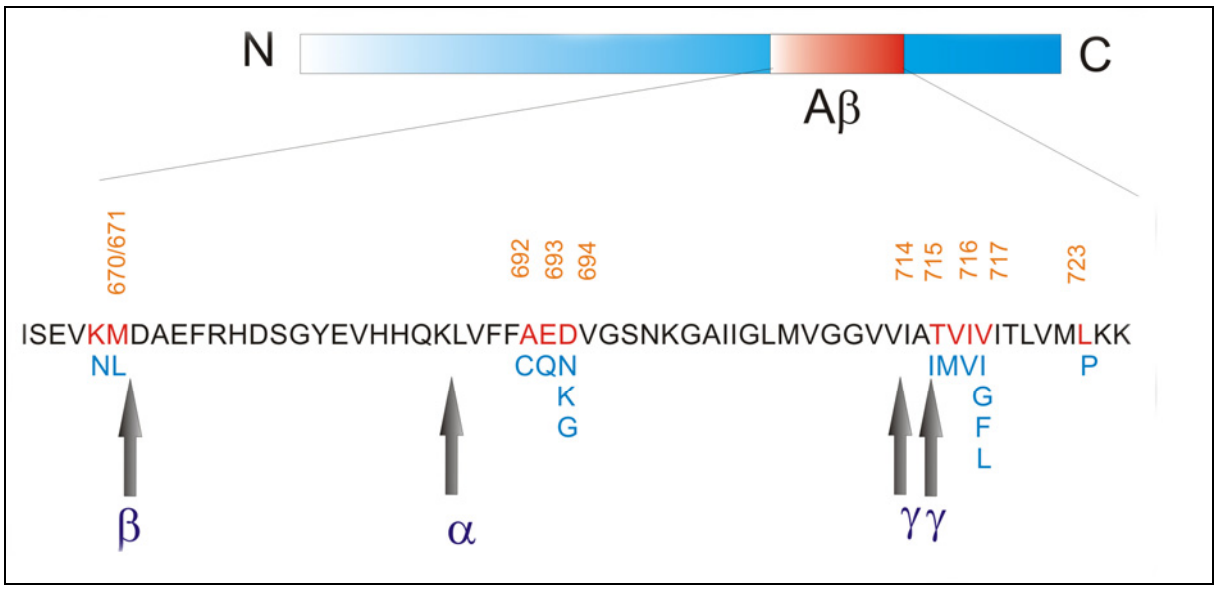


**Figure 5: βAPP mutations linked to familial Alzheimer´s disease**

The sequence within APP that contains the Aβ and transmembrane region is expanded and shown by the single-letter amino acid code. The bold letters below the line indicate the currently known missense mutations identified in certain patients with familial Alzheimer's disease and/or hereditary cerebral hemorrhage with amyloidosis. Three-digit numbers refer to the residue number according to the β-APP770 isoform. – Source: Figure adapted from [17]

### 5.5.2.2 Missense mutations in the Presenilins

Genetic linkage analysis identified Presenilin 1 (PS1) on chromosome 14 and Presenilin 2 (PS2) on chromosome 1 as genes involved in autosomal dominant FAD. The name "Presenilin" indicates that mutations in those genes result in a particularly early "pre-senile" onset of disease (please see footnote ‡ for an extensive databank of mutations and references ). As many as 146 missense mutations in PS1 and 12 in PS2 have been identified, mutations in PS1 being the most aggressive, commonly causing onset of symptoms before the age of 50 [17]. Insights into the mechanism of Presenilin will be presented in the following chapters.

### 5.5.2.3 Apolipoprotein E4 Allele

The apolipoprotein E epsilon 4 genotype (e4), which is overrepresented in AD cases in comparison to the general population, appears to predispose to the development of AD [1]. The Rotterdam study, a population-based cohort of 7983 people aged 55 or older, showed that the apoE epsilon 4 (e4) allele was strongly associated with the risk for AD and vascular dementia: Carriers of the e2/e4 and e3/e4 genotypes each had a relative risk of dementia about double that of e3/e3 carriers. Carriers of the e4/e4 genotype had a relative risk of dementia about eight times that of e3/e3 carriers [46]. In a prospective population-based study, ApoE, elevated total cholesterol, and systolic hypertension all increased the risk for AD in an independent and additive manner. The risk associated with treatable factors was greater than that for ApoE epsilon 4 [1]. The mechanism by which Apo E4 acts is not fully understood but it is assumed that it increases the steady state level of Amyloid-β presumably by decreasing its clearance from the brain and increasing aggregation [17].

## 5.6 Proteolytic processing of APP

### 5.6.1 The α-Secretase

In the non-amyloidogenic processing pathway, APP is proteolytically cleaved by α-secretase at the Lys16-Leu17 bond within the amyloid β domain [47, 48]. This prevents deposition of intact amyloidogenic peptide. Furthermore, the large ectodomain, sAPPα released by the action of α-secretase seems to have several neuroprotective properties [49].

Studies with a range of hydroxamic acid-based compounds, such as batimastat, indicate that α-secretase is a zinc metalloproteinase. Members of the ADAMs (A Disintegrin And Metalloproteinase) family of proteins, TACE, ADAM10 and ADAM9 all fulfill some of the criteria required of α-secretase. APP is constitutively cleaved by α-secretase in most cell lines [50].

From the set of putative α-secretases, the disintegrin metalloprotease ADAM 10 was specified to have both constitutive and regulated α-secretase activity [21]. Expression of a dominant negative mutant of ADAM 10 in HEK cells decreases the secretion of sAPPα. [51].

‡ http://www.molgen.ua.ac.be/ADMutations/default.cfm?MT=0&ML=1&Page=AD

As the α-secretase cleavage within the Amyloid-β region of APP both prevents the deposition of the Aβ peptide and releases the neuroprotective sAPPα, pharmacological up-regulation of α-secretase may provide alternative therapeutic approaches for Alzheimer`s disease [22]. The beneficial action of cholinesterase inhibitors, for instance, may in part be due to activation of muscarinic receptors, resulting in an up-regulation of α-secretase. Other agents can also increase the non-amyloidogenic cleavage of APP including estrogen, testosterone, cholesterol lowering drugs, various neurotransmitters and growth factors [50].

Interestingly, Postina et. al could show by crossing mice overexpressing ADAM10 in neurons with transgenic human APP mice, that the production of Amyloid-β peptides was reduced, deposition in plaques was prohibited and functional defects in hippocampal neurophysiology (LTP) as well as memory deficits in the Morris water maze were rescued. The authors thus conclude that increasing the activity of ADAM10, as one efficient α-secretase, could potentially be helpful as an alternative therapeutic strategy besides attempts to selectively inhibit β- or γ-secretase [52]. This could theoretically be achieved by activation of second messenger cascades, like the protein kinase C, known from studies in cells to enhance α-secretase activity. However, more has to be learned about the underlying pathways and mechanisms. Also, activation of the second messenger cascade could prove to be too nonselective [22].

## 5.6.2 BACE2 has a non-amyloidogenic effect

The identification of the BACE homologue BACE2 incited great interest concerning the question on whether it has a similar enzymatic profile as BACE or whether it is involved in completely different cellular processes.

Saunders et. al published a technical report [53] in which they performed a database search with the complete amino acid sequence of BACE and found two full-length cDNAs that were highly homologous to BACE which were thus called BACE2. They furthermore mapped BACE 2 to chromosome 21 and more precisely to the obligate Down syndrome (DS; trisomy 21) region, a minimal region of chromosome 21 that must be inherited in a trisomic state for expression of the constellation of features and symptoms characteristic of DS. Bennet, Vassar and colleagues stated by referring to the publication by Vassar et. al. [54] that they think that BACE2 is not likely to be the major β-secretase, at least in HEK 293 cells because the antisense-used in the study to decrease BACE activity by up to 80% are not complementary to BACE2 mRNA and therefore cannot cross-hybridize with and inhibit BACE2 mRNA. The residual 20% of β-secretase cleavage they observed is thus more likely to be explained by residual cells which escaped transfection with the oligos. The authors thus conclude that BACE is the major β-secretase, at least in HEK 293 cells, and that BACE2 does not compensate for loss of BACE function in these cells [53].

Yan et. al similarly found BACE2 together with BACE in a search of vertebrate expressed sequence tag (EST) databases with their 10 sequences found in C. elegans. They also mapped BACE2 to human chromosome 21q22 within the Down's syndrome critical region. The authors furthermore showed that BACE2 is only expressed at low levels in brain and that only those antisense oligomers targeting BACE considerably decreased the release of Aβ peptides into the medium, whereas those against BACE 2 did not.

These data thus in line with the results by Vassar et. Al. suggested that BACE is the essential β-secretase for Amyloid pathology [55]. In parallel to the technical comment by Saunders et. al, two other groups started from an analysis of the so-called `Down critical region' in 21q22.3 within the chromosome 21 and also identified BACE2 [56, 57].

### 5.6.2.1 Sequence Structure of BACE2

BACE and BACE2 exhibit 52% amino acid sequence identity and 68% similarity (see Figure 6 below). BACE2 contains two aspartyl protease active sites at virtually identical positions to the two active sites in BACE [53]. Both endoproteases share similar structural organization including a prodomain, a catalytic domain formed via DTG and DSG active site motifs, a single transmembrane domain, and a short C-terminal tail. The amino acid sequences of BACE and BACE2 are divergent only at the COOH-terminal 30 amino acids and the NH2-terminal 80 amino acids. Which contain predicted single membrane-spanning domains [53].

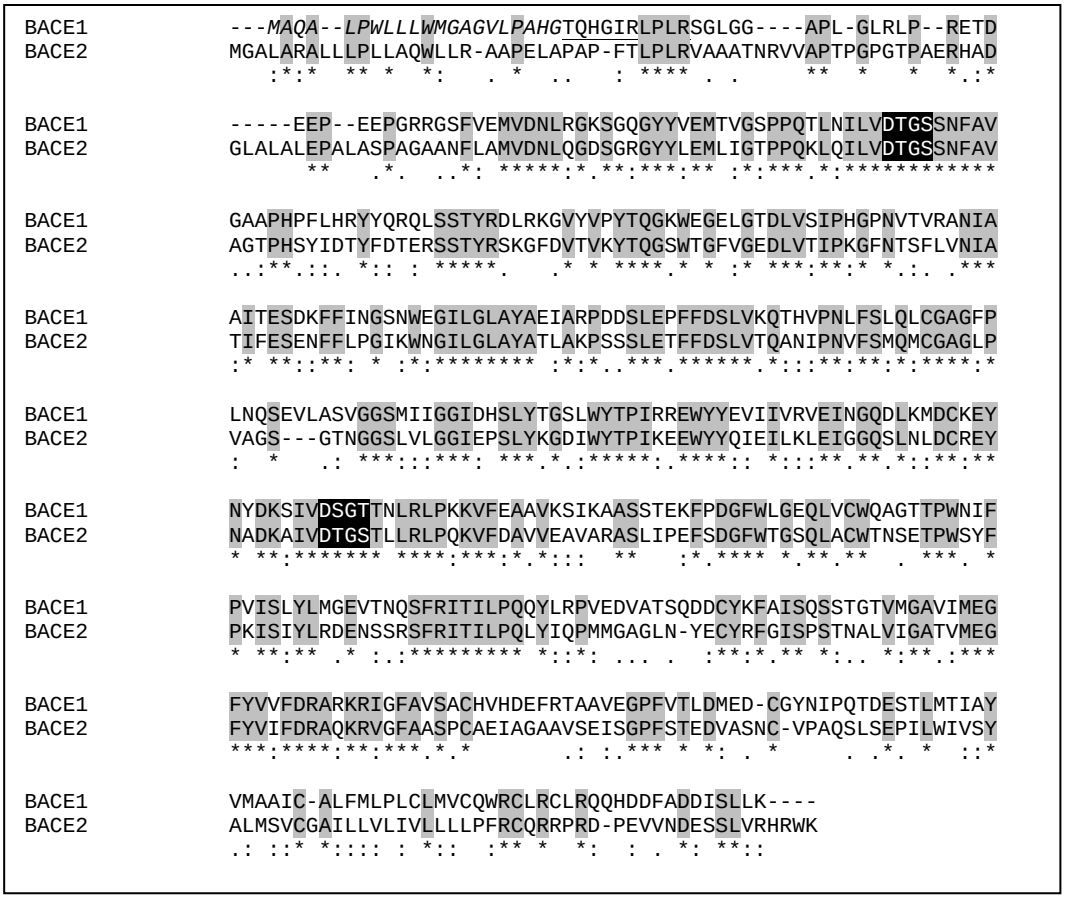


**Figure 6: Homology between BACE and BACE2**

BACE (Accession number AF204943) and BACE2 (Accession number AF204944) were aligned with CLUSTALW[§]. Regions of identity are shown in grey. The active site motifs DTGS and DSGT are shown in black. The *signal peptide* of BACE is shown in *italic*, the prodomain of BACE1 is underlined.

In vivo, BACE2 is expressed as a precursor protein containing pre-, pro-, protease, transmembrane, and cytosolic domains/peptides [58]. It is a 518 amino acid protein with a

[§] http://www.bork.embl-heidelberg.de:8080/Alignment/alignment.html

20-residue signal peptide, and two putative N-glycosylation sites. In addition, and similarly to BACE, BACE2 differs from the other members of the human aspartic protease family in the number and distribution of putative disulfide bonds and in the presence of an extended C-terminal region which contains a predicted transmembrane segment [57].

The prodomain processing of BACE2 was shown to occur auto-catalytically between Leu(62) and Ala(63) [59]. BACE2 cleaves itself in vitro whereas an inactive mutant in which one of the catalytic aspartates is mutated to an asparagine can not auto-activate nor was the pro-peptide of this mutant cleaved by another proteinase in vivo. The study furthermore showed that the prodomain processing occurred intramolecularly within the endoplasmic reticulum/early Golgi [59]. Autoactivation of purified BACE2 was confirmed by another group [60].

### 5.6.2.2 Tissue Expression of BACE2

Yan et. al. initially reported that BACE2 was expressed only at low levels in brain [55]. This finding was extended by Northern analysis which revealed that BACE2 mRNA is expressed at low levels in most human peripheral tissues and at higher levels in colon, kidney, pancreas, placenta, prostate, stomach, and trachea. Human adult and fetal whole brain express very low or undetectable levels of BACE2 mRNA and in situ hybridization of adult rat brain showed that BACE2 mRNA is expressed at very low levels in most brain regions [61]. Other studies agree with the broad tissue distribution of BACE2 [57] and also found by Northern blotting that the mRNA for BACE2 is present at a low level in brain when compared to BACE [62]. However, using sensitive TaqMan analysis, Hussain et. al. conclude that the mRNA for BACE and BACE2 correlate as they are highest for example in the substantia nigra and tend to be equally low in other subregions, for example in the striatum. In addition, immunohistochemical analysis showed that BACE protein is present in neurons within the hippocampus, frontal cortex, and temporal cortex in brain from both AD and aged control subjects [62].

### 5.6.2.3 Localization of BACE2

BACE2 was localized in the endoplasmic reticulum, Golgi, trans-Golgi network, endosomes [60], where it co-localizes with APP [62]. In comparison to BACE, it has a more diffuse localization pattern and is present throughout the Golgi compartments even at low expression levels [60]. Also, BACE2 was found at the plasma membrane [59, 60]. Removal of the C-terminus of BACE2 alone did not alter its cellular localization, whereas removal of both the C-terminal domain and the transmembrane domain resulted in a diffuse fluorescent signal over the entire cytoplasm, suggesting that the Transmembrane domain governs the localization of BACE2 [60].

### 5.6.2.4 Cleavage Site of BACE2

Although BACE2 also cleaves at the β site within APP, its preferential site is in the middle of the Amyloid-β domain after two Phenylalanines at positions 19 and 20. This was measured by in vitro cleavage products analyzed by MALDI-TOF, which also revealed a second cleavage site between Phe-19 and Phe-20 [63]. The major cleavage

site after Phe-20 and the minor site between Phe-19 and Phe-20 was confirmed by another study which analyzed cleavage products by MALDI-TOF and subsequently quantified by reverse-phase HPLC [60]. Using Radiosequencing of [3H]valine-labeled CTF-α and Amino acid sequences matching, the site between Phe-19 and Phe-20 was again confirmed [64].
It can be concluded from these data, that BACE2 functions more like an alternative α-secretase and thus has a non-amyloidogenic effect [60, 63, 64].
As a further conclusion, BACE2 can be distinguished from BACE on the basis of autoprocessing of the prosegment, APP processing specificity, and subcellular localization patterns [60].

#### 5.6.2.5 3D Structure of BACE2

Although the overall structural topology between BACE and BACE2 protease domains is quite similar, the former contains 3 disulfide bonds but the latter only two. Analysis of the crystal structure of BACE also revealed that there are subtle structural difference around the DTG/DSG active site between the two BACE species that could potentially be exploited to achieve better specificity of BACE inhibitors [65].

## 5.7 The amyloidogenic pathway

As outlined above, two secretases process APP in the amyloidogenic pathway, the β-secretase and the γ-secretase.

### 5.7.1 The Presenilin Complex

Whereas the γ-secretase activity was known for quite some time, it proved to be difficult to identify the corresponding gene. The discovery of the Presenilin 1 and 2 (PS1 and PS2) as major genes for early onset FAD finally lead to the identification of the γ-secretase. The genes are homologous and encode polytopic transmembrane proteins [66, 67].
Several lines of evidence support the association between these genes and the described activity: mutations of PS in FAD patients shifted the cleavage of γ-secretase from position 40 to 42 of Amyloid-β, γ-secretase activity was tamed in cells from PS knockout mice [68-71] and replacements of either of the two aspartate residues within the PS abolished the γ-secretase activity [72] suggesting that the γ-secretase might be a novel form of a membrane bound aspartate protease [73-75].
Endoproteolysis within the cytoplasmic loop of PS leads to the characteristic N-terminal and C-terminal fragments (NTF or CTF respectively) [76]. The resulting Presenilin-complexes consist of NTF and CTF are the stable and active species within the cell [77-79].
It has been put forward, that Presenilin is probably the active center of this γ-secretase complex [75, 80, 81]. In favor of this hypothesis is that the γ-secretase could be characterized pharmacologically as an aspartyl protease [82]. The two aspartates of Presinilin lie within its transmembrane domains 6 and 7 across from each other within the membrane. They could therefore cooperatively catalyze substrates within the membrane, which is a novel site of action for aspartate proteases [80, 83]. Interestingly, the position of the γ-secretase cleavage seems to be dependent on the length and the

structure of the substrate rather than its sequence of amino acids [80, 84]. Moreover, the sequences close to the aspartates within the Presenilins show homologies to known aspartate proteases, such as polytopic aspartyl proteases of bacterial origin [85]. There has been long-standing debate on whether PS directly codes for the γ-secretase activity or just for an essential cofactor of the yet to identify γ-secretase. The purification of the γ-secretase activity by means of chromatography and glycerol gradients indicated that γ-secretase was a high molecular weight complex [86, 87]. Prompted by this finding, Presenilin cofactors were identified as members of the γ-secretase complex, namely Nicastrin [88], APH-1[89-91] and PEN-2 [90, 92]. Edbauer and colleagues reconstituted an active γ-secretase complex in yeast cells devoid of endogenous PS1 and γ-secretase activity and could demonstrate that in fact, PS, Nct, APH-1 and PEN-2 are the necessary and sufficient components for γ-secretase activity [93]. It was also shown by Kimberly et. al. that these four factors co-assemble in mammalian cells [94]. Using RNAi technology in Drosophila S2 cells, Takasugi and colleagues could dissect the stepwise assembly of this complex (Figure 9) and show that APH-1 stabilizes the PS holoprotein in collaboration with NCT, whereas PEN-2 elicits the final maturation of the γ-secretase complex, conferring its activity and inducing endoproteolysis of PS [95]. APH-1 and Nicastrin were also shown to form a stable intermediate prior to the association with PS holoprotein [96, 97] which in a synopsis supports the model below.

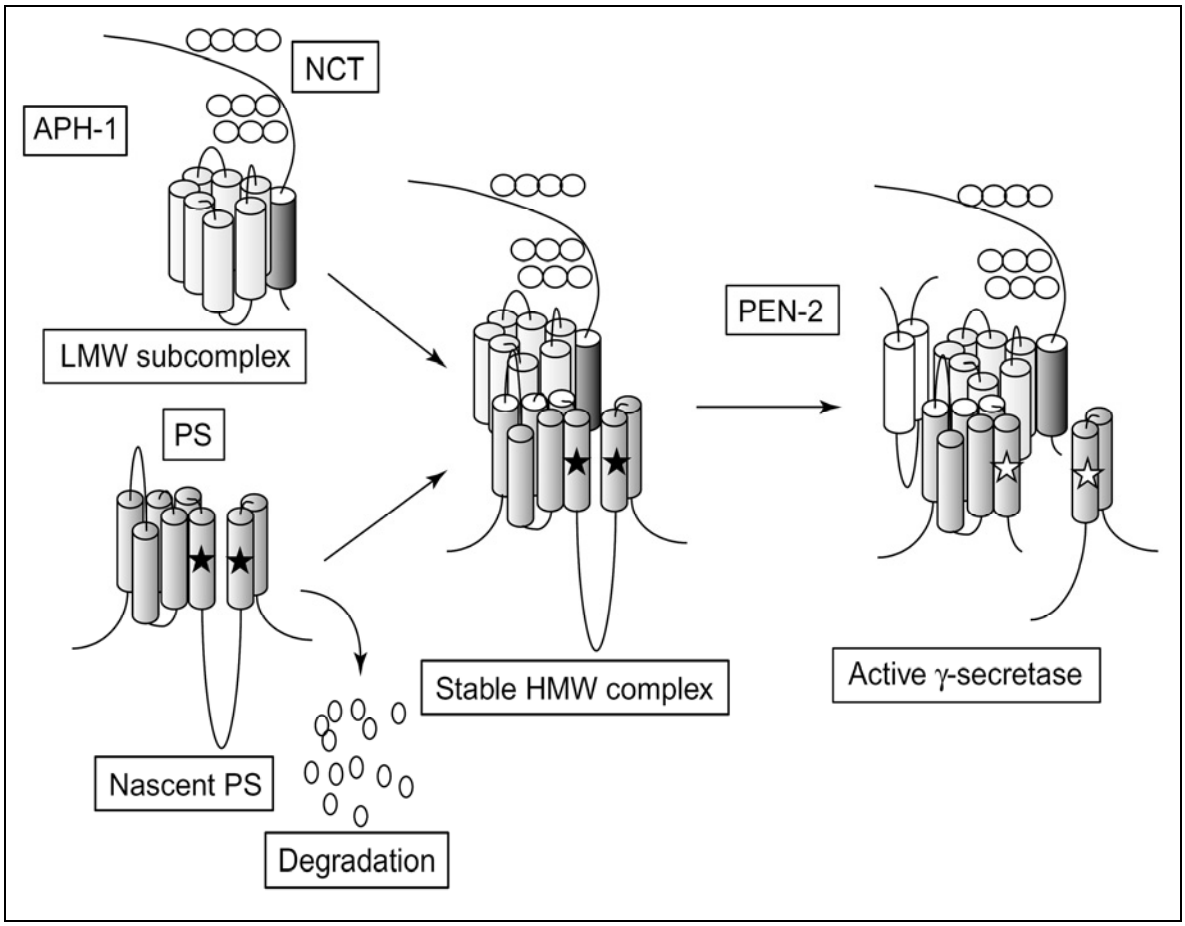


**Figure 7: Stepwise assembly and activation of the γ-secretase complex**

Schematic depiction of the stepwise assembly and activation of the γ-secretase complex. Nascent PS holoprotein is rapidly degraded while a fraction of PS is stabilized to form a HMW complex by binding to the sub-

complex formed by APH-1 and NCT. PEN-2 elicits the final step of maturation of the γ-secretase complex, facilitating endoproteolysis of PS and conferring γ-secretase activity. Tubes represent the putative transmembrane domains (TMD) of each protein, and stars within the 6/7th TMD of PS symbolize active (unfilled) and inactive (black) aspartate residues involved in γ-secretase activities.
Source: Figure adapted from [98]

### 5.7.1.1 Role of the Presenilin complex in signal transduction

In addition to its critical role in APP processing, the γ-secretase complex is also involved in signal transduction via the NOTCH pathway, [70, 99] which has an important function in cell differentiation and development. Notch is a type 1 transmembrane protein that is transported to the plasma membrane through the secretory pathway. During its transport through the Golgi network it is cleaved by a furin-like enzyme. Notch can function at the surface as a receptor for ligands as Delta and Serrate who upon binding induce a second cleavage of Notch by the Metalloprotease ADAM17/TACE [100]. This cleavage than results again in an extracellular Notch fragment and a membrane bound fragments which subsequently is processed by the Presenilin complex liberating the intracellular domain of Notch (NICD). NICD is consequently translocated to the nucleus where it binds to a transcription factors of the CLS family [101].
A comparison of the processing of Notch and APP, as shown in Figure 10, reveals strong similarities: cleavage of both molecules liberates a N-terminal fragment in a process often called “ectodomain shedding” [102]. The subsequent processing of the respective C-terminal fragments by the γ-secretase complex generates a fragment that subsequently moves to the nucleus. This type of signal-transduction is also called “regulated intramembrane proteolysis” or RIP. It has been reported that the receptor tyrosin kinase ErbB4 is another molecule that is analogously processed by the metalloprotease ADAM17/TACE in cooperation with the γ-secretase complex [103] [104]. Similar to NICD, the “APP intracellular domain” (AICD) (see Figure 2) can assemble with other factors such as Fe65 to a complex which translocates to the nucleus to control transcription [105-107]. Regulation of retinoid gene expression and modulation on the transcriptional effect of NICD itself are discussed. AICD is selectively degraded by Insulin degrading enzyme (IDE) [108] which could thus serve to terminate the signal. Together this system would thus be able to entertain a conrolled signal transduction.

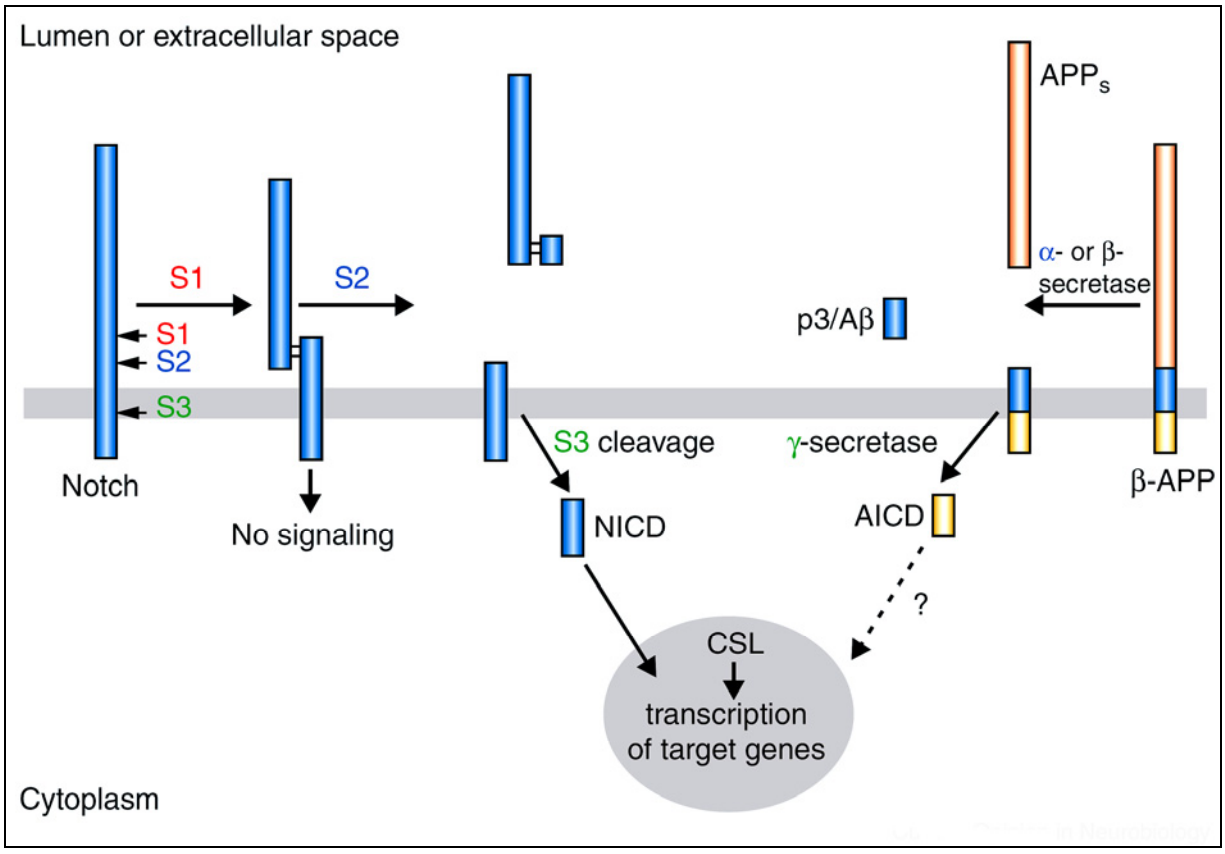


**Figure 8: Notch- Signal Transduction Pathway in comparison to APP-processing**

Notch signalling relies on three endoproteolytic cleavages. Notch maturates in the Golgi apparatus by furin-mediated cleavage at site 1 (S1). At the cell surface, Notch is cleaved at S2 (after binding to its ligands Delta/Serrate/Lag-2). Finally, PS-dependent cleavage at S3 liberates the NICD, which translocates to the nucleus, thereby regulating the transcription of target genes by binding to transcription factors of the CSL (CBP/SuH/LAG-1) family. β-APP is processed by a similar pathway Initial cleavages of β-APP by α- or β-secretase leads to the generation of a membrane-bound CTF. γ-Secretase cleavage then liberates p3 or Aβ, and the APP intracellular domain (AICD). The biological function of AICD remains to be determined
– Source: Figure adapted from [109]

## 5.7.2 The β-Secretase

The cleavage of the β-secretase (BACE) of APP is the rate limiting step of amyloid production (see Figure 2). Whereas β-secretase activity has been known for a long time, the identification of the β-secretase protein proofed to be rather difficult until several findings finally converged to a common result.

### 5.7.2.1 Identification of β-Secretase (BACE)

The gene encoding for the β-secretase, termed Asp2 or BACE, was identified in 1999 almost simultaneously by four independent groups using different approaches. Whereas Vassar and colleagues [54] successfully used an expression cloning strategy, Yan et al. [55] identified BACE via a database search for aspartyl proteases using the genome of C. elegans followed by a databank search on human sequences. Sinha et al. [110] purified the β-secretase activity to homogeneity from human brain. Hussain et al. [111] also used a cloning approach to identify BACE. In addition, a homologous protein to BACE was identified by Hussain et. al [111] which was called BACE2. The BACE gene maps to

chromosome 11, whereas BACE2 is encoded on chromosome 21 close to the region associated with Down syndrome [56].

### 5.7.2.2 Domain Structure of BACE

BACE is a 501-amino acid protein with an amino-terminal signal peptide of 21 amino acids followed by a proprotein domain spanning amino acids 22–45 [112]. The luminal domain of the mature protein extends from residues 46–460 and is followed by a transmembrane domain of 17 residues and a short cytosolic tail of 24 amino acids (Figure 11). BACE contains two active site motifs at amino acids 93–96 and 289–292 in the luminal domain, each containing the conserved signature sequence of aspartic proteases D T/S G T/S. BACE is predicted to be a Type I transmembrane protein with the active site on the luminal side of the membrane where β-secretase cleaves APP. BACE2, displays 64% amino acid sequence similarity to BACE and also shows a C-terminal transmembrane domain [112]. Together, BACE and BACE2 define a new family of transmembrane aspartic proteases, related to the pepsin family and more distantly related to the retroviral aspartic proteases or other aspartic proteases [112].

```
  1 MAQALPWLLL WMGAGVLPAHG*TQHGIRLPL RSGLGGAPLG LRLPRETDEE PEEPGRRGSF
 61 VEMVDNLRGK SGQGYYVEMT VGSPPQTLNI LVDTGSSNFA VGAAPHPFLH RYYQRQLSST
121 YRDLRKGVYV PYTQGKWEGE LGTDLVSIPH GPNVTVRANI AAITESDKFF INGSNWEGIL
181 GLAYAEIARP DDSLEPFFDS LVKQTHVPNL FSLQLCGAGF PLNQSEVLAS VGGSMIIGGI
241 DHSLYTGSLW YTPIRREWYY EVIIVRVEIN GQDLKMDCKE YNYDKSIVDSGT TNLRLPKK
301 VFEAAVKSIK AASSTEKFPD GFWLGEQLVC WQAGTTPWNI FPVISLYLMG EVTNQSFRIT
361 ILPQQYLRPV EDVATSQDDC YKFAISQSST GTVMGAVIME GFYVVFDRAR KRIGFAVSAC
421 HVHDEFRTAA VEGPFVTLDM EDCGYNIPQT DESTLMTIAY VMAAICALFM LPLCLMVCQW
481 RCLRCLRQQH DDFADDISLLK
```

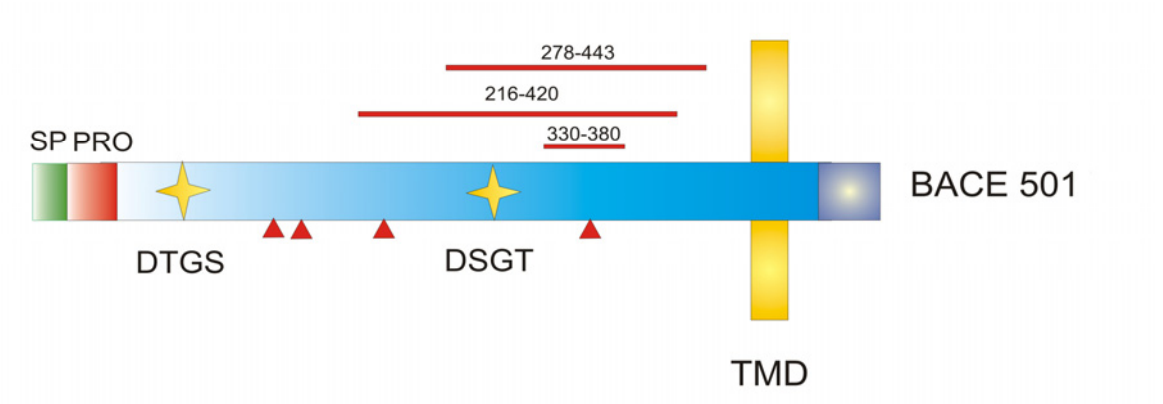


**Figure 9: Amino Acid sequence of BACE and Domain structure**

BACE sequence (accession number AF190725 in genbank) as well as a schematic drawing of the BACE domain structure are shown. The signal peptide (SP) is shown in green, the prodomain (PRO) of BACE is colored in red, the cleavage site for the SP is indicated by an asterisk * in the sequence. The active site aspartate is highlighted in yellow and indicated in the schematic drawing by large yellow asterisks. The transmembrane domain is displayed in bold letters underlined with a punctuated

line. The four N-glycosylation sites are shown in italic and underlined and as red arrowheads in the drawing. The six cysteines involved in intramolecular dissulfide bonds are boxed and the corresponding bonds indicated by red bars. Source: The schematic drawing was adapted from [113]

## 5.7.2.3 Mouse Models studying BACE

### 5.7.2.3.1 BACE Knock-out Mice

The role of BACE in Aβ-production was demonstrated in several mouse models. Studies in BACE knock out mice showed that in neurons, BACE expression is strong whereas BACE2 expression is weak. Furtermore, since Amyloid-β generation is abolished in BACE–/– neurons [114] BACE is thought to represent the principal β-secretase. Interestingly, the BACE knock out mice were healthy and fertile and showed no structural abnormalities upon microscopic examination, a result that was confirmed by other groups [115]. Similarly, Roberds and colleagues did not detect any abnormalities in brain histochemistry, blood and urine chemistry or blood-cell composition in their BACE-KO mice [116]. Also there was no compensatory change in gene expression of the homolog BACE2, nor were there amyloid plaques detected even if the BACE-KO mice were crossed into an APP overexpressing strain of mice [117]. Pastorino et. al. furthermore reported that their BACE knockout animals exhibited the lack of formation of the β-secretase-dependent C99 and C89 C-terminal fragments but they did not comment on any overt phenoypic alterations [118].

In terms of behavioral alterations, a knockout mouse in which LacZ replaces the first exon of murine BACE was described to a more timid and less exploratory behavior in comparison to a mouse model that overexpressed BACE, suggesting to the authors that BACE may have an unexpected role in neurotransmission [119]. More precisely, it could be shown that the Amyloid-β-dependent hippocampal memory deficits of mice overexpressing human APP Tg2576(+) are rescued both behaviorally and electrophysiologically by knocking out BACE in those mice. This improvement correlates with a reduction of cerebral Amyloid-β 40 and 42 levels before amyloid deposition in Tg2576 mice occurs, suggesting that soluble Amyloid-β assemblies and CTFs may be causing memory dysfunction in part by disturbing cholinergic functions [120].

Taken together, these studies validate BACE as the necessary and sufficient β-secretase in the brain. BACE acts as the rate-limiting step for AD´s structural and functional pathology.

### 5.7.2.3.2 Transgenic Mice overexpressing BACE

In good keeping with these BACE-KO models are the data from BACE overexpressing mice. BACE overexpression in those mice show decreased levels of full-length APP and increased levels of C99 and C89 in vivo [121] as well as intracellular β-amyloid immunoreactivity that was co-localized with transgenic BACE in neurons [122] whereas increased brain levels of Amyloid-β peptides and Amyloid-β deposition was only observed upon co-Expression of human APP wild-type [123] or carrying the wild type or the swedish mutation [121, 122]. Interestingly, in another BACE and APP double-transgenic mouse, an inverse relationship between increased parenchymal amyloid deposition and decreased vascular deposition of Amyloid-β as compared with APP overexpressing mice

was observed. Further analysis found that the increased Amyloid-β levels were mainly composed of N-terminally truncated species of Amyloid-β, especially Amyloid-β (11-40) and Amyloid-β(11-42) which are directly produced by BACE (see section 5.7.2.10 on enzyme kinetics) but that those N-terminally truncated Amyloid-β forms prevented the vascular amyloid deposition. The authors suggest, that a lower solubility of those truncated Amyloid-β species might decrease their drainage from the neuronal site of production along the perivascular space into the cerebrospinal fluid and thus result in a lower amount of vascular deposition [124]. A high overexpression of BACE in transgenic mice decreased Amyloid-β production as compared to moderate overexpression in another mouse model. Further experiments suggested an explanation for this by showing that high BACE expression shifted the subcellular location of APP cleavage to the neuronal perikarya early in the secretory pathway, thereby increasing β-cleavage of APP but probably decreasing subsequent axonal processing of the CTFs [125].

### 5.7.2.4 Posttranslational Maturation of BACE

BACE is synthesized as a 70kDa large, N-glycosylated pro-enzyme (the calculated weight is 50kDa) with an N-terminal 24 amino acid long propeptide [126, 127].

#### 5.7.2.4.1 The role of the pro-domain of BACE

Upon exit from the ER, the propeptide is cleaved off in the TGN by Furin, or a furin-like proprotein convertase [126-128]. Pinnix however, showed that the propeptide could also be cleaved off in a Furin-deficient mutant thus suggesting that propetide-convertases other than Furin might play a role [129]. Sidera and colleagues also report an autocatalytic cleavage of the pro-peptide by purified BACE at pH5 but not at pH8 [130]. This finding remains however controversial whereas autocatalytic activity could be clearly shown for BACE2 (Hussain, Christie et al. 2001).

The release of the pro-domain does not seem to be necessary for the activation of the enzyme, because pro-BACE produces significant amounts of the β-cleaved C99 [128, 131]. Furthermore, pro-BACE only has a 2.3 fold lower $K_{cat}$ / $K_M$ ratio than mature BACE indicating that BACE is not a strict zymogen that has to be activated by propeptide cleavage to become a fully potent enzyme. (Shi, Chen et al. 2001). The Crystal structure of BACE holds a mechanistic explanation of the function of the pro-domain by demonstrating, that catalytical water within the active center of pro-BACE is not blocked by a salt bridge of the pro-peptide which would have been a common mechanism known for pepsinogen and other proteases [132]. It follows from this that cleavage of the pro-peptide cannot effectively regulate the activity of BACE. Furin and similar propeptide-convertases are thus not suited as a target for pharmacological intervention.

#### 5.7.2.4.2 Posttranslational Modifications of BACE

Maturation is continued in the Golgi by complex N-Glycosylation [127] at 4 asparagine residues [133], resulting in the mature 75 kDa endo H resistant BACE [127].

Additionally, BACE undergoes further post-translational modification. Three cysteine residues within the transmembrane domain and the cytoplasmatic domain are palmitoylated and mature, N-glycosylated residues are sulfated. [128].

#### 5.7.2.4.3 Dissulfide Bonds in BACE

BACE establishes three disulfide bonds of which the bond between residues 330 and 380 which lies close to the active center of the protease seems to be especially important for the correct folding and enzymatic activity [113]. Those disulfide bonds (Figure 11), not conserved in members of the pepsin family, are all intramolecular linkages, which are thus not available for forming intermolecular disulfide bonds with other proteins [133].

### 5.7.2.5 Localization and Trafficking of BACE

##### 5.7.2.5.1.1 Cellular localization of BACE

Numerous studies using mostly Human Embryonic Kidney (HEK) cells have localized BACE by means of immunofluorescence techniques to acidic compartments such as the TGN and the endosomal system with minor amounts in the ER and at the plasma membrane [54, 111, 127, 134-136]. As pointed out by Yan and colleagues, endogenous BACE has a more stringent Golgi-like pattern whereas the additional stainings could be an effect of overexpression [136].

##### 5.7.2.5.1.2 Cellular localization of β-secretase activity

Given its mildly acidic pH optimum BACE [54, 137] would theoretically cleave APP most efficiently within endocytic compartments or the TGN. APP has been demonstrated to undergo active internalization from the cell surface providing a ready source of substrate [18]. In addition, the cycling of BACE to and from the plasma membrane and TGN would theoretically result in even greater access to APP, which could be cleaved directly or upon return to acidic compartments [135]. However, several studies using various techniques like temperature block [138], pulse chase experiments and experiments using pharmacological treatment [64, 136, 139], as well as sucrose gradient fractionation [136] showed that the β cleavage can occur as early as in ER/Golgi fractions in HEK cells, neuro glioma cells and neurons. Further support stems from studies that selectively retained APP in the ER by addition of a di-leucine retention motif [140, 141], or retained BACE in the ER respectively [142] and thereby demonstrated efficient β-secretase cleavage of APP in the ER. These data also underline the finding discussed above that pro-BACE, which is the major species of BACE in the ER, is significantly active. A study using Fluorescence Resonance Energy Transfer (FRET) demonstrated close contact between BACE and APP at approximately 250nm not only in the Golgi, but also at the cell surface and in early endosomes of H4 neuro glioma cells [143]. Since these studies overexpressed constructs of BACE and/or APP, the exact site of action of BACE within the different cell types has not been entirely clarified.

##### 5.7.2.5.1.3 Trafficking through the Exocytotic Pathway

BACE travels along the exocytotic pathway through the Golgi-apparatus to the plasma membrane [136] from where it is internalized and transported to endosomal compartments. A fraction can reach the endosomes directly from the Trans- Golgi Network (TGN). BACE is assumed to recycle several times between surface and endosomes during its relatively long half-life of approximately 12-16 hours (Huse and Doms 2000).

The signals regulating this transport have been studied. The pro-domain appears to be important for the exit of BACE from the ER, because a construct in which the prodomain was deleted accumulates in the ER [128]. Localization to the TGN seems to be significantly mediated by the Transmembrane Domain (TM), supported by experiments in which the TM fused to a GFP protein was sufficient to localize the TM-GFP-fusion protein to the TGN (Yan, Han et al. 2001).

Recycling between plasma membrane and endosomes is guided by a di-leucine motif LL 499/500 at the C-terminus (see amino-acid sequence of BACE), as deleting LLK (Huse and Doms 2000) or replacing it by LLAA (Pastorino, Ikin et al. 2002) leads to prolonged presence of BACE at the surface during steady state conditions. Pastorino and colleagues explain this by reduced endocytosis of the LLAA construct (Pastorino, Ikin et al. 2002). Huse and co-workers propose instead that an accelerated recirculation to the membrane due to defective sequestration to endosomes and reduced direct transport form TGN to endosomes might be responsible (Huse and Doms 2000). There is evidence that the serine residue S498 can be phosphorylated by Casein Kinase 1 which does not influence reinternalization but promotes the consecutive transport from early to late endosomal compartments as well as the TGN. Non-phosphorylated BACE consequently resides in early endosomal compartments [109, 144-146]. A putative transport mechanism is proposed by He and colleagues who postulates that the conserved motif DisLLk (essential residues in capital letters) is an „acid-cluster-dileucine motif“ which in analogy to the mannose-6-phosphate receptor binds to N-terminal VHS-domains of GGA proteins, establishing an association to the Golgi membrane resulting in its subsequent transport to the endosomes [147, 148]. These authors furthermore demonstrate that phosphorylation of the Serine S498 facilitates binding of GGA proteins which control the recycling to the cell surface. The BACE mutant S498A which can not be phosphorylated remains in endosomal compartments from where it directly recycles to the cell surface, whereas the mutant S498D, which mimics phosphorylated BACE, is transported to vesicles that mediate transport to the TGN. This retrograde transport to the TGN was furthermore shown to be inhibited by a dominant negative form of GGA1 supporting a direct interaction of GGA1 with the C-terminus of BACE [149]. A study based on fluorescence lifetime-imaging which can quantify close interactions of proteins using modified FRET experiments confirms that phosphorylation of S498 enables the dileucine motif of BACE to bind to GGA1 primarily in the TGN which consequently accelerates recycling to the surface. Phosphorylation itself can occur in various compartments including areas close to the cell surface where it could be used as a means of regulation [150]. The X-ray crystal structure of a hetero-dimeric crystal of the BACE C-terminus and GGA1 VHS domain demonstrates that increased GGA affinity for phosphorylated BACE arises by increased hydrogen bonding and electrostatic interactions between the two proteins leading to a reversible increase in affinity [145]. It is important to note however, that neither BACE phosphorylation [144] nor mutation of the BACE dileucine motif [146] leads to altered Amyloid-β production or APP shedding, at least under overexpressing conditions.

#### 5.7.2.5.1.4 Role of the TM domain of BACE

Yan and co-workers studied the contribution of the TM domain to trafficking of BACE and generated several deletion constructs and GFP-fusion proteins to dissect that it is necessary and sufficient for targeting BACE to the TGN [136]. Interestingly, the isolated C-terminal Dileucine Motif or the entire C-terminus are dispensable for TGN localization which is in good agreement with the function of the Dileucine motif in the transfer from the TGN to endosomes after the TM has addressed BACE to the TGN. Moreover, the authors studied the enzymatic activity of their constructs and showed that the TM is important for effective substrate binding and processing, because β-secretase activity was abolished in a construct lacking the TM and the C-terminus. BACE activity was lost even if the construct was artificially retained in the ER by an attached KDEL motif and additionally presented with excess APP retained by BFA treatment. According to the authors, the loss of activity can thus not be attributed to the defective localization of the construct which is secreted into the supernatant due to the lack of the TM. Since wild-type BACE (wt BACE) is enzymatically active under these conditions, the authors conclude that the TM is necessary for BACE to access APP [136].

#### 5.7.2.5.1.5 Polarized Sorting of BACE

Studies in Madin-Darby canine kidney (MDCK) cells, which are epithelial polarized cells frequently used as a system for the analysis of polarized sorting, revealed that BACE is largely sorted to the apical surface which corresponds to the axons of hippocampal neurons [151]. In contrast, the majority of APP is transported to the opposite basolateral surface where also α-secretase activity resides whereas activity of γ-secretase was found on both surfaces. This means that the minor amount of APP reaching the apical surface is an almost exclusive substrate for BACE. On the basolateral surface however, BACE has to compete with the resident predominant α-secretase for cleavage of APP. Since membrane bound C-terminal C99 produced by BACE still contains a known sorting signal which directs C99 to the basolateral surface, γ-secretase converts C99 to Amyloid-β nearly exclusively at the basolateral surface. Because of the opposite targeting of substrate and enzyme, the authors conclude that APP is not a major physiological substrate of BACE in polarized MDCK cells [151].

#### 5.7.2.5.1.6 Lipid Rafts and BACE

A number of in vivo and in vitro studies have shown that β-amyloid production is sensitive to cholesterol levels, and while some of the published results are contradictory, the bulk of them consistently indicate that high cholesterol ester levels correlate with increased amyloid production both in cells and in transgenic animals expressing human APP [26]. Hence the β- and γ-secretase activities may be positively regulated by cholesterol. Cellular cholesterol may act in part by partitioning the proteinases into distinct lipid microenvironments within the plasma membrane. In the membrane, cholesterol enriched microdomains or “rafts” are zones in which proteins involved in signal transduction, protein trafficking, and proteolytic processing accumulate [152]. Rafts can be partially purified because of their relative insolubility in detergent such as Tx-100 or CHAPS at low temperature and their different buoyant density compared with the bulk

of the cellular membrane. Rafts are thus also referred to as Detergent resistant membranes (DRMs) [152, 153].

Interestingly, APP, Aβ, and the γ-secretase have all been found in lipid rafts [154]. A series of studies provide evidence that BACE is also associated with rafts. Riddel and colleagues demonstrated in three different cell lines (CHO, SH-SY5Y and HEK) and using different detergents (Triton X-100, CHAPS, Carbonate and Lubrol WX yielded the best results) that BACE is present in light membrane raft fraction which also contained APP and PS1 [155]. Only the mature form of BACE is associated with rafts, suggesting that, in line with many other raft-associated proteins, BACE localizes to cholesterol-rich microdomains following transit from the ER to the Golgi complex. Furthermore, CTFβ co-fractionated with BACE in rafts. This implies that intracellular β-cleavage may indeed occur in these cholesterol enriched microdomains. In contrast, CTFα consistently floated to a light membrane fraction that was relatively poor in cholesterol. Interestingly, only a minor proportion of APP co-fractionates with BACE in lipid rafts, suggesting that BACE does not have ready access to large amounts of APP within the cell. These observations suggest that the cholesterol-dependent partitioning of β-secretase into lipid rafts may underlie the cholesterol sensitivity of β-amyloid production because it promotes the association of BACE with APP and PS1 to generate a proteolytically active assembly [155].

Based on these findings, Cordy and co-workers [156] chose a more direct approach and targeted BACE virtually exclusively to raft domains of SHSY-5Y cells by replacing the transmembrane and cytosolic domains of BACE with a GPI-anchor attachment sequence. In general, a GPI anchor is attached to certain proteins by the action of a GPI transamidase. This enzyme cleaves the peptide bond at the GPI-anchor attachment site — the ω-site, and simultaneously transfers the carboxyl group of the newly generated C-terminus to the terminal amino group of a preformed GPI anchor. [157, 158]. By attaching a GPI anchor to BACE, Cordy et. al. could indeed show that amyloidogenic processing was substantially increased, presumably because targeting BACE to lipid rafts should cause it to co-localize with the small fraction of APP present in rafts, substantially increasing its amyloidogenic processing. They have also shown that disruption of the rafts by lovastatin treatment caused GPI-BACE to dissociate from rafts and that this treatment inhibited production of sAPPβ. This result demonstrates that expression of GPI-BACE alone is not sufficient to cause increased APP processing, and that the raft localization of the enzyme is critical for the observed increase in sAPPβ and Amyloid-β production. The authors conclude that strategies such as cholesterol reduction might segregate BACE away from its substrate APP, and may therefore be therapeutically viable [156].

To further specify the parameters governing how BACE and APP associate with rafts at the cell surface, Ehehalt et. al. [159] used an established cross-linking assay whereby artificial clustering of distinct membrane patches can be induced on the surface via cross-linking membrane bound proteins with antibodies. They could show that a small fraction of APP and BACE co-patched on the surface of living cells with each other and with PLAP as a GPI-anchored raft-associated protein. Because only a small fraction of APP and BACE are associated with detergent resistant membranes, the authors assumed that these proteins are probably found in two distinct membrane pools, one raft associated and another localized outside of rafts. The authors thus hypothesized that it

is very unlikely that cleavage of APP can take place at the surface and they could show that blocking endocytosis prohibits CTFβ and Amyloid-β production probably due to the prevention of subsequent clustering of APP and BACE into the same raft platform. However, cross-patching of BACE and APP reconstituted Amyloid-β production at the surface under strict inhibition of endocytosis presumably due to artificially induced clustering thereby mimicking the process normally taking place after internalization. The authors also show that cholesterol depletion inhibits Amyloid-β production and conclude that β-secretase activity is critically dependent on an intact raft environment and that BACE outside rafts should not be active [159].

### 5.7.2.6 Tissue Expression and Tissue localization of β-secretase activity

There is a wealth of literature on tissue expression of BACE, altered expression in AD patients and its diagnosis, modifiers of expression and mechanisms of regulation.

#### 5.7.2.6.1 BACE mRNA – distribution

Detection of BACE mRNA levels in mural brains in two studies showed similar hybridization signals in neurons of the cerebral cortex, hippocampal formation, thalamus and cholinergic basal forebrain nuclei, while astrocytes did not display labeling [160, 161]. The local expression pattern of BACE mRNA did not correlate with the distribution of β-amyloid deposits [160] and immunohistochemical destruction of the basal forebrain produced no significant changes in the distribution of BACE mRNA [161]. A comparison of BACE mRNA levels in mouse and human brain demonstrated the co-expression of β-APP with BACE and ADAM10 which is in keeping with the postulated role of ADAM10 and BACE as authentic α- and β-secretases [162].

#### 5.7.2.6.2 Tissue Expression of the BACE protein

As mentioned above, studies in BACE knock out mice showed that in neurons BACE, but not BACE2, is strongly expressed and represents the principal β-secretase because Amyloid-β is abolished in BACE–/– neurons [114]. Interestingly, an alternative Amyloid-β species starting at Glutamate 11 instead of Aspartate 1 in APP was shown to be the major Amyloid-β species in mural neurons dependent on the presence of BACE, thus indicating an alternative β-secretase cleavage (see separate section 5.7.2.8 on subsite specificity below) known from previous cell studies [114]. Another study confirmed the neuronal expression of BACE protein in the brains of mice, with the most robust immuno-cytochemical labeling present in the cerebral cortex, hippocampal formation, thalamus, and cholinergic basal forebrain nuclei. In transgenic Tg2576 mice overexpressing swAPP, amyloid plaque formation was shown to stimulate astrocytic BACE expression. This work thus supports the hypothesis that neurons are the primary source of β-amyloid peptides in brain and that astrocytic β-amyloid generation may contribute to amyloid plaque formation when activated. Whereas BACE was expressed at high levels in brain, lower levels could also be detected by Western blot analysis in heart and liver, at very low levels in pancreas, kidney, and thymus and at almost absent levels in spleen and lung [163]. Immunohistochemical analysis demonstrated that BACE immuno-reactivity in the brain was predominantly neuronal and was found in tangle-bearing neurons in AD [164].

#### 5.7.2.6.3 Altered protein expression of BACE in AD patients

Several studies using different techniques found elevated BACE expression levels and increased BACE activity in AD brains compared to controls. By comparative Western blot analysis, a 2.7-fold increase in protein expression of BACE correlated to a nearly twofold increase in C99 levels in the cortex of AD patients as compared to age-matched controls without significant changes in mRNA levels [165]. Similarly, a study using an antibody capture system showed that BACE activity and protein levels were significantly increased in brains with AD in the frontal and temporal cortex but not in the cerebellum. Immunohistochemical analysis demonstrated that BACE immunoreactivity in the brain was predominantly neuronal and was found in tangle-bearing neurons in AD [164]. The temporal cortex was confirmed to show a large increase of BACE activity as opposed to a decrease in α-secretase activity in of AD patients [166]. Also, the sAPPβ immunostaining, used to localize BACE activity, was reported to be stronger and more extensive in gray matter in Alzheimer disease (AD) cases than controls [167]

In line with these findings, a study that analyzed BACE protein expression and activity in tissue within three hours after rapid autopsy of sporadic AD patients showed that BACE levels were significantly higher by Western Blot analysis and Enzyme-Linked Immunosorbent Assay (ELISA) in the temporal cortex of AD brain than in brain from non-demented controls. Moreover, enzymatic activity of BACE, measured both using fluorescent substrate and by Immunoprecipitation of C99 from tissue, was increased significantly in AD samples compared with controls. There was also a significant correlation between BACE expression levels and plaque numbers in AD brains. The authors conclude that elevated BACE expression resulting in increased activity and Amyloid-β production could be causally involved in sporadic AD, although it could also be reactive to the pathologic process itself [168]. A follow up study found a correlation between BACE enzymatic activity in AD and brain Amyloid-β (1-x) and Amyloid-β (1-42) production. Elevated BACE expression was mirrored in elevated BACE mRNA levels although no mutations in the ORF of the BACE gene explicative of this elevation were found [169]. Furthermore BACE activity as measured by fluorescent substrate increased significantly with age in mouse, monkey, and human brains, independent of brain region [170].

Some analyses found no association between BACE levels and AD histopathology. BACE mRNA amounts were measured to be similar in patients and controls, as opposed to a twofold increase in ADAM10 mRNA levels in AD samples, however without relationship to the severity of anatomical damage [171]. This finding is mirrored by two other works which found no change in BACE mRNA levels neither in AD brains relative to controls [172, 173], nor in peripheral tissue [173]. In terms of BACE activity, aging Tg2576 mice showed unaltered APPsβ levels with aging and no evidence for altered presynaptic cholinergic activity [174].

#### 5.7.2.6.4 Mechanisms regulating BACE expression

The regulation of BACE expression have been studied with respect to the transcriptional as well as on the translational level.

The promoter of the rat BACE gene was cloned and expressed and shows highly conserved regions between rat, mouse and human which contain a number of putative transcription factor binding sites including MZF1, Sp1, four GATA-1 sites, and one YY1 site. Direct mutagenesis and deletion mutants showed that the GATA-1 elements are involved in regulation of BACE expression and identified two regions that might contain activators or suppressor elements [175].
The human BACE promoter was cloned subsequently and confirmed the conservation of transcription factor-binding sites. The promoter region and 5' UTR was shown to contain multiple transcription factor binding sites, in particular a stimulating protein (SP)1 site [176].
Functionality of the identified Sp1 response element was demonstrated by a study which reported an activating effect of SP1 on BACE expression as assessed by overexpression or knockout of SP1 respectively 177.
Some investigators critically discuss results presented above by pointing out that no significant increase in mRNA BACE levels in AD were found despite reports on increased BACE protein levels in AD [165, 171-173]. They thus conclude that BACE protein levels are more likely to be controlled on the translational level.
Lammich and co-workers demonstrated with an extensive deletion approach that the 5'-untranslated region of BACE can decrease the rate of BACE translation whereas it does not affect transcription. This effect of the (5'UTR) does not seem to be exerted by the GC-richness of the upstream open reading frame (uORF) which are thought to down-regulate the efficiency of translation initiation of the main ORF, but rather by its tightly folded secondary structure [178].

### 5.7.2.7 Crystallographic Structure of BACE

The 3-dimensional structure of the BACE ectodomain was resolved by Hong et. al in a crystal with the BACE inhibitor OM-99 [179]. In comparison to the lead structure human pepsin, which displays 22% sequence identity, BACE shows four insertions that increase the molecular diameter significantly. In addition, it is remarkable that the active site cleft is more extended than in other human aspartic proteases and it is partly covered by a “flap” structure that could potentially regulate substrate binding. Hong and colleagues assign special importance to a couple of residues with respect to the substrate affinity. Please note that the numbering of the residues in the structural publications follows the sequence of Renin such that the corresponding BACE numbering can be obtained by adding 61 amino acids (amino acid position in BACE=amino acid position in Renin + 61). The positively charged residue R235 (R296 in BACE sequence) is predicted to build a hydrogen bond to the P2 asparagine of the inhibitor OM-99 with the sequence (EV N KAAEF), which shares the asparagine (N) at P2 with swedish APP (EV NL DAEF) [179, 180]. Therefore R235 might be critical for the binding of the substrate swedish APP.

**Figure 10: 3D- structure of BACE**

Depicted is the Ribbon structure taken from entry "1FKN" (structure resolved by [179]) in the Protein Data Bank http://www.rcsb.org/pdb/index.html. The active site aspartates are shown in black.

Sauder et. al. predicts an additional hydrogen to the Asp+1 residue in APP, which would imply that Swedish APP (NL D) (Figure 5 above) would establish one more hydrogen bond than wt APP (KM D) which could explain the much higher affinity of sweAPP to BACE [180]. Furthermore, the structure by Hong et. al. predicts an unfavorable interaction between the positively charged P2 lysine in wt APP with the equally positive R235 (R296 in BACE sequence) in BACE [179]. Hong et al. improved their structure two years later by using the modified inhibitor OM99-2 (EV N LAAEFF) which ameliorated the definition of the structure at the S(3)' and S(4)' subsites [181].
In addition, there were BACE structures published as bound to another hydroxyethylamine inhibitor which revealed significant active-site movements[182], as well as from glycosylated BACE zymogen (proBACE) derived from Trichoplusia ni (High 5) cells in the absence of a bound inhibitor [183].

## 5.7.2.8 Subsite Specificity of BACE

It has been mentioned above (See section 5.4.2 on proteolytic processing), that BACE can cleave at Aspartate 1 (Asp1), as well as at Glutamate 11 (Glu11). Some studies have analyzed the conditions for those different cleavages and there is also data on the ideal residues at each subsite of the enzyme.

### 5.7.2.8.1 Cleavage at Asp 1 and the "swedish mutation"

Citron et. al [44] investigated the double mutation found in a Swedish family with early onset familial AD, in which the two amino-acids KM before Asp+1 are exchanged by NL (KMD to NLD) (Figure 5 above). A study on the cellular mechanism responsible for the

increased production of Aβ of this mutant found that the β-secretase cleavage at the NLD occurred already in secretory Golgi vesicles where it can compete with the non-amyloidogenic α-secretase cleavage explaining the strong increase in Amyloid-β generation [184] Since this finding, the swedish mutation has been widely used as a tool to increase the sensitivity of measuring β-secretase activity in cell culture and animal models as well as for in vitro kinetic assays.
Kinetic in vitro studies showed that a peptide derived from the β-secretase site of Swedish APP has a kcat/KM value about 60-fold higher than that from native APP [185] and that the greatest impact comes form the change K to N at the P2 site [186].

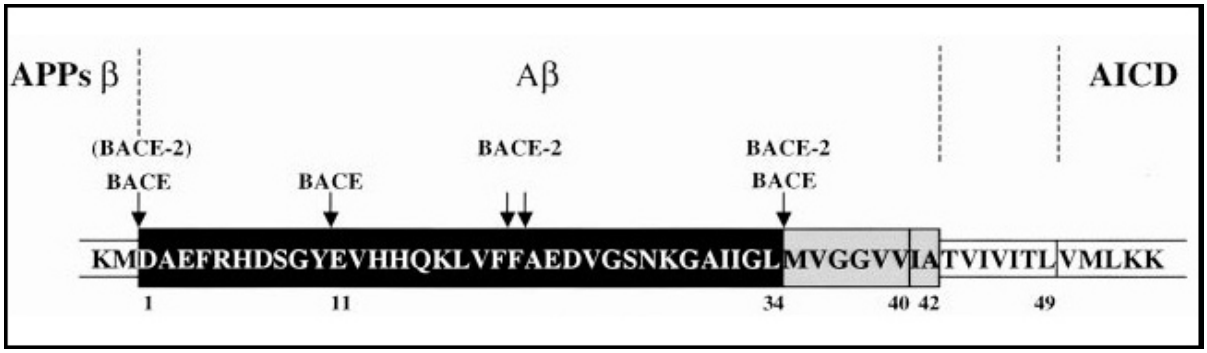


**Figure 11: Cleavage sites of BACE in APP**

The Aβ domain is depicted schematically in this figure. The known BACE and BACE-2 cleavage sites are indicated by arrows. The BACE cleavages at Asp+1, Glu+11 and position 34 respectively will be explained below. The Aβ sequence is the „sum" of the black and light gray colored residues. As described above, it results from cleavage at Asp+1 by β-secretase and at residues 40 or 42 respectively by γ-secretase. The remaining N-terminal fragment (APPsβ) as well as the C-terminal fragment (AICD) are also labeled – Source: [187].

### 5.7.2.8.2 Alternative cleavage at Glu11 by BACE

In addition to the majority of Amyloid-β from HEK cells starting at Asp +1, there were also minor amounts of peptides found starting at Val +3 and Glu +11 [18]. In contrast, the predominant species in rat primary neurons seems to be Amyloid-β beginning at +Glu11 [188]. Vassar and co-workers confirmed that overexpression of BACE in 293 cells exclusively increases cleavage at position Asp +1 and Glu +11 and that BACE inhibition with antisense oligonucleotides could greatly reduce all Amyloid-β species (Amyloid-β x-40 as well as Amyloid-β x-42) to about 60-70% of those in controls [54]. In another study, BACE overexpression similarly increased the secretion of Amyloid-β(1-40/42) and Amyloid-β (11-40/42) in both NT2- cells and NT2N neurons as well as increased intracellular Amyloid-β(1-40/42) and Amyloid-β(11-40/42) confirming that Amyloid-β(11-40/42) is generated prior to deposition in senile plaques [189]. Cai and colleagues furthermore showed in mural neuronal cultures that besides BACE-dependent Amyloid-β 1-40 production there is considerable Amyloid-β 11-40 production which is completely abolished in BACE -/- neurons. Moreover, a structural analysis showed that a mutual structural compatibility in addition to the sequence feature influences which cleavage occurs. The cleavage of APP at the β-site by BACE is readily disrupted through limited structural twists, whereas the +Glu11 site is relatively better positioned to gain access to the BACE catalytic cavity. Insertion or deletion of residues between the +Asp1 and

+Glu11 site also favors cleavage of APP at latter site. On the other hand, but significantly shortening the loop region impairs the ability of BACE to process APP unselectively at both sites [190].

#### 5.7.2.8.3 Sequence of alternative cleavages of BACE

Since data strongly supported that BACE was responsible for both cleavages, at Asp+1 and Glu+11 respectively, it was interesting to investigate which factors determine which cleavage occurs and in which sequence. It was found that Glu+11 cleavage is a function of the expression level of BACE, that it depends on the membrane anchorage of BACE [131], and that Asp+1 cleavage can be followed by Glu+11 cleavage which might be an explanation of the dependence on the quantity of BACE expression [131, 191]. Two studies found that the localization of BACE within the cell determines, which cleavage occurs. Pharmacological treatment with BFA and Monensin [64] as well as artificial targeting of BACE plus pharmacological treatment to either the ER or, the Golgi [139] showed, that cleavage at Asp+1 predominates in the ER, whereas the cut at Glu+11 occurs subsequently in the TGN. Huse et. al. furthermore demonstrated that the difference in pH between the ER (neutral) and the TGN (mildly acidic) or the different degree of maturation of BACE and APP in terms of complex glycosylation (takes place in the TGN) alone are not sufficient to explain the differential cleavage in the two compartments. Since Glu+11 cleavage did not significantly occur in the ER even upon trapping of BACE and APP in this compartment, the authors conclude, that rather than absolute amounts of BACE leading to a subsequent BACE cleavage of pre-processed C99 (Asp+1) to yield C98 (Asp+11) as proposed by Creemers [131], the accumulation of overexpressed BACE in the TGN might favor Glu+11 cleavage, although the exact environmental factors could not be identified. The authors propose that the presence of the prodomain could be an interesting parameter, as well putative interaction partners that might constitute a multi-component catalytic complex around BACE [139].

By using immunoprecipitation and Mass Spectroscopy, another study revealed that the major isoform of Amyloid-β from N2a cells and BACE overexpressing HEK cells were Amyloid-β1-40 and Amyloid-β11-40 but also Amyloid-β11-34 and Amyloid-β1-34 which were detected earlier in primary rat embryonic neuronal cultures [188] and in brains of transgenic mice overexpressing both mutant APP and mutant Presenilin 1 [192]. Interestingly the investigators found that overexpression of BACE, besides an increase in Glu+11 cleavage also results in an increase in Amyloid-β(x)-34, but not Amyloid-β(x)-40, and that this cleavage at position Leu 34 could be inhibited by the γ-secretase inhibitor DAPT. The authors thus concluded that the +34 cleavage could be mediated by γ-secretase itself or by a γ-secretase dependent process and that the suppression by DAPT could be explained by that fact that cleavage at 34 depends on prior cleavage of Amyloid-β at position 40/42 by γ-secretase [193].

It could be shown in subsequent studies, that the +34 cleavage is indeed dependent on prior cleavage by γ-secretase and that this postulated γ-secretase dependent process is in fact β-secretase activity. Fluhrer et al. reproduced the +34 cleavage in vitro using purified Amyloid-β 1-40, which was inhibited by a specific BACE inhibitor, and also in vivo by incubation of conditioned media containing Amyloid-β-(1–40) and Amyloid-β-(1–42) with BACE expressing cells in which PS1 activity and thus de novo synthesis of

Amyloid-β were excluded by expression of a loss-of-function PS1 variant, controlled against cells expressing the inactive PS1 variant alone. Thus, BACE was identified as the protease responsible for the +34 cleavage. It could theoretically truncate Amyloid-β near or at the cell surface or after endocytosis of Amyloid-β, although the physiological relevance remains unclear [194]. This cleavage of BACE at position +34 of Aβ was confirmed in another study which similarly showed, that in vitro the substrate Amyloid-β 1-40 is cleaved by BACE and BACE2 at +34 and that in vivo this cleavage was suppressed by specific inhibitors against Presenilin which left BACE activity unaffected [195].

#### 5.7.2.8.4 The ideal substrate sequence of BACE

In a kinetic study using a randomly generated library of synthetic peptide and mass spectrometry for initial rate determination, Turner et al. have investigated the subsite specificity of BACE for each individual subsite. Whereas in the native wtAPP the sequence is EVKM-DAEF [following the subsite nomenclature Schechter and Berger [196]]: and EVNL-DAEF (Figure 12) in the sweAPP respectively they identified an "optimal" consensus peptide defined as EIDL-MVMD which was cleaved with a $K_{cat}$ / $K_M$ value 14-fold better than the analogous APPsw derived peptide. Interestingly, the increased ratio is due to improvement in the $K_M$ , („OK" 1,4 +/- 0,2 µM vs. "swe" 35,8 +/- 2 µM) whereas $K_{cat}$ changed much less. These data also suggest that there might be much better physiological BACE-substrate than APP [186]. In comparison, another study found that replacing the P3-P2' sequence in wt APP VKM-DA by ISY-EV yielded a substrate that was cleaved by BACE seven times faster than the corresponding swedish APPS peptide, SEVNL—DAEFR and was also superior to swAPP in cellular assays [197].
Again, this shows that even swAPP is far from being an optimal substrate for BACE.
Further kinetic studies revealed the substrate residues P(5)-P(7) as important binding positions for the enzyme. The addition of these substrate residues contributes to the decrease in $K_M$ and increase in $K_{cat}$ values, suggesting that these residues contribute to both substrate recognition and transition-state binding [198].
A comparison of BACE to other aspartic proteases such as cathepsin D and E, napsin A, pepsin, and renin showed little similarity with respect to the substrate preference and inhibitor profile [137]. In contrast, the homolog BACE2 however showed very similar parameters as BACE. As in the study by Turner et al., the authors found that BACE displays poor kinetic constants toward its known substrates (wild-type substrate, SEVKM/DAEFR, K(v) = 7 µM, $K_{cat}$ = 0.002 s(-1). Swedish mutant, SEVNL/DAEFR, $K_M$ = 9 µM, $K_{cat}$ = 0.02 s(-1)) and that a much better substrate could be generated (VVEVDA/AVTP, $K_M$ = 1 µM, K(µM) = 0.004). Based on a collection of decameric substrates, the authors furthermore showed that BACE has a loose substrate specificity and that the substrate recognition site in BACE extends over several amino acids. BACE prefers a leucine residue at position P1. BACE accepts polar or acidic residues at positions P2' and P1 but prefers bulky hydrophobic residues at position P3 [137].

### 5.7.2.9 Known substrates for BACE

As presented above, there has been a long-term doubt that APP is the only physiological substrate for BACE, given its poor kinetic constants towards BACE. Indeed, so far, three other substrates for BACE have been identified.

The Golgi-resident sialyltransferase, ST6Gal I was shown to be a substrate for BACE by the following experiments. BACE co-localized with ST6Gal I, overexpression of BACE resulted in the increased secretion of ST6Gal I, whereas overexpressed swAPP competed with ST6Gal I processing and BACE cleaved a protein A-ST6Gal I fusion protein in vitro [199].

The authors emphasize that surprisingly ST6Gal I is a type II membrane protein, although it was predicted that a possible substrate of BACE, would be a type I membrane protein like APP, given that BACE itself is a type I membrane protein. The authors hypothesize that the stem region of ST6Gal I may be flexible enough to be accessed by catalytic site of BACE and that similarly other type II glycosyltransferases might be additional substrates for BACE [200]. In terms of the physiological function of this enzyme-substrate-interaction the authors remark that the interaction of a sialylα2,6galactose residue, which is synthesized solely by ST6Gal I, with a B cell-specific lectin, CD22/Siglec-2, is important for B cell function. They refer to the finding from Luo et al. [115] that mice deficient in BACE appeared to exhibit abnormal levels of serum globulin and suggest that BACE deficiency may cause an abnormality in B cells through aberrant ST6Gal I processing [199].

In a screen for putative BACE substrates known to also undergo processing by metalloproteases, P-selectin glycoprotein ligand 1 (PSGL-1) was identified [201]. PSGL-1 is a type I membrane protein which is expressed as a homodimer and is known to mediate leukocyte adhesion to endothelial cells in inflammatory reactions in brain and peripheral organs. PSGL-1 was demonstrated to be cleaved in human monocytic U937 cells as well as in HEK cells by endogenous or transfected BACE, to yield a soluble ectodomain and a C-terminal transmembrane fragment. This processed fragment was absent in BACE deficient mice but could be produced in an in vitro assay by BACE. By the use of deletion constructs, the cleavage site could be mapped to the juxtamembrane region within the ectodomain and was more specifically located by mass spectrometry between a Leu-Ser peptide bond within the motif NL-S which is very similar to the swAPP site NL-D (Figure 12). Since PSGL-1 is constitutively expressed on most leukocytes and mediates adhesion to the endothelium, the authors propose that BACE could modify the binding of the N-terminal ectodomain of PSGL-1 to its receptor and thus influence inflammatory processes. The authors thus furthermore suggest that BACE null mice might not have an overt phenotype but could display some aberrant immune responses if immunologically challenged [201].

Interestingly, this additional substrate again is involved in immune responses like ST6Gal I thus suggesting the intriguing hypothesis, that BACE could be somehow involved in the regulating of immune response.

Furthermore, APLP1, and APLP2 which are closely related and exhibit the same domain structure as APP, were shown to be a substrate for BACE [202]. APP, APLP1, and APLP2 are functionally redundant as shown by Knock-out mice revealed that and similar to APP,

APLPs appear to be cleaved by extracellular proteases followed by proteolytic processing by γ-secretase [202].

The authors demonstrated that co-transfection of BACE 1 with APLP1 or -2 results in the production of a APLP- CTF as well as specific increase in the secretion of soluble APLPs fragments. Since AICD, the γ-secretase generated intracellular domain, of APP (section 5.7.1.1 on Presenilin and signal transduction) was shown to control transcription by translocation to the nucleus in a Fe65 dependent manner, the authors tested whether APLP1 can substitute for APP in an assay for the transcriptional function involving Gal4 dependent transactivation of a nuclear target Tip60. Indeed, increasing amounts of BACE 1 enhance transactivation of Gal4-Tip60 mediated by APLP1 suggesting that consistent with a common transcriptional function for APP and APLPs. The BACE 1 cleavage site was located to a position next to the TM of APLPs but the cleavage sequences are not conserved in APLP1 or -2, and no similar sequence motif can be readily identified in APLP1 or -2 [202].

In another study, APLP2 proteolytic products were decreased in BACE KO mice. Reduced levels of secreted extracellular soluble APLP2 were paralleled by the lack of formation of the APLP2 C-terminal fragment. Opposite effects were seen in BACE transgenic mice. Overexpression of BACE in cultured cells also caused increased APLP2 processing [118].

| **Substrate** | **Sequence** | | | | | | | | | | | | | |
|---|---|---|---|---|---|---|---|---|---|---|---|---|---|---|
| **Subsite Nom.** | | | | | | **P3** | **P2** | **P1** | | **P1`** | **P2`** | **P3`** | | |
| wtAPP (+Asp1) | E | E | I | S | E | V | K | M | * | **D** | A | E | F | R |
| SweAPP(+Asp1) | E | E | I | S | E | V | N | L | * | **D** | A | E | F | R |
| wtAPP (+Glu11) | | | R | H | D | S | G | Y | * | **E** | V | H | H | Q |
| Amyloid-β+34 [194] | N | K | G | A | I | I | G | L | * | M | V | G | G | V |
| ST6Gal1 | S | D | Y | E | A | L | T | L | * | Q | A | K | E | F |
| PSGL1 | I | P | M | A | A | S | N | L | * | S | V | N | Y | P |
| APLP1 | E | Q | Y | E | R | K | V | N | * | A | S | V | P | R |
| APLP2 | E | T | L | D | V | K | E | M | * | I | F | N | A | E |
| Endoproteolysis [203] | P | L | N | Q | S | E | V | L | * | A | S | V | G | G |
| "Ideal substrate" OK [186] | | | | | E | I | D | L | * | M | V | M | D | |
| Optimized substrate [197] | | | | | S | I | S | Y | * | **E** | V | E | F | R |

**Figure 12: Comparison of the cleavage sites of the known substrates for BACE**

The BACE Cleavage site is indicated by an asterisk *. Please note that negatively charged residues at P1` are written in bold letters. Subsite Nomenclature is indicated according to [196]

#### 5.7.2.10 Enzyme Kinetics of BACE

Since it is much easier to obtain and purify the ectodomain of BACE than the intramembranous full length BACE, most of the kinetic studies were done with the BACE ectodomain. However there are two studies who also report on a comparison of the kinetic properties between the BACE ectodomain and full length BACE. Moreover, the published kinetic parameters for BACE-NT (a BACE ectodomain lacking the transmembrane domain and the C-terminus) vary to a large extent because of different substrates and methods used. Most studies used "swedish-like" substrates, although two studies published kinetic parameters for substrates with optimized sequences (Figure 13). In terms of methods, fluorogenic substrates as well as matrix-assisted laser desorption ionization time-of-flight (MALDI-TOF) and HPLC were applied to determine substrate cleavage. Interestingly, as Gruninger-Leitch point out, BACE displays structural similarities with other aspartic proteases like Renin but its catalytic efficiency is 250 fold lower than that of for instance cathepsin D (Gruninger-Leitch, Schlatter et al. 2002).

##### 5.7.2.10.1 Comparison of BACE ectodomain and full length BACE

There has been one study so far which published kinetic parameters for full length BACE (BACE-FL). Kopcho et. al compared the kinetics of BACE-FL enriched in unpurified membrane preparations of Chinese hamster ovary cells with purified versions of BACE NT and detected no significant kinetic differences using a Swedish APPlike substrate. It was furthermore mentioned in another study that identical catalytic activity for the purified ectodomain of BACE and a full-length version of the enzyme was observed. However, the authors did not publish the kinetic parameters of their BACE-FL preparations [137].

##### 5.7.2.10.2 Kinetic parameters of the pro-domain

As presented in the section 5.7.2.4.1 "Role of the prodomain", The $K_{cat}$ / $K_M$ of propeptide-containing BACE was measured only 2.3-fold less than that of mature BACE. An inhibitor also had similar inhibitory potency for both BACE species suggesting that the Pro domain has little effect on the BACE active site.

### 5.7.3 Interaction partners of BACE

As BACE is the rate limiting step of Amyloid-β production, interactions of BACE as with other possibly regulating proteins are of great interest.

Among the AD related proteins, it was proposed that Nicastrin co-immunoprecipitates with BACE and also increases β-secretase activity in COS-7 cells, as measured by amount of soluble APP produced [204]. Also, a direct binding between BACE and PS1 was suggested as shown by co-localization studies in human cultured cells as well as coimmunoprecipitation that preferentially detected immature BACE, leading to the author's hypothesis, that Presenilin might potentially act as a regulator of BACE maturation [205]. In addition, a study presented data that the ectodomain of BACE, when exogenously added to cells expressing APP, can interact with the ectodomain of APP on the cell surface leading to its internalization. This interaction does not seem to be dependent on substrate binding to the active site of BACE, since neither antibodies direct

against the active site nor competitive inhibitors could decrease internalization. Also, co-immunoprecipitation of full length BACE and APP from lysates was shown [206].

The C-terminus of BACE possibly interacts with proteins of the cellular trafficking machinery like the GGA proteins [147, 148], which may regulate the phosphorylation dependent endocytosis of BACE [144] as presented above in the section on BACE trafficking. In addition, binding of the cytoplasmic region of BACE, likely the Di-leucine motif, to the C-terminus of phospholipid scramblase 1 (PLSCR1), a type II integral membrane protein, was shown by Co-immunoprecipitation and Co-localization with buoyant lipid microdomains in SH-SY5Y cells [207]. The authors propose that by this mechanism BACE could be recruited into detergent-insoluble lipid rafts.

A yeast two-hybrid system furthermore identified the brain-specific type II membrane protein BRI3 as an interaction partner with the C-terminal cytosolic tail of BACE, which interestingly is also converted by Furin as is BACE [208].

| Reference | Substrate Sequence | Enzyme type | Method | $K_M$ (µM) | $K_{cat}$ (min-1) | $K_{cat}$ / $K_M$ (µM-1 * min-1) |
|---|---|---|---|---|---|---|
| | **“Swedish-like” substrates** | | | | | |
| 209 | Substrate„FS-2“: (MCA)SEVNL*DAEFK(DNP) | BACE-NT | Fluorogenic | 4,5 | 0,25 | 0,056 |
| 186 | Substrate „SW“: EVNL*DAEFWHDR | BACE-NT | MALDI-TOF | 35,8 | 54,7 | 1,528 |
| | | | | | | |
| 137 | SEVNL*DAEFR | BACE-NT | Fluorogenic | 9 | 1,2 | 0,133 |
| | | BACE-FL | | not speci-fied | not speci-fied | |
| 210 | AcEVNL*DAEFK(DNP) | BACE-NT from S2 insect cells | FRET-methoxycumarin group | n.d. | n.d. | 0,004 |
| “” | | BACE-NT from CHO cells | | n.d. | n.d. | 0,005 |
| “” | | BACE-FL from HEK cells | | n.d. | n.d. | 0,003 |
| 185 | SEVNL*DAEFR | | HPLC | 1000 | 2,45 | 147 |
| 211 | AcEVNL*DAEFK(DNP) | | Reverse Phase Column | n.d. | n.d. | 0,008 |
| 212 | TEEISEVNLDAEFRHDSGK | truncated PreProBACE (amino acids 1–460) insect cells | reverse-phase HPLC | | | 186600 |
| “” | | PreProBACE treated with Furin to generate mature BACE | | | | 438000 |
| | **Substrate with „optimized“ sequences** | | | | | |
| 213 | Substrate “OK“: EIDL*MVLDWHDR | | HPLC | 5,2 | 19,2 | 3,692 |
| 186 | Substrate “OK“: EIDL*MVLDWHDR | | MALDI-TOF | 1,4 | 28,6 | 20,429 |

**Figure 13: Overview of kinetic parameters of BACE from the literature**

The entries of the table are categorized into “swedish-like substrates” and “optimized sequences”. The BACE cleavage site is indicated by an asterisk *.

# 6 Goals of the current work

BACE cleavage is the rate limiting step in generating Amyloid-β. Since the identification of BACE, important knowledge, of its tissue expression and regulation, its maturation and trafficking, its substrate profile and putative interaction partners has been generated. However, attempts to inhibit this enzyme based on information from crystal structures of the soluble BACE ectodomain encounter the difficulty that BACE seems to have an unusually wide cleft of its active center. It is thus of paramount interest to study the conformation and the enzymatic characteristics of BACE in its native configuration. The present work thus aimed at clarifying whether native BACE functions in a complex or in cooperation with other proteins and whether this might influence its physiological function. This knowledge could have important impact on our understanding of the physiologic function of BACE with respect to its interaction with substrates and the regulation of its enzymatic activity. In addition these insights might open alternative pathways for therapeutic intervention.

For this purpose the following specific aims were formulated:

1) Development of an appropriate method to study the native conformation of BACE
    a. In particular it was intended to adapt Blue-Native Polyacrylamide Electrophoresis (BN-PAGE), which was successfully used for the study the γ-secretase complex [93, 214], for the study of native BACE. To this end, a method for native preparation of protein complexes for BACE derived from neuronal tissues and cultured cells had to be optimized. Moreover, the BN-PAGE separation technique should be improved for BACE and a detection of native BACE by Western Blot with an appropriate sensitivity for endogenous levels should be achieved.
    b. The native size of BACE should consequently be identified in native samples from different tissues and cell lines in comparison to the size of BACE under denaturating conditions on SDS-PAGE.

2) Characterization of the quaternary structure of BACE
    a. The putative oligomeric structure of native BACE should be analyzed by appropriate methods such as co-immunoprecipitation studies.
    b. The posttranslational modification of native BACE within the putative complex should be identified.

3) Differences in quaternary structure with respect to subcellular localization
    a. Subcellular sites of assembly of the putative BACE complex should be identified with appropriate constructs containing retention motifs which control the subcellular localization of the corresponding proteins.

4) Identification of domains within BACE involved in the putative binding interface
    a. A domain deletion analysis should be performed by generating appropriate constructs with intact enzymatic function. The native size of the constructs should subsequently be analyzed by BN-PAGE.

5) Investigation of the potential physiological role of a putative BACE complex
    a. A putative influence of the native quaternary conformation on stability, trafficking and subcellular localization should be investigated in comparison to the properties of BACE under denaturating conditions.
    b. With respect to the fact that BACE is the rate-limiting enzyme for the generation of Aβ, it was furthermore an intended goal of this study to characterize the enzymatic properties of the putative native BACE complex in vivo and in vitro.

# 7 Material and Methods

## 7.1 Cloning

### 7.1.1 Existing constructs used

- full length BACE (BACE-FL) in pcDNA 3.1/Zeo (+) (Invitrogen) obtained from Michael Willem (Haass laboratory) , described in [127].
- full length BACE, HA-tagged, in peak 12 obtained from Stefan Lichtenthaler (Haass laboratory), subsequently subcloned into pcDNA3.1/Hygro(-) vector (Invitrogen)
- BACE ectodomain (BACE-NT) in pcDNA4/myc-His A/Zeo (Invitrogen) obtained from Michael Willem (Haass laboratory) , described in [127].
- BACE lacking the C-terminus (BACE-ΔC) in pcDNA4/myc-His A/Zeo (Invitrogen) obtained from Michael Willem (Haass laboratory) , described in [127].

### 7.1.2 Cloning Vectors

- pcDNA 3.1/Zeo (+) (Invitrogen)
- pcDNA 3.1/Hygro (-) (Invitrogen)
- pcDNA4/myc-His A/Zeo (Invitrogen)

#### 7.1.2.1 Maps of the Vectors

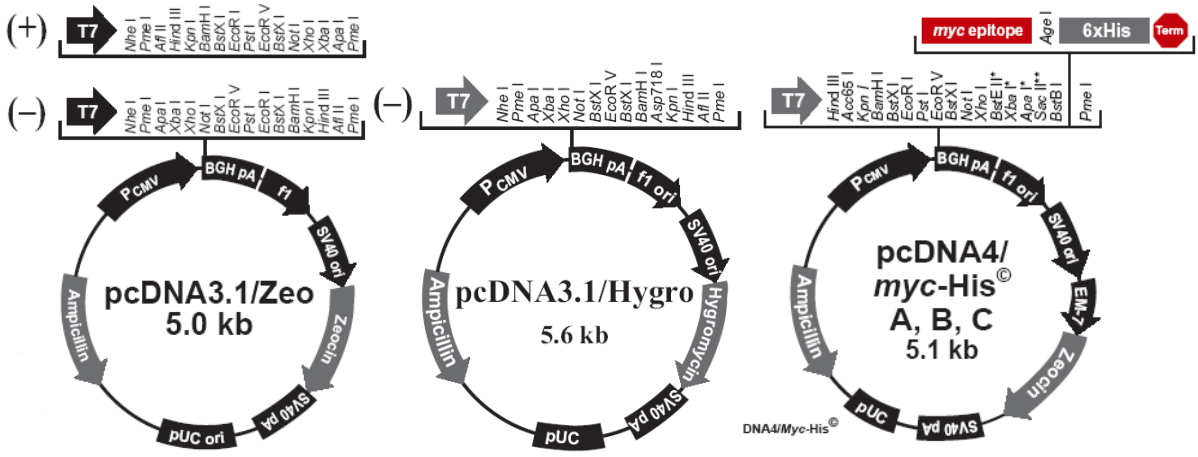


### 7.1.3 Summary of Cloning of BACE expression constructs

Full length BACE (BACE-FL) was tagged at its C-terminus with a myc-His-tag in pcDNA4/Zeo(+) vector (Invitrogen) or was fused to the Hemagglutinin-tag (HA) in the pcDNA3.1/Hygro(-) vector (Invitrogen) using the GC-Rich-PCR kit (Roche). For the purification of soluble BACE, a myc-His-tag was fused to the soluble ectodomain of BACE truncated at amino acid 454 and cloned into the pcDNA4myc/His/A vector [127]. The BACE-poly-alanine (BACE-pA) construct had the wild-type transmembrane domain (amino acids 455-477) replaced by a stretch of 23 alanine residues. To establish a GPI-linked BACE-NT (BACE-GPI), the BACE-NT sequence was fused to the GPI anchor of CD59 (amino acids ASLENGGTSLSEKTVLLLVTPFLAAAWSLHP). To retain BACE within the KKXX (BACE-KKXX) recognition signal was attached by replacement of the original C-term ISLLK with AKKAA [215]. All cDNAs were verified for the correct sequence by automated sequencing at GATC-Biotech AG (Konstanz)

## 7.1.4 Generation of myc-tagged BACE variants

To obtain myc/his tagged BACE-FL and BACE-NT, the both were subcloned via EcoRI and XhoI into the pcDNA4/myc-His A/Zeo (Invitrogen) thereby fusing the myc or his epitope to the C-terminus.

### 7.1.4.1 Primers used for cloning

#### 7.1.4.1.1 BACE-pA:

The BACE-pA construct contains a poly-alanine residue stretch in replacement of the TM domain. Furthermore, the construct was designed such that it enables one to easily cut out the base pairs coding for the TM domain to ligate oligonucleotides directly into the construct. This can be done by subcloning BACE into the Stratagene pKS+ bluescript vector via Eco RI and XHOI to eliminate a NotI present in pcDNA3.1 Zeo + and subsequently cutting out the base pairs coding for the TM by SacII and SPH1. One Alanine flanking the TM domain on either side will remain in the corresponding protein.

Forward Primer:
5'd[ATTT GCG GCC GCA GCA GCA GCA GCA GCA GCA GCA GCA GCA GCA TGC CAG TGG CGC TGC CTC]3'

Reverse Primer:
5'd[ATTTG CGGC CGC AGC AGC AGC AGC AGC AGC AGC AGC CGC GGT TGA CTC ATC TGT CTG TGG]3'

#### 7.1.4.1.2 BACE-GPI

BACE was cloned into a peak12/ HA (EdgeBiosystems) expression vector containing RFP –CD59 (obtained form Stefan Lichtenthaler – Haass laboratory) via a HindIII and a NheI-site. The GPI sequence from CD59 starts just behind the NheI site. As an upstream primer T7 could be used with pcDNA3.1 as a template, such that the HindIII site was conserved. The reverse primer introduced a NheI site.

Forward Primer: T7
5'd[TAATACGACTCACTATAGGG]3'

Reverse Primer:
5'd[CTA GCTAG CGAGGGTTGACTCATCTGTCTG]3'

#### 7.1.4.1.3 BACE-KKXX

The C-terminal Dileucine motif ISLLK was replaced with AKKAA.

Forward Primer : T7
5'd[TAATACGACTCACTATAGGG]3'

Reverse Primer:
5'd[GAT GAC ATC GCA AAA AAA GCT GCA TGA CTC GAG GATC]3'

## 7.1.5 PCR

All used primers were purchased from Invitrogen.
GC-Rich-PCR kit (Roche) was used for PCR in combination with dNTP Mix (Invitrogen) and Pwo DNA Polymerase (Roche). The PCR machine used was a Master Cycler Gradient (Eppendorf).

### 7.1.5.1 PCR reaction solution

3 µl template (~10-20 ng/µl)
1 µl forward primer (~10 ng/µl)
1 µl reverse primer (~10 ng/µl)
1 µl dNTPs (10 mM)
1 µl Pwo DNA Polymerase (~1U/µl)
1 µl GC rich enzyme (~1U/µl) (GC-Rich-PCR kit)
20 µl GC resolution buffer (GC-Rich-PCR kit)
20 µl GC reaction buffer (GC-Rich-PCR kit)
ad 100 µl with distilled water

### 7.1.5.2 PCR Program

95 °C, 4 min
30 cycles:
95 °C, 30 sec
65 °C, 30 sec than decreased by 1° C in every cycle until 52° C was reached (“touch down”)
72 °C, 2 min
72 °C, 20 min

## 7.1.6 Gel electrophoresis

The electrophoretic separation of DNA molecules was performed according to standard protocols (see [216], Chapter 6).
1% agarose gels (Agarose obtained from Gibco) was used in TAE buffer (0,04 M Tris-Acetate, 0,001 M EDTA). DNA was visualized by Ethidium Bromide (Sigma). 1µg of a 1Kb DNA ladder (Gibco) was used as molecular weight marker. The 6x loading buffer contained 15% Ficoll (Sigma) and 0.25% Bromophenol Blue (Sigma) and Xylene Cyanol (Merck) respectively. The desired bands were cut out with a scalpel and extraction of DNA was subsequently achieved with the Nucleo Spin Extract Kit (Macherey-Nagel) according to the manufacturer´s instructions.

## 7.1.7 Restriction Digest and Ligation of DNA

For Restriction Digests, restriction enzymes were used in the appropriate buffers according to the manufacturer´s protocol.

- EcoRI (Fermentas)
- XhoI (Fermentas)
- NotI (Fermentas)
- SPH1 (Fermentas)

Prior to restriction, DNA concentrations were measured with a photometer (SmartSpec 3000 von Biorad) to equilibrate DNA-concentrations.
In case a vector had to be linearized, dephosphorylation was performed subsequent to restriction to avoid re-ligation by using shrimp alkaline phosphatase (Roche) according to the standard protocol.
Restricted DNA was separated on agarose gels. DNA concentrations of inserts and linearized vector were estimated from signals derived from Ethidium Bromide, cut out of the gel and eluted.
For Ligation, vector and insert were used in a 5:1 ratio and ligation was performed with the Rapid DNA Ligation Kit (Roche) following the respective standard protocol.

## 7.1.8 Transformation of E. Coli preparation of plasmids

Transformation of the competent E. coli strain DH5α was done following the standard procedure ([216], chapter 1) applying a heat shock for 90 seconds. Clones containing the respective selection marker

were resistant to 100 µg/ml Ampicillin (Sigma) and could be selected from respective plates to be amplified in o/n cultures containing fluid selection media.
DNA purification at small scale ("miniprep") was done from 5 ml of E.coli o/n cultures according to the instructions of the NucleoSpin Plasmid Kit (Macherey-Nagel). DNA purification at a larger scale ("maxiprep") were done from 200 ml o/n culture following the instructions from QIAfilter Plasmid Maxi Kit (Qiagen).

### 7.1.9 Screening of positive clones and sequencing of the constructs

An analytical restriction digest was performed from minipreps. Maxipreps were obtained from constructs which yielded appropriate fragments in the restriction digest. In parallel, constructs were sequenced over the full range at GATC-Biotech AG (Konstanz) for verification.

## 7.2 Cell lines and cell culture

### 7.2.1 Existing Cell lines

| | |
|---|---|
| H4 cells | human glioma cell-line |
| 293 cells | Hyman Embryonic Kidney (HEK) cells |
| Swe cells | Swe cells: HEK (human embryonic kidney) 293 cells, stably expressing APP Swe (K595N/M596L double mutation in APP first discovered in a swedish familiy suffering from FAD) resulting in enhanced Amyloid-β production [18]<br>- cultivated in basic media containing G418 |

### 7.2.2 Newly Generated cell lines

| | |
|---|---|
| Swe BACE-FL | Swe cell-line stably expressing BACE-FL |
| Swe BACE-NT | Swe cell-line stably expressing BACE-NT |
| Swe BACE-ΔC | Swe cell-line stably expressing BACE-ΔC |
| Swe BACE-pA | Swe cell-line stably expressing BACE-pA |
| Swe BACE-GPI | Swe cell-line stably expressing BACE-GPI |
| Swe BACE-KKXX | Swe cell-line stably expressing BACE-KKXX |
| Swe BACE-FL-myc | Swe cell-line stably expressing BACE-FL-myc |
| Swe BACE-NT-myc | Swe cell-line stably expressing BACE-NT-myc |
| Swe BACE-FL-HA | Swe cell-line stably expressing BACE-FL-HA |

#### 7.2.2.1 Standard medium

Human embryonic kidney 293 cells (HEK 293) were maintained in Dulbecco's modified Eagle's medium High Glucose (PAA) (Gibco/Invitrogen) supplemented with 2 mM L-Glutamine (Invitrogen), 10% fetal bovine serum 50 U/ml penicillin (Invitrogen) und 50 µg/ml streptomycin (Invitrogen).

#### 7.2.2.2 Media for Selection

Cell lines expressing constructs with the pcDNA3/Zeo or the pcDNA4/Zeo vector respectively were selected with 400 µg/ml Zeocin (Invitrogen) Cells transfected with the pcDNA3.1/Hygro vector were selected with 100 µg/ml Hygromycin (Invitrogen). Expression of swe APP was maintained by addition of 200 µg/ml G418. H4 glioblastoma cells were used without transfection.

### 7.2.3 Transient and stable transfection of cells

All stable transfections of HEK 293 cells were performed with lipofectamine reagent (Invitrogen) as described by the manufacturer.
Cells were transfected at ~40% confluency. In case of pre-experiments, transient transfection was performed and cells were analyzed within 48 hours. For selection of stably expressing clones, cells were split to generate different dilutions and plated into selection media. Subsequently, stable clones were scraped using a tip of a pipette and transfered into 24 well plates.

### 7.2.4 Splitting and Freezing

The culturing of the cells (Splitting and Freezing) was performed according to standard protocols ([217]). Trypsine was obtained from PAA and the medium for freezing was composed of FCS (PAA) with 10% DMSO (Roth) added.

### 7.2.5 Mouse lines and tissue preparation

The construct used to generate the transgenic BACE overexpressing mouse line contains a human BACE cDNA insertion in the Thy-1 cassette at the XhoI site of the pTSCα plasmid [218]. Transgenic mice were generated by pro nuclear injection of DBA/ C57Bl6 embryos (N. Smyth, University of Cologne). Brain from BACE-deficient (obtained from Paul Saftig, Kiel) and control littermates were used for endogenous BACE-1 expression analysis. Mice were sacrificed at an age of 5 days (P5) or 3 months and tissue was snap frozen in liquid nitrogen. Genotyping was performed by Michael Willem [124]. All animal manipulations were performed in full accordance with current German laws.

## 7.3 Immunocytochemistry and fluorescence microscopy

### 7.3.1 Antibodies

All antibodies used were diluted in I-Block (Tropix).

#### 7.3.1.1 Primary antibodies

- N-terminal antibody to amino acids 46–60 of BACE (EE-17, Sigma), 1:500
- C-terminal antibody to amino acids 482–501 (LK-16, Sigma), 1:500

#### 7.3.1.2 Cell markers

- Mouse Anti-Rat Giantin Monoclonal Antibody, 1: 500
- Anti-BiP (GRP78) Monoclonal Antibody, 1:40

#### 7.3.1.3 Secondary antibodies

Alexa 555 or Alexa 586 labeled secondary antibodies were used (Molecular Probes, Netherlands).

### 7.3.2 Preparation of Cells for Immunofluorescence

Cells subjected to immunofluorescence were grown on polylysine-coated cover glasses. Cover glasses were treated with 100 µg/µl polylysine solution (Poly-L-Lysin von Sigma) for 30 minutes and subsequently washed x3 with PBS.

The following solutions were used :

- PBS (ph 7.4): 140 mM NaCl, 10 mM Na2HPO4, 1,75 mM KH2PO4
- PBS (Ca, Mg): 1 mM CaCl2, 0,5 mM MgCl in PBS (pH 7.4)
- Fixing solution: 4% paraformaldehyde (J. T. Baker) and 4% Saccharose (Merck) in PBS
- Ammonium Chloride Solution: 50 mM ammonium chloride (Sigma) in PBS
- TritonX-Solution: 0,2 % Triton X 100 (Sigma) in PBS
- Blocking Solution: 1% FCS, 1% BSA (Sigma) und 0,1 % Gelatine (Sigma) in PBS
- Mowiol Solution: 15% Mowiol (Hoechst), 50 mg/ml DABCO (Sigma)

Cells were washed in PBS (pH 7,4) and fixed in fixing solution for exactly 20 minutes. Subsequently, cells were washed again several times and remaining paraformaldehyde was quenched with Ammonium Chloride Solution. After 2 washing steps with PBS, cells were treated with TritonX- solution for 5 minutes followed again by several washing steps. After blocking with blocking solution for 10 minutes, cells were incubated with primary antibody for 20 minutes. Washing steps and incubation with secondary antibody for 20 minutes followed. Finally, after several washing steps with PBS, cells were washed with distilled water and mounted on cover slips with mowiol solution.

For surface stainings, cells were washed twice with PBS (Ca, Mg) and incubated with the primary antibody on ice for 20 minutes. Subsequently cells were washed twice with PBS prior to fixing cells and detection with secondary antibody as described above.

### 7.3.3 Microscopy

Cells were analyzed on a Zeiss LSM 510 Meta confocal microscope (Zeiss, Oberkochen, Germany) equipped with a 63x/1.25 objective and standard FITC and TRITC Fluorescence filter sets. Images were obtained with Metaview system software (Universal Imaging Corporation). For Image processing, Photoshop 5.5 (Adobe) was used.

## 7.4 Protein Biochemistry

### 7.4.1 Production of Protein extracts

#### 7.4.1.1 Total Cell lysates for SDS PAGE and CoIP

STEN-Lysis buffer: 50 mM Tris pH 7.6, 150 mM NaCl, 2 mM EDTA, 1% Nonidet P-40 (USB), containing Protease Inhibitor Cocktail (Sigma) , diluted to 1:500
CHAPS Lysis buffer: 150 mM Na Citrate, pH 6.4, 2% CHAPS (Fluka BioChemika) containing Protease Inhibitor Cocktail (Sigma) , diluted to 1:500

90 % confluent cells were washed twice on ice with ice-cold PBS (pH 7.4) . Subsequently cells were scraped in 1 ml STEN-Lysis buffer (for co-IP experiments CHAPS lysis buffer was used instead) per 10 cm plate using a cell scraper and transferred to an Eppendorf cup and incubated on ice for 30 minutes. After

10.000 g clearance at 4°C for 60 minutes, the supernatant (=STEN-lysate) was either analyzed directly or frozen at -20°C.

### 7.4.1.2 Membrane Preparations

The protocol for membrane preparations, was optimized for subsequent BN-PAGE analysis. Cells were grown to confluency and washed with PBS. The 1.000 x g cell-pellet was homogenized in hypotonic buffer (20 mM sodium citrate, pH 6.4, 1mM EDTA, 5% glycerol, protease inhibitor cocktail P-8340, Sigma) and frozen in liquid nitrogen for cell rupture by thawing. Protein fractionation was done at a concentration of 1% of each Lubrol WX and Brij35 (Pierce) by centrifugation at 5.000 x g and continued with the 5.000 x g-supernatant (5% Glycerol added) at 130.000 x g for 30 min. at 4°C in a Beckman ultracentrifuge (OptimaTM Ultracentrifugation, Beckman, Germany) to remove non membranous material. Membrane pellets were solubilized in 20 mM Sodium citrate-buffer (pH 6,4; 1mM EDTA; protease Inhibitor cocktail P-8340, Sigma) with 1% Triton X-100 for 10 minutes on ice. Insoluble material was removed by 130.000 x g ultracentrifugation for 30 min. at 4°C.
Native lysates, containing all proteins of the secretory pathway and cytosolic components, were obtained by adding Triton X-100 to the 5.000 x g-supernatant at a final concentration of 1% and a clearing centrifugation at 130.000 x g in 20 mM Sodium citrate-buffer (pH 6,4; 1mM EDTA; protease Inhibitor cocktail P-8340, Sigma).

## 7.4.2 Assessment of total protein amount

Measurement of total protein concentration in lysates was done by photometry using a calibration curve obtained from BSA standard dilutions using the standard protocol provided by the Bio-Rad Protein Assay Kit (Bio-Rad).

## 7.4.3 Immunoprecipitation of proteins

The following solutions were used for Immunoprecipitation:

- Protein A-Sepharose solution: 100 mg/ml Protein A Sepharose (Sigma) in STEN buffer
- STEN Buffer: 0,05M Tris pH 7,6, 2 mM EDTA, 0,2% NP-40, 0,15M NaCl

Immunoprecipitation of BACE was performed from lysates in 20 mM sodium citrate (pH 6.4, 2% CHAPS (Merck, Germany), 1 mM EDTA, Protease Inhibitor Cocktail (Sigma, Germany)). Lysates were incubated with anti-myc-Agarose (Sigma) and anti-HA-Agarose (Sigma) and incubated at 4° C on a shaker. Protein A Sepharosebeads were subsequently pelleted at 10 000 g for 2 minutes and washed 3 times with 750 µl STEN (150 mM NaCl, 50 mM Tris-HCl, 1 mM EDTA, 0.2 % NP-40) . 2x Laemmli buffer was added to washed pellets and samples were boiled at 95° C for 10 minutes prior to analysis on SDS PAGE.

## 7.4.4 Antibodies for immunoprecipitation/ immunoblotting

The following polyclonal antibodies to BACE were applied at the indicated dilutions in standard immunoblotting procedures:

- N-terminal antibody to amino acids 46–60 of BACE (EE-17, Sigma) at 1:2000
- C-terminal antibody to amino acids 482–501 (LK-16, Sigma) at 1:2000
- BACE-propeptide antibody GM190 to amino acids 22–45 from Gerd Multhaup, FU Berlin [127] at 1: 500
- The neoepitope-specific antibody sw192 (Elan) was used at 1:1000 to specifically detect soluble Swedish ßAPPs [184].
- The monoclonal HSP70 (1:1000) antibody SPA-820 was purchased from Stressgen. HRP labeled secondary antibodies (Promega) were used for ECL detection (AmershamPharmacia Biotech).

- For the immunoprecipitation studies of myc-tagged proteins anti-myc-Agarose (Sigma) was used and anti-HA-Agarose (Sigma) for HA-tagged proteins respectively.
- The monoclonal antibody 9E10 (1:1000) to the Myc epitope was obtained from the hybridoma bank.
- For HA (1:1000) detection the anti-HA monoclonal antibody HA.11 was used (Covance Inc., Princton, USA).
- 6687: polyclonal antibody from rabbit to the last 20 amino acids of the C-term of ßAPP (C. Haass), at 1:300
- Hsp70: monoclonal antibody form mouse to Hsp70/Hsc70 (Stressgen), at 1:750

## 7.4.5 PAGE and Western Blotting of proteins

Buffers used:

- Tris-Glycine buffer: 25 mM Tris and 0,2 M glycine in $H_20$
- Tris-Glycine-SDS buffer: 25 mM Tris, 0,2 M glycine, 0,01% SDS in $H_20$
- Tris-Tricine buffer: 0,1 M Tris, 0,1 M Tricine, 3 mM SDS
- Laemmli buffer: 50 mM Tris, pH 7,2, 20% Glycerol, 10% ß-Mercaptoethanol, 4% SDS
- Urea buffer: 50 mM Tris, pH 7,2, 4 M Urea, 20% Glycerol, 10% ß-Mercaptoethanol, 4% SDS

SDS polyacrylamide-electrophoresis (SDS-PAGE) for separation of proteins with respect to their sizes was performed following standard protocols ([219], chapter 18).
For detection of BACE, 8% polyacrylamide gels and Tris-Glycine-SDS Puffer were used. Samples were boiled at 95°C for 10 minutes in Laemmli sample buffer. See Blue Plus 2 (Invitrogen) was utilized as molecular weight standard.
For detection of APP CTFs, 10-20% Tris-Tricine gels (Novex) and Tris-Tricine buffers were used.
Samples were boiled at 95°C for 10 minutes in Laemmli sample buffer. Prestained Protein MW Standards Lows (Gibco) was loaded as molecular weight standard.
Western Blotting of proteins on PVDF Membrane (Millipore) was performed according to standard protocols using Tris-glycine as blotting buffer ([219], chapter 18).

## 7.4.6 Blue Native PAGE (BN-PAGE)

Native 6-16 % gradient gels were prepared according to the protocol of Schagger et al. [220-223]. Protein concentrations were measured with the Bradford Assay (Biorad, Germany) according to the supplier's instructions. Triton-X 100-solubilized membrane fractions, native lysates or soluble BACE-NT were subjected to BN-PAGE essentially as described before [214, 223]. Marker proteins used in BN-PAGE were BSA, 66 kDa; β-amylase, 200 kDa; apoferritin, 443 kDa and thyroglobulin, 669 kDa (Sigma).

## 7.4.7 Detection of proteins with antibodies

The following solution was used for blocking WB membranes and dilution of detection antibodies:
Blocking Solution: PBS with 0.5 g/l I-Block (Tropix) und 0,1% Tween 20 (Roth).

Blocked membranes were incubated with the respective primary antibody for 1-2 hours prior to frequent washing steps in TBS (25 mM Tris, ph 7,6, 140 mM NaCl, 2,7 mM KCl) with 0,3% TritonX 100 (Sigma). Subsequently HRP-coupled α-mouse or α-rabbit secondary antibodies (Promega) diluted to 1: 10000 were incubated with the membranes for 30 minutes until additional washing steps were applied. Detection of the secondary antibodies was performed using ECL (enhanced chemoluminescence) technique (Amersham Pharmacia) according to the manufacturer´s instructions.
Light sensitive films (Super RX, Fuji) were developed with a Curix 60 (Agfa).
Developed Films were scanned with a SnapScan 1236 S (Agfa) and images were processed with Photoshop 5.5 (Adobe)

### 7.4.8 Stripping of Western Blot membranes

To analyze the same blot with several antibodies, membranes were stripped and re-blotted.
Membranes were incubated at 50°C for 30 minutes in : 62,5mM Tris-HCl, ph 6,7, 2% SDS, 0,7% ß-Mercaptoethanol (Merck). Subsequently, membranes were washed in PBS 0,2% Tween 20 (Roth) and blocked in blocking solution for 20 minutes prior to incubation with antibodies as described above.

### 7.4.9 Radiolabeling of cellular proteins

To radiolabel cellular proteins, cells were incubated at 37°C in methionine-free, serum-free MEM (Gibco Life Sciences) for 90 minutes. For BFA treatment of cells, 10 µg/ml BFA was added to the starvation media, whereas control cells were incubated with the carrier (ethanol) alone. Subsequently, cells were incubated with fresh medium supplemented with [$^{35}$S]methionine (Promix; Amersham Pharmacia Biotech, Freiburg, Germany) and kept at 37°C in the incubator for 3 hours for the pharmacological experiments. For the temperature block experiments, cell were alternatively labeled for 1.5 hours and then incubated at 15°C, 20°C or 37°C respectively in a water basin [224-226]. Cells were buffered in 10mM Hepes buffer at pH 7.4.
For immunoprecipitations, cells were lysed in STEN buffer (50 mM Tris, pH 7.6, 150 mM NaCl, 2 mM EDTA) supplemented with 1% nonidet P-40 (NP-40)/1% Triton X-100/2% bovine serum albumin (BSA) on ice for 10 min. Lysates were clarified by centrifugation for 20 min at 14 000 g and immunoprecipitated for 3 h at 4°C using the APP specific antibody 6687. After separation by sodium dodecyl sulfate–polyacrylamide gel electrophoresis (SDS–PAGE), proteins were transferred to a polyvinylidene difluoride (PVDF) membrane (Imobilon, Millipore Corporation, Eschborn, Germany) and analyzed by autoradiography.

### 7.4.10 FPLC purification of His-tagged soluble and membrane bound BACE

For the purification of BACE, membrane bound BACE-FL with a myc-His tag was obtained from large-scale membrane preparations. To obtain soluble BACE for purification, HEK 293 cells expressing BACE-NT with a myc-HIS tag were kept in OPTIMEM (Invitrogen) for 24 hours. Supernatants containing BACE-NT or Triton X-100 extracted membrane preparations (see above) were purified on a FPLC ÄKTApurifier system (Amersham Pharmacia Biotech) with a Ni-NTA-Sepharose column (Amersham Pharmacia Biotech) by a 10 mM Imidazole washing step and a 10-500 mM Imidazole gradient each in PBS, 0.1% Triton-X 100. The eluted material was pooled and dialyzed against PBS, 0.1% Triton-X 100 and concentrated by using a Vivaspin 6 ml concentrator with a MWCO of 5000 Dalton (Vivascience, Hannover, Germany). The purity of BACE was verified by Coomassie staining with Colloidal Blue staining solution (Novex, San Diego, USA). For size determination in 8% SDS gels the Seeblue marker (Invitrogen) was used.

## 7.5 Enzymatic assays

Purified BACE-FL and BACE-NT were dialyzed against PBS 0.1 % Triton X-100 and stored at –80°C in aliquots. Protein concentrations were estimated by Bradford assay (Biorad). Active enzyme concentrations were obtained by active site titration using the statine-based inhibitor H-EVN-Statin-VAEF-NH2 and by fitting data from inhibition experiments approaching titration conditions to the general equation for tight binding inhibitors [227]. The kinetic measurements were performed in 100 µl reaction mixtures containing the substrate (Cy3-SEVNLDAEFK-(Cy5Q)-NH2 from Amersham Pharmacia Biotech) at a concentration ranging from 1 to 27 µM in 50 mM acetate buffer with 0.25 mg/ml bovine serum albumin, pH 4.5 at 26 °C. To calibrate the fluorescent measurements, increasing substrate concentrations corresponding to 2% of 5, 15, 25, and 35 µM respectively (this corresponds to the approximately 1% of the substrate which was converted during the first 20 minutes in which initial velocities were determined) where completely hydrolyzed during 20 minutes of incubation with BACE enzyme and maximum values for RFU recorded. Subsequently, the inner filter effect was measured. The inner filter effect is a an apparent decrease in emission quantum yield and/or distortion of bandshape as a result of reabsorption of emitted radiation known to occur with fluorogenic substrates especially at higher concentrations, (IUPAC Compendium of Chemical Terminology 2nd Edition (1997)), To

assess the inner filter effect, 5, 15, 20 and 25uM of the uncleavable substrate Cy3 -LVFFAEDVK(Cy5Q)-NH2 were added to the fully converted substrate to simulate the presence of high concentrations of quenching groups. The conversion factor m= RFU / [S] was determined to be 2.8 whereas the inner filter effect was found to be not significant up to a substrate concentration of 30 µM. DMSO concentrations were adjusted in all assays and did not exceed 5%.
Reactions were started by addition of enzyme, and the increase in fluorescence at 590 nm (excitation at 530 nm) was measured in 96-well plates (Nunc) on a Fluoroskan Ascent FL Fluorescence plate reader (Labsystems), while gentle shaking of the samples was applied during the intervals between measurements. Initial velocities were determined for the first 20 minutes of the progression curve via linear regression. Initial velocities transformed to µmol/ sec * µmol Enzyme were plotted against increasing substrate concentrations (1-27 µM). KM and kcat were calculated from a nonlinear least squares best fit to the Michaelis-Menten equation. For the commercial BACE-NT, purchased from OncogeneTM, the second order rate constant kcat/KM was calculated from a quasilinear plot of velocity as a function of substrate concentration (Table in Figure 7). To cleave off the pro-domain, purified BACE-NT was treated over night with Furin (NEB) in 100 mM HEPES, pH 7.5; 0.5% Triton-X 100, 5 mM CaCl2, whereas a control was incubated in buffer only. The absence of the pro-domain was controlled by immunoblotting with the pro-peptide antibody GM190. BACE-NT with and without pro-peptide were subjected to the enzyme activity assay.

## 7.6 Machines/Devices used

- pH meter: Inolab ph Level 1 (Wissenschaftlich Technische Werkstätten Weilheim)
- PCR machine: Master Cycler Gradient (Eppendorf)
- agarose gel analysis: UV transilluminator (UVP)
- photometer: Smart Spec 3000 (Biorad)
- table centrifuge: Biofuge Fresco (Heraeus)
- ultracentrifuge: Optima Max-E ultracentrifuge (Beckman Coulter)
- film-developer: Curix 60 (Agfa)
- Scanner: SnapSace 1236 S (Agfa)

# 8 Results

## 8.1 Molecular Size of Native BACE

Since it was of interest to study BACE in its native configuration to address the question whether it assembles to a higher molecular weight complex, native membrane preparations had to be optimized for the separation of BACE by Blue Native Polyacrylamide Gel Electrophoresis (BN-PAGE). In particular, different detergents wrere tested for their ability to carefully extract BACE from membrane preparations and their compatibility with BN-PAGE. A combination of Lubrol WX, Brij35 and Triton X-100 (Material and Methods) gave the best results. With this setup, endogenous BACE was studied in untransfected HEK 293 cells as well as in the glioblastoma cell line H4 by means of BN-PAGE as compared to SDS-PAGE (Figure 14 A and B respectively). BN-PAGE identified the native size of BACE as 140 kDa whereas no signal appeared at the expected range around 70 kDa (Figure 14 A, lanes 5 and 6) which is the known size of BACE under denaturing conditions as verified by SDS-gel analysis (Figure 14 B, lanes 5 and 6). To validate the specificity of the signals, Triton-X 100 solubilized membrane preparations were furthermore analyzed from the neocortex of 5 day old (P5) BACE knock out mice in contrast to P5 wt mouse brains. Indeed, a sharp band at 140 kDa could be detected in the P5 wt brains which was absent in the knock-out P5 mice (Figure 14 A and B, lanes 3 and 4). This indicated that in murine brains, where BACE is prominently expressed in neurons [54], BACE has approximately double the size in its native conformation than under denaturing conditions. Interestingly, the signal derived from adult wt mice (Figure 14 A and B, lane 2) was much weaker than that from P5 wt mice, indicating that BACE might be upregulated during early development, a finding that has not been addressed in the literature so far. As expected, the strongest signal from the BN gel was measured in membrane preparations of a transgenic mouse (Thy-1-BACE; TB) which overexpresses neuronal human BACE under the control of a Thy-1 cassette [124]. Taken together, these data show that under native conditions, BACE has approximately double the size as under denaturing conditions as shown in two independent cell lines as well as from intact murine brain tissue from different mouse strains at different stages of development.

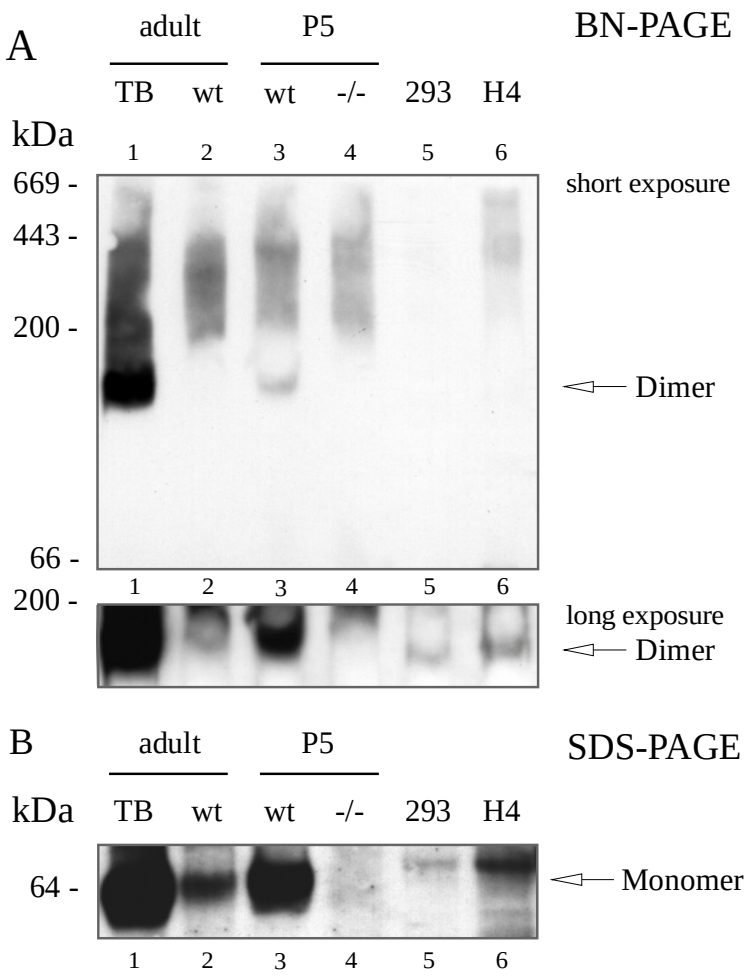


**Figure 14: Endogenous and transgenic BACE migrates at 140 kDa on a BN gel.**

Membrane proteins were extracted with 1% Triton X-100 and separated on a 6-16% gradient BN-PAGE (A: short and long exposure) or on an 8% SDS-PAGE (B). Antibody (EE-17) against the N-terminus of BACE was used for detection. BACE recovered from brains of transgenic mice overexpressing human BACE in neurons (TB) has a size of approximately 140 kDa band on the BN gel in contrast to ~70 kDa on the complementary SDS gel. Endogenous BACE from P5 wt mice was clearly detected controlled by the absence of a signal from BACE -/- mouse P5 brain membrane preparation. In HEK 293 and the glioblastoma cell line H4, endogenous BACE migrates to 140 kDa (A: long exposure). Nonneuronal BACE has a slightly larger molecular size on the SDS-PAGE gel.

## 8.2 Identification of the BACE dimer

The fact that native BACE had double the size of denatured BACE prompted us to investigate, whether BACE could exist as a dimer under native conditions which is destabilized by the denaturing SDS-PAGE analysis procedure. It was therefore decided to generate two differentially tagged BACE-FL constructs and tested whether those constructs dimerize by performing Co-immunoprecipitation (Co-IP) analysis. Since prior data from our laboratory showed [127] that a C-terminal epitope tag did not influence BACE activity, a C-terminal myc (BACE-FL-myc) or a HA tag (BACE-FL-HA) was chosen. Control experiments revealed that both constructs were active and had a native size of approximately 140 kDa (data not shown). Immunoprecipitation of either the myc or the HA tag was subsequently performed from total cell lysates of cells expressing either one of the tagged BACE versions in isolation or co-

expressing both of them. To control for the confounder that the BACE molecules could artificially cluster together after lysis, a mixture of cell lysates containing myc or HA tagged BACE variants was included in the analysis. The captured BACE molecules were consequently separated on an SDS-PAGE and detected by myc or HA antibodies respectively (Figure 15). As can be seen in the two lanes indicated by the arrows in Figure 15, the two differently tagged BACE species could be co-immunoprecipitated, if co-expressed, by capturing either tag and detecting the respective opposite tag, whereas no signal was detected from cells exclusively only expressing one species. Also, there was no signal seen when lysates of cells only expressing one species were mixed, indicating that no post-lysis aggregation takes place. There was also cross pull down of immature, pro-peptide containing BACE dimmers, whereas the immature species was only faintly detected in the direct lysate (Figure 15, lowest panel). One likely explanation of these different signal intensities is that under the conditions of immunoprecipitation the antibodies might have a higher affinity to immature than to mature BACE.

Taken together, these experiments indicate that BACE-FL can occur as homodimers within cells. Given that the size of native BACE was found to be 140 kDa these data suggest in a synopsis, that BACE exists primarily as a homodimer. The finding that pro-peptide containing, immature BACE was also co-immunoprecipitated suggests that dimerization can occur already in compartments like the ER [126, 128] which contain immature BACE.

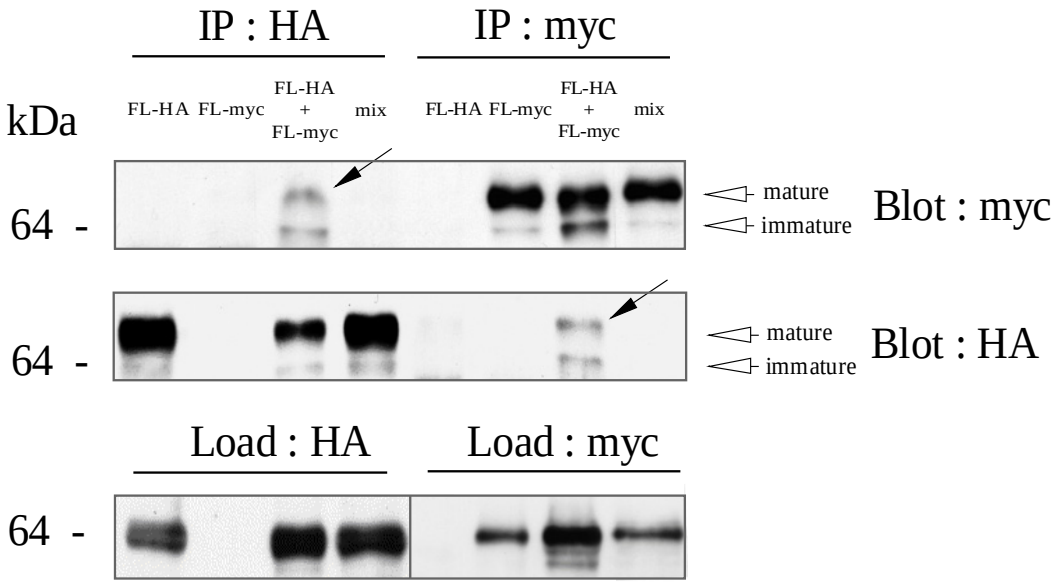


**Figure 15: Co-immunoprecipitation of differentially tagged BACE.**

Immunoprecipitation with anti-myc-agarose beads or with anti-HA-agarose beads were performed in 2 % CHAPS lysates of cell lines stably expressing BACE-FL-myc and BACE-FL-HA. Myc-tagged BACE-FL could be specifically detected after anti-HA immunoprecipitation (arrow in upper panel). Vice versa, HA-tagged BACE-FL was co-isolated with an anti-myc-antibody (arrow in lower panel). This indicates that both BACE-FL variants interact with each other. In both cases, mature and immature BACE were observed. Artificial post-lysis aggregation was excluded by combining lysates from BACE-FL-HA and BACE-FL-myc expressing cell lines respectively (mix). The load shows the expression levels of the respective BACE variants.

## 8.3 Conditions for Dimerization

Having established that native BACE adopts a dimeric quaternary structure, it was next of interest to identify the conditions for dimerization of BACE and perform a domain deletion analysis and a subcellular localization study.

### 8.3.1 The native conformation of the BACE-ectodomain

BACE was shown to undergo ectodomain shedding [128, 228, 229] and the BACE ectodomain is enzymatically active and has widely been used for kinetic studies (see section 5.7.2.10 on enzyme kinetics above).

The first construct to be studied was a construct which has a deletion of the entire transmembrane domain and the cytosolic domain (BACE-NT; also see Figure 18 for a schematic overview of the constructs used) to study the soluble BACE-ectodomain under native conditions.

Myc-tagged BACE-NT obtained form native lysates of overexpressing cells (material and methods section 7.4.1.2) was directly compared to untagged BACE-FL on BN-PAGE (Figure 16). Interestingly intracellular myc-tagged BACE-NT like secreted BACE-NT migrated to a size of approximately 70 kDa under native conditions (Figure 16 , lanes 1 and 3 on both panels). Furthermore, a cell line co-expressing untagged BACE-FL (FL) together with a myc-tagged BACE-NT (NT-myc) showed a 70 kDa band in addition to the 140 kDa band (arrow in left panel of) as detected with an N-terminal antibody. When analyzing the same probes with the myc antibody however, thus specifically detecting myc-tagged BACE-NT (arrow in right panel of), there was no signal observed at the dimeric size, indicating that intracellular BACE-NT does not bind to itself nor to BACE-FL to form a multi-protein complex.

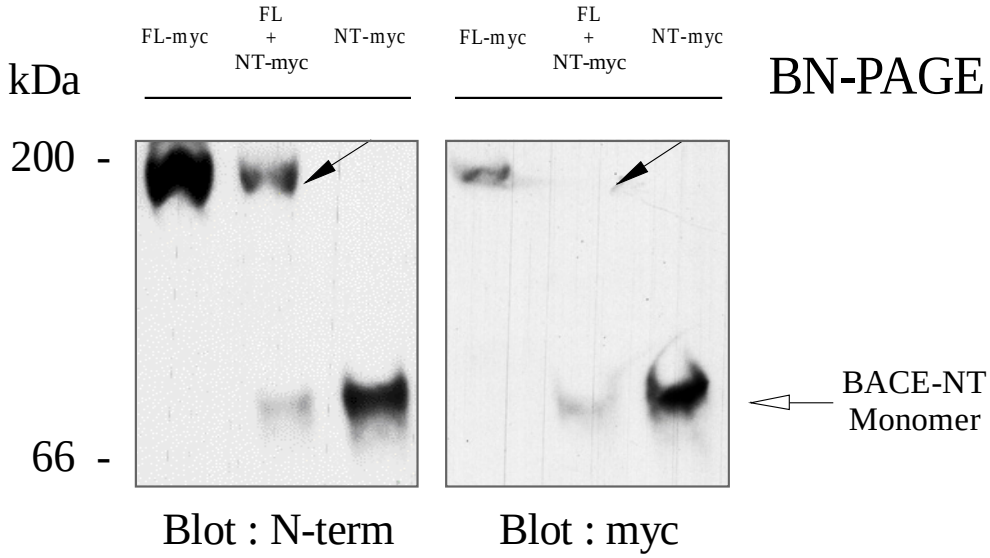


**Figure 16: BACE-NT is a monomer on BN-PAGE**

BN-PAGE analysis of native lysates from cells expressing BACE-FL-myc and BACE-NT-myc alone, or co-expressing untagged BACE-FL together with BACE-NT-myc was performed. A signal from the N-terminal epitope (EE-17) is compared to the myc-signal. The BACE-FL-myc dimer is detected by EE 17 (left panel, first lane) and the myc antibody (right panel, first lane). A cell line co-expressing untagged BACE-FL together with a myc-tagged BACE-NT shows an EE-17-positive band at 140 kDa (arrow on left panel) which is not detected by the myc antibody (arrow on right panel) and a 70 kDa band, which is selectively myc positive. The same EE-17-positive and myc-positive monomeric band is detected in the BACE-NT-myc sample.

To confirm these findings by an independent method, a co-IP experiment analogous to that described above was performed using BACE-FL-HA and BACE-NT-myc. As can be seen in Figure 17, there the ectodomain of BACE could not be co-immunoprecipitated with full length BACE which is in line with the results of the BN-PAGE analysis.
It can be concluded from these data that whereas BACE-FL assembles to homodimers under native conditions, BACE-NT exists as a monomer and does not bind to BACE-FL.

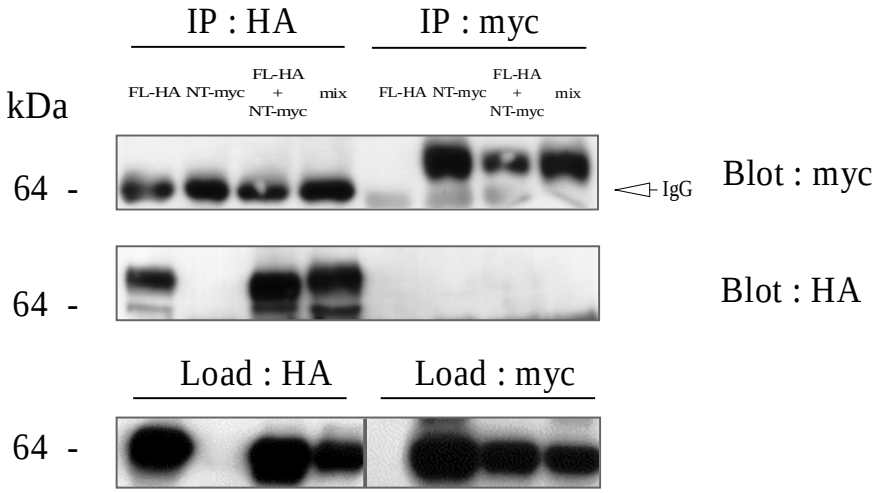


**Figure 17: Differently tagged BACE-NT does not co-immunoprecipitate**

2 % CHAPS lysates of cell lines stably expressing BACE-NT-myc and BACE-FL-HA were analyzed by immunoprecipitation in analogy to the experiment displayed in Figure 15.

## 8.3.2 Essential Domains for Dimerization

The failure of BACE-NT to dimerize suggested that either the transmembrane domain, the cytosolic domain or both were necessary for dimerization. To dissect these theoretical alternatives, a BACE construct that lacks the cytoplasmic domain (BACE ΔC) was generated. Also, a BACE variant in which the transmembrane domain (TM) was replaced by a polyalanine stretch was cloned to abolish any specific structure of the TM that might be important for dimerization while preserving the membrane attachment (BACE pA). An overview of all the construct used in the present investigation is schematically depicted in Figure 18.

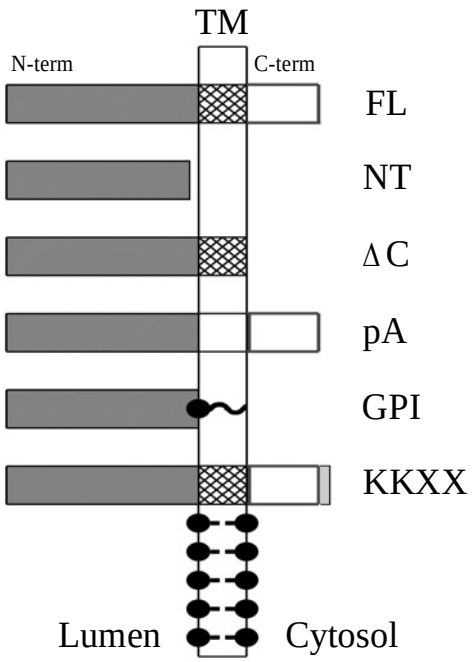


**Figure 18: Schematic representation of BACE constructs**

Full length BACE (FL) has a luminal catalytic ectodomain and is integrated in the membrane by its transmembrane domain (TM; hatched box). BACE-NT lacks the TM region and the cytoplasmic tail. BACE-ΔC (ΔC) lacks the cytoplasmic domain and BACE pA represents a construct in which the TM was replaced by a poly-Alanine-stretch. GPI-anchored BACE corresponds to a membrane linked BACE-NT (GPI). Attachment of a C-terminal KKXX-ER-retention signal is used to retain the full length construct in the ER/Cis-Golgi compartment.

Membrane attachment of both construct was controlled by cell surface immunostaining of intact cells with an N-terminal antibody against the extracellular domain and showed invariant surface staining of both constructs as compared to BACE-FL (Figure 19). In contrast, BACE-NT was not detected at the surface but only intracellulary after permeabilization of the cells (Figure 19 and inserts) indicating as expected that it is rapidly secreted into the medium.

Cellular activity of both constructs was furthermore confirmed by the specific detection of the N-terminal cleavage product sAPPß accumulated over 12 hours in the supernatants of Swedish APP expressing cell lines using the neo-epitope specific antibody sw192 (Figure 20 and Figure 2 for a scheme of the detected APP products). BACE ΔC as well as BACE pA showed a clear increase in sAPPß levels, while cellular APP levels were roughly equal. The amounts of retained APP stubs showed more variability which might be due to different compartementalization and/or further processing of the stubs (Discussion section 9.5.1.) Cell densities were roughly equal as measured by the signal intensities from HSP70.

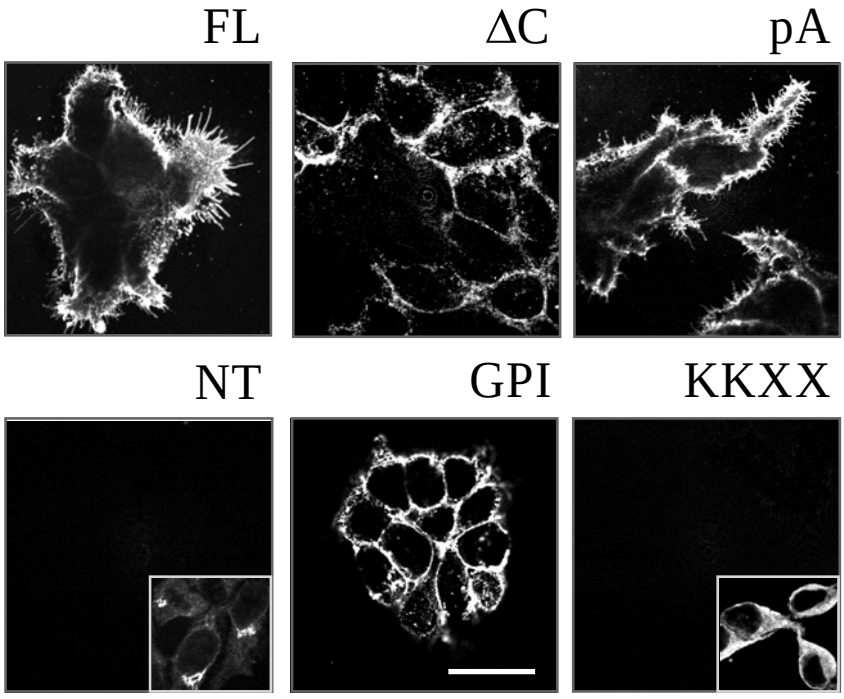


**Figure 19: Plasma membrane expression of BACE variants**

Non-permeabilized cells were stained with the ectodomain antibody EE-17. The plasma membrane-anchored BACE variants (FL, ΔC, pA, GPI) are recognized by surface staining. Secreted BACE-NT is not bound to the membrane. As expected, the ER retained KKXX version is also not found at the cell surface. BACE-NT and BACE-KKXX are only detected in permeabilized cells (inserts). Scale bar: 20 µm. Note that the constructs BACE-GPI and BACE-KKXX are described later in separate sections but are included in this figure to ensure comparability and avoid redundancy.

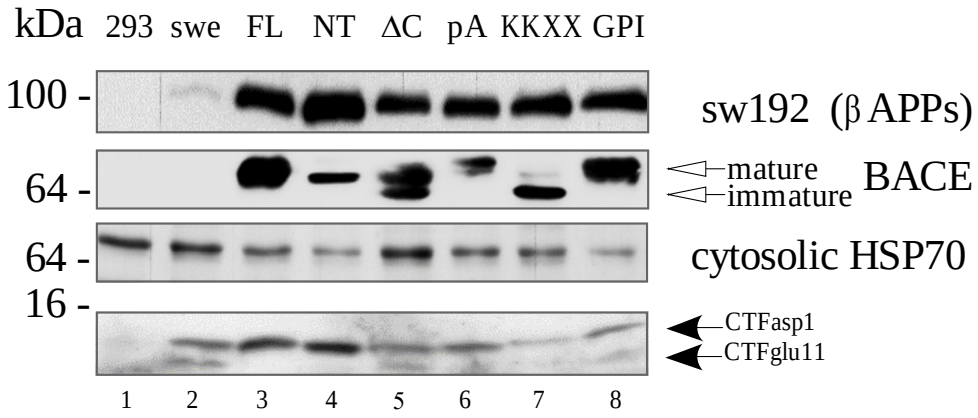


**Figure 20: Intracelllular enzymatic activity of BACE variants**

The BACE-constructs shown in (Figure 18) were stably expressed in a Swedish APP expressing cell line and cultured in serum free medium overnight. The medium was subsequently collected and BACE activity was assessed by the identification of Swedish APPsß using the neoepitope specific antibody sw192 (upper panel). C-terminal fragments CTF produced by BACE cleavage starting at Asp+1 and Glu+11 respectively are shown in the lowest panel. Expression of the BACE variants is shown in the middle panel. Equal amounts of protein loaded were controlled with an antibody to HSP70 (lower panel). Please note that the

constructs BACE-GPI and BACE-KKXX are described later in separate sections but are included in this figure to ensure comparability and avoid redundancy.

Interestingly, the direct comparison on BN-PAGE showed that both BACE ΔC and BACE pA were detected at dimeric size as opposed to BACE-NT serving as a molecular marker for monomeric BACE (Figure 21, lanes 1-4).
This falsified the initial hypothesis by showing that neither the authentic TM domain nor the C-terminus of BACE were necessary to promote dimerization.

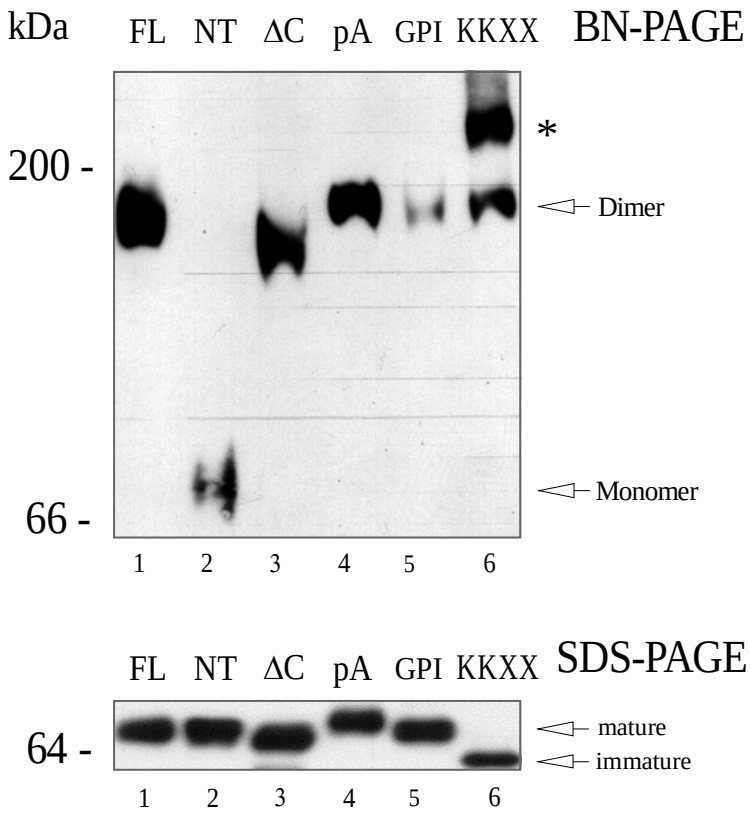


**Figure 21: Analysis of BACE variants on BN-PAGE in comparison to SDS-PAGE**

Membrane Preparations of full length BACE (FL) expressed in HEK 293 cells migrates as a sharp band at 140 kDa on a BN-PAGE (upper panel) in contrast to a 70 kDa band on the SDS-PAGE gel (lower panel). The secreted ectodomain of BACE-NT obtained from media of the cells migrates to approximately 70 kDa (upper panel), which is within the range of the expected monomeric size seen on a SDS-PAGE gel (lower panel). Please note that the constructs BACE-GPI and BACE-KKXX are described later in separate sections but are included in this figure to ensure comparability and reduce redundant information.

### 8.3.3 Membrane Association

The question that was addressed next was whether the lack of membrane attachment could explain that the BACE ectodomain is incapable of dimerization. Since a GPI anchor is an efficient way to attach proteins to membranes and was shown to be compatible with BACE function previously [156], the GPI anchor motif of CD59 was added to the ectodomain of BACE (BACE-GPI, Figure 18). As expected, the BACE-GPI species showed a strong surface expression as compared to the absence of a corresponding signal on the surface of BACE-NT cells, indicating that the GPI signal is sufficient to attach BACE-NT to the membrane (Figure

19). The functionality of BACE-GPI was furthermore confirmed with experiments analogous to those described above (Figure 20).
Analysis of native BACE-GPI on BN-PAGE subsequently demonstrated that addition of the GPI anchor signal shifts BACE-NT from a size of ~70 kDa to a size of ~140 kDa which is the same size as BACE-FL (Figure 21). Furthermore it was tested whether the GPI anchor successfully attaches BACE-NT to the membrane. BACE-NT was not detected in native solubilized membrane fractions but exclusively in native lysates containing proteins of the secretory pathway and cytosolic proteins (material and methods section 7.4.1.2). On the other hand, BACE-GPI was found together with membrane-bound BACE-FL in the membrane fractions but not in the native lysates, indicating that the GPI anchor successfully attaches the ectodomain of BACE to the membrane (Figure 22).

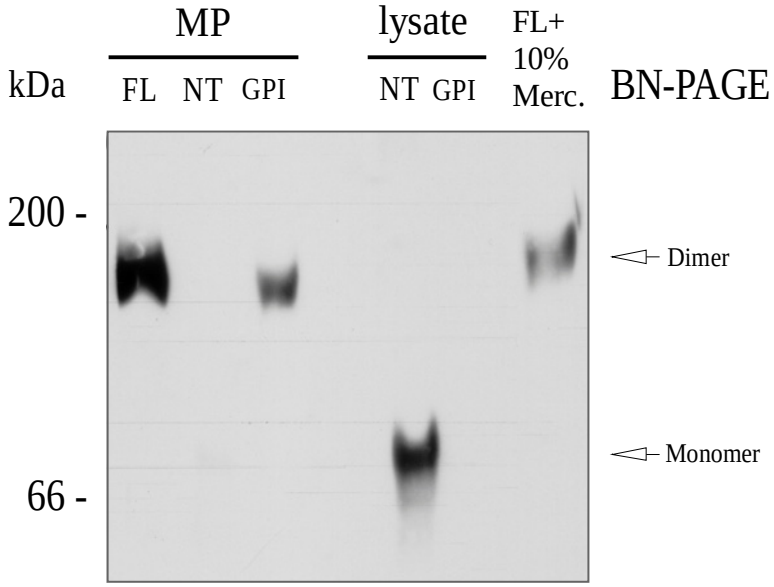


**Figure 22: Membrane preparations compared to native lysates on BN-PAGE**

Membrane preparations (MP) of full length BACE (FL), BACE-NT (NT) and BACE-GPI (GPI) compared to native lysates (lysate) of NT and GPI respectively. In the last lane, BACE-FL was run with 10% (w/v) β-Mercaptoethanol added.

The differences in native molecular size cannot be explained by the size of the GPI recognition sequence and the GPI anchor itself (see Discussion section 9.6.1 for a detailed argument) but rather suggests that the GPI anchor rescues the deficiency of BACE-NT to dimerize. This implies that the ectodomain of BACE is sufficient for homodimerization as long as it is bound to the membrane.
It was furthermore examined, whether the cysteine residues within BACE are used for intermolecular interactions between two BACE molecules leading to a BACE dimer. However, addition of 10% β-Mercaptoethanol to the BACE-FL sample, which reduces disulfide bonds, did not impair dimeric configuration. This indicates that the cysteine residues of BACE are reserved for intramolecular linkages which is in keeping with the literature [133].

### 8.3.4 Cellular assembly of the BACE Dimer

The finding that mature as well as immature BACE species could be co-immunoprecipitated (Figure 15) evoked the assumption that dimerization of BACE could take place very early in the secretory pathway. Moreover, in light of the finding that native BACE is a dimer, it were a tempting hypothesis to assume that the subsite specificity for Asp+1 or Glu+11 could be modulated by a difference in the oligomeric state of BACE between the ER and the TGN.
In this regard, experiments partly published in [64] demonstrated that cleavage at Asp+1 predominates in the ER, whereas the cut at Glu+11 occurs subsequently in the TGN. Selective low-temperature incubations of cells at 15°C or 20°C are known to block the secretory pathway at the pre-Golgi intermediate compartment or the trans-Golgi network respectively [224-226]. Application of this technique to cells either expressing wt APP or swe APP with or without co-expressing BACE-FL (Figure 23 A) showed that the ratio between Asp+1/Glu+11 cleavage is markedly increased at 15° C in comparison to the control incubation at 37° C whereas it decrease at 20° C compared with 15° C although it is still considerably larger than at 37° C. This indicates that Asp+1 cleavage takes place early in pre-Golgi intermediate compartments, whereas the Glu+11 cut occurs later in the TGN.
In agreement with this, treatment with BFA (Figure 23 B), which blocks the secretory pathway by disrupting the movement of material from the ER to the Golgi apparatus [230] established that in the presence of BFA, the Asp+1 cleavage product is increased whereas the Glu+11 is suppressed. It can also be seen, that overexpression of BACE increases Glu+11 and Asp+1 cleavage in a wt APP background, whereas the Asp+1 cleavage is even more prominent if sweAPP is expressed harboring the preferred cleavage site which is in agreement with earlier publications [184, 186]. Two independent methods thus established the sequential cleavage of wt APP as well as swe APP by BACE, whereby the Asp+1 cleavage is followed by the Glu+11 cleavage.

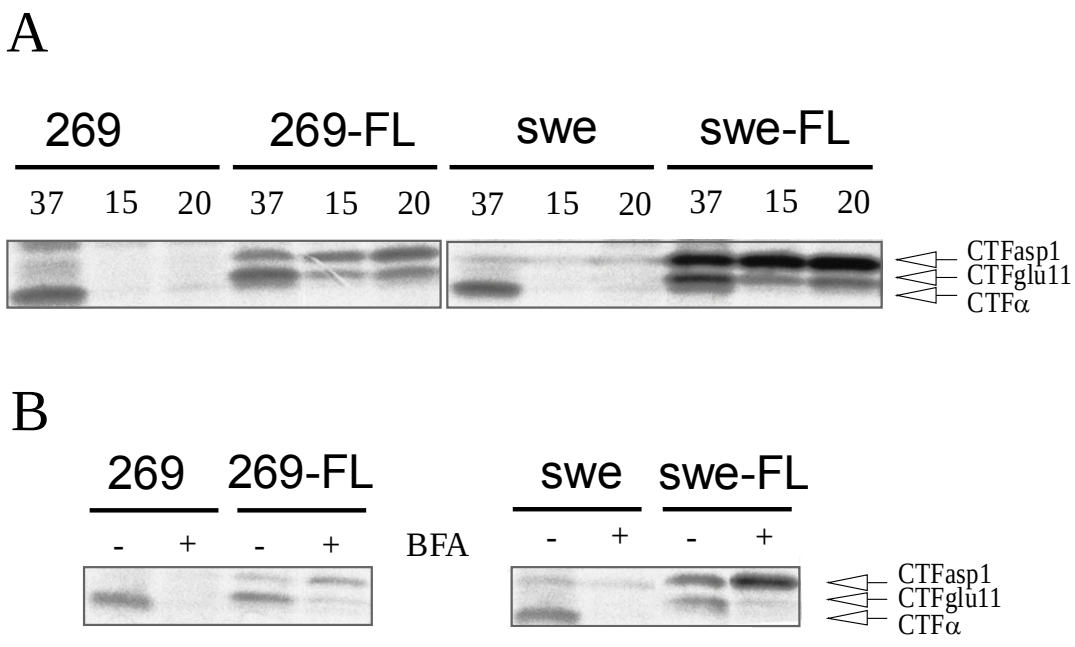


**Figure 23: Subsite specificity of BACE in distinct subcellular compartments.**

(A) 293 Cells expressing either wt APP (269) or swe APP (swe) alone or in combination with BACE (FL) were radiolabeled with [$^{35}$S] methionine and subsequently cooled to 15°C or 20°C, while control cells where incubated at 37°C (upper panel). All cells were buffered in 10 mM Hepes buffer at pH 7.40 to compensate for the lack of carbon dioxide buffer present in the incubator. Radiolabeled intracellular βAPP was subsequently precipitated from cell lysates with antibody 5313 and detected by autoradiography. (B) The same cell lines as in the upper panel radiolabeled with [$^{35}$S] methionine in the presence or absence of BFA or monensin. Radiolabeled newly generated intracellular βAPP was subsequently precipitated from cell lysates with antibody 6687 and detected by autoradiography (lower panel). Arrows indicate CTFasp1, CTFglu11 and CTFα respectively.

It was therefore studied next whether retaining BACE in the ER would interfere with dimerization.

A BACE construct with the classical KKXX ER-retention motif [231] attached to the C-terminus of BACE-FL was produced and characterized (BACE-KKXX). Retention to the ER/cis Golgi compartment of this construct was confirmed by the obligatory presence of its pro-peptide as detected by the pro-peptide specific antibody GM190. The pro-domain is known to be cleaved off in the TGN by Furin, or a furin-like proprotein convertase, suggesting that BACE-KKXX resides in compartments before the TGN [128]. This was confirmed by the surface staining, which showed that BACE-KKXX does not reach the plasma membrane but is instead retained in the ER as demonstrated by a prominent ER-staining in permeabilized cells (Figure 19 and insert ). Enzymatic activity of BACE-KKXX in the ER was however preserved (Figure 20) which is in line with earlier studies on BACE activity in the ER [64, 139]. Sometimes, a higher molecular weight band was seen around 220 kDa which might be due to association of BACE-KKXX with an ER resident factor like a chaperone as it was demonstrated for the inactive pancreatic splice variant [232, 233]. On BN-PAGE, native BACE-KKXX migrated to dimeric size, suggesting that homodimerization of BACE occurs as early as in the ER/cis-Golgi, since the KKXX motif retains BACE in this compartment.

Summarizing the above sequence of experiments, the data are consistent with the model that the BACE ectodomain can promote homodimerization of BACE under the condition that BACE is membrane attached. This homodimerization occurs as early as in the ER and leads to a proteolytically active, 140 kDa large dimeric enzyme. A difference in quaternary structure of BACE is therefore unlikely to account for the different subsite specificity of BACE in different compartments.

## 8.4 Kinetic Properties of dimeric BACE

The ectodomain has widely been used in enzymatic assays for the determination of kinetic parameters and inhibitor studies mainly because it is much easier to obtain in large amounts from cells and it is active when measured with in vitro assays [185, 209-211, 213]. Knowing of the deficiency of BACE-NT to dimerize, it was asked whether the native BACE dimer has different kinetic properties with respect to those published for the monomeric BACE ectodomain. There are only two studies which reported on enzyme kinetics of BACE-FL without however assessing the conformation of BACE [137, 210]. A purification scheme as described in Material and Methods that was therefore devised as a compromise between obtaining sufficiently pure enzyme which would allow for kinetic analysis and preserving the integrity of the native dimer-configuration. BACE-NT was purified in parallel to BACE-FL and purity was compared to unpurified material on Coomassie-stained SDS-PAGE. Purity was furthermore validated against commercially available purified BACE-NT (O-NT) to show that BACE has been purified to almost homogeneity (see Figure 24 A). On the corresponding Western blot, the pro-domain

specific antibody GM190 [127] indicated that BACE-NT-onco and BACE-NT produced in our laboratory still carried the pro-domain (Figure 24 A, lower panels), which is in agreement with earlier reports [127, 131, 209, 212]. The BN-PAGE analysis confirmed that purified BACE-FL still had a dimeric quaternary structure as compared to monomeric purified BACE-NT (Figure 24 B).

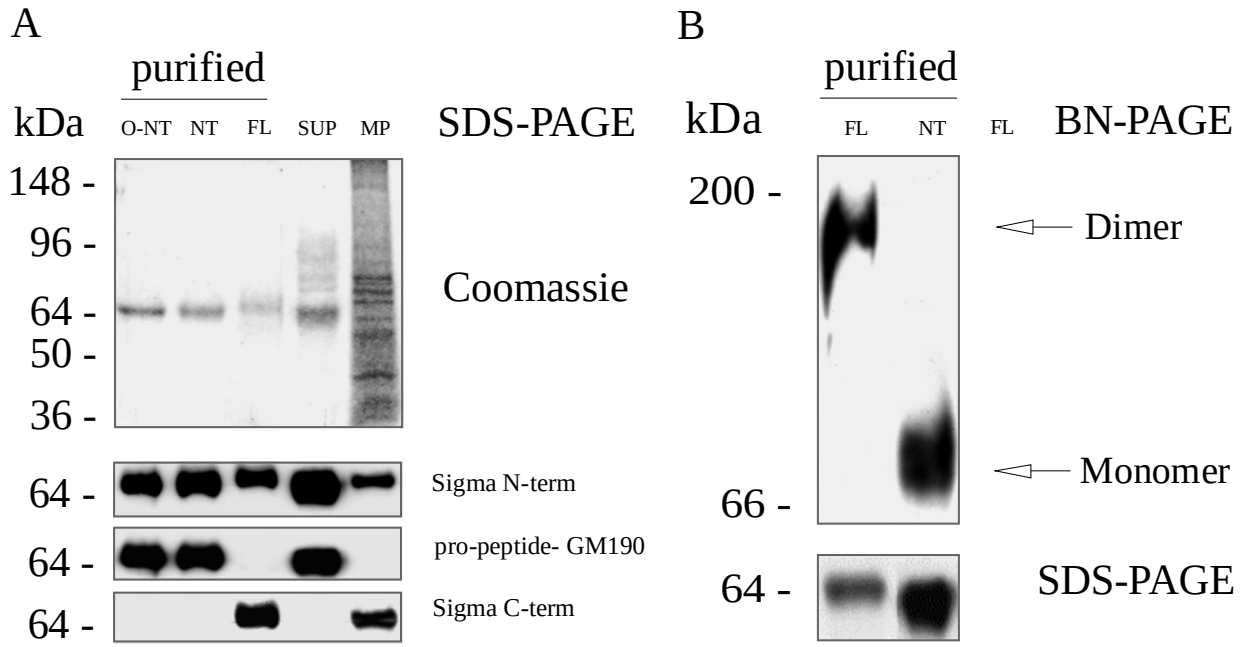


**Figure 24: Purification of native dimeric BACE-FL and monomeric BACE-NT**

(A) Coomassie-stained SDS-PAGE with commercial BACE-NT (O-NT), purified BACE-NT (NT) and BACE-FL (FL) compared to unpurified supernatant (SUP) and a total membrane preparation (MP). The corresponding Western blot shows signals detected with the pro-peptide-, N-terminal and C-terminal antibodies. Note that BACE-NT carries the pro-domain.
(B) BN-PAGE demonstrates the purification of dimeric BACE-FL and monomeric BACE-NT. 10 ng of purified BACE-NT (NT) and BACE-FL (FL) were separated on a 6-16% BN-PAGE and detected with the myc epitope specific antibody 9E10. Purified BACE-NT (NT) migrates to 70 kDa while BACE-FL (FL) migrates to 140 kDa.

Using purified BACE, measurements of enzyme kinetics were subsequently performed. The Michaelis-Menten kinetic obtained for the quenched fluorogenic substrate Cy3-SEVNLDAEFK-(Cy5Q)-NH2 harboring the Swedish APP cleavage site [151] showed a higher affinity and catalytical activity for dimeric BACE-FL compared to monomeric BACE-NT and the commercial BACE-NT-onco which served as a means of validation of the measurements (Figure 25 and Table 27).

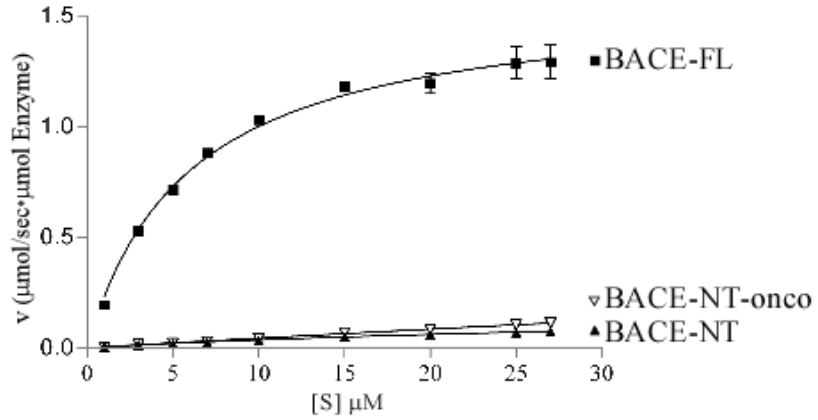


**Figure 25: Michaelis-Menten kinetics of BACE-FL compared to BACE-NT**

Enzymatic kinetics of the HPLC purified BACE-Dimer compared to the monomer: Michaelis-Menten curves of BACE-FL in comparison to BACE-NT and commercial BACE-NT-onco (Oncogene) show significant differences in $K_M$ and $k_{cat}$ of the enzymes.

As can be seen in Figure 25, saturation kinetics for BACE-NT could not be obtained under the experimental conditions used since much higher substrate concentrations would have been needed. For a valid comparison, kcat at 10 µM was determined which shows that BACE-FL is about 30 times more catalytically active than BACE-NT at this substrate concentration. Due to a nearly linear Michaelis-Menten curve within the range of substrate concentrations used, kcat and KM for the commercial BACE-NT could not be estimated by a nonlinear fit. Thus, the second order rate constant kcat / KM from a quasilinear plot of velocity as a function of substrate concentration as described in Material and Methods. The obtained value is nearly identical to the one for the BACE-NT produced in our laboratory, as is the kcat at 10 µM (Figure 25 and Table 27).

To further exclude the possibility that the presence of the pro-domain in BACE-NT was responsible for the difference in kinetics, the pro-domain was removed by incubation of the purified BACE-NT with Furin which was reported to cleave the prodomain of BACE [127]. Subsequently, the kinetics were compared between the pro-domain free BACE-NT (nopro BACE-NT) and untreated BACE-NT (Figure 26 A). Both versions of the enzyme showed a similarly low affinity to the substrate with an almost linear Michaelis-Menten plot within the range of substrate concentrations utilized (Figure 26 B).

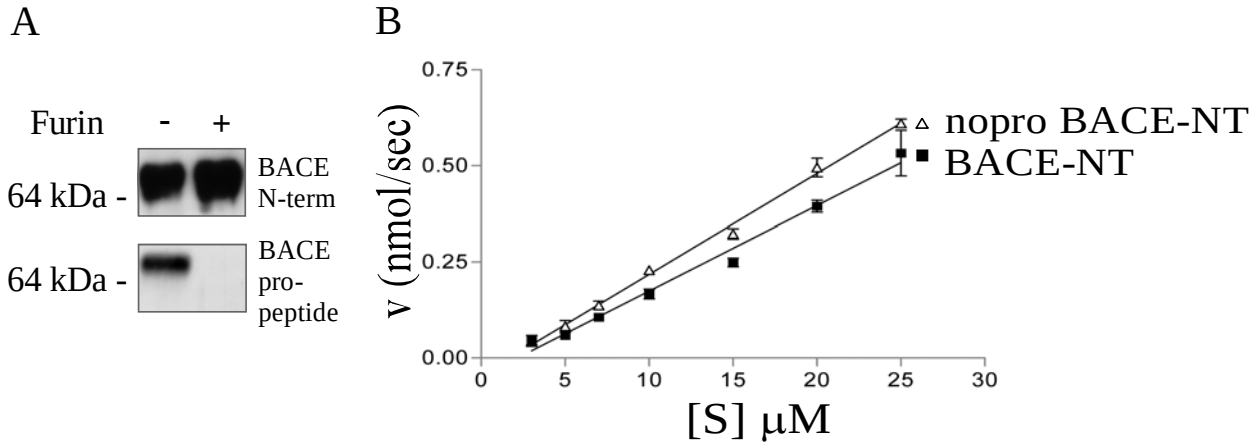


**Figure 26: Effect of the pro-domain of BACE on its enzymatic efficiency**

(A) HPLC purified BACE-NT was processed with Furin to remove the pro-domain. The immunoblot demonstrates the absence of the pro-peptide after Furin-cleavage as shown by the absence of a signal with the pro-peptide specific antibody GM190. The N-terminal antibody detects both cleaved and uncleaved protein. (B) The enzymatic kinetics of BACE-NT without pro-domain (nopro BACE-NT) and BACE-NT are nearly identical over a range of substrate concentrations from 2-25 μM. Note that due to the small amounts of noproBACE-NT obtained, the concentration of the enzyme was not determined via active site titration and the graph consequently displays the initial velocities instead of the turnover rates.

In accordance with Shi et al. [212] it is thus proposed that the pro-domain of BACE has little effect on the BACE active site. The kinetic data rather suggest that the relatively poor kinetic parameters of BACE-NT are due to its inability to dimerize, although the differences in amino acid sequence between BACE-FL and BACE-NT in themselves could theoretically also have an impact on the differences in kinetic properties observed.
Interestingly, an in-vitro cleavage experiment published earlier in [201] only yielded sufficient cleavage products when membrane preparation of BACE-FL were used, whereas no cleavage was observed with BACE-NT as enzyme, again suggesting that both species might also vary in enzymatic efficiency with respect to other substrates than APP.
Summing up, these kinetic data support the notion that homodimerization of BACE optimizes the enzymatic efficiency with respect to the substrate APP.

| Enzyme | $K_M$(μM) | $k_{cat}$($sec^{-1}$) | $k_{cat}$([S]=10μM) ($sec^{-1}$) | $k_{cat}/K_M$ ($\mu M^{-1}sec^{-1}$) |
|---|---|---|---|---|
| BACE-FL | 5,9 ± 0,5 | 1,59 ± 0,08 | 1,03 ± 0,02 | 0,269 ± 0,017 |
| BACE-NT | 50,5 ± 5,2 | 0,21 ± 0,02 | 0,0330 ± 0,0006 | 0,0042 ± 0,0001 |
| BACE-NT -onco | nd | nd | 0,0422 ± 0,0007 | 0,0043 ± 0,00006* |

**Table 27: Table showing the kinetic properties of BACE-FL compared to BACE-NT**

Note, that for commercial BACE-NT-onco the second order rate constant kcat/ KM was calculated from a quasilinear plot of velocity as a function of substrate concentration (*). "nd" = not determined.

# 9 Discussion

## 9.1 Evidence for a BACE-Dimer

Huse and colleagues hypothesized that BACE might form oligomeric proteins which could be a prerequisite for exit from the ER. These authors found that in the absence of the reducing agent β-mercaptoethanol (BME) in the SDS-PAGE gel loading buffer, BACE migrated faster and as a single band as compared to the characteristic doublet in the presence of BME, indicating that non-reduced BACE is able to build intramolecular dissulfide bonds. When they incubated BACE in the absence of BME only at 37°C or 55°C as opposed to 95°C, they detected small amounts of BACE migrated as a higher molecular weight species around 220 kDa suggesting BACE oligomers with some degree of SDS resistance. To exclude the possibility that these bands were due to artificial SDS aggregation, Huse et. al. loaded BACE on continuous sucrose velocity gradient in the presence of either Triton X-100 or CHAPS, but could not detect significant amounts of BACE in higher density fractions. The authors thus conclude that BACE exists primarily as a monomer [134].

Sidera et al. performed a Ni2+ – affinity purification of BACE to study whether BACE can cleave off its pro-domain in an autocatalytic manner which they found to be true in contrast to the papers suggesting Furin as the pro-peptide convertase. They also analyzed the molecular weight of Ni2+ – affinity purified full-length, histidine tagged BACE on SDS-PAGE gels and detected a larger band at around 140 kDa and a 200 kDa band in addition to the monomeric size. They hypothesized that this might represent a putative dimer and trimer, although the 200 kDa band was more prominent upon longer storage and at higher protein concentrations indicating that it was partly due to non-specific aggregation. Removal of N-linked sugars by PNGase reduced the size of the putative 140kDa large Dimer to about 100kDa, which is in agreement with the calculated weight of two non-modified BACE molecules [127]. Reduction with DTT and β-mercaptoethanol almost completely removed the ~200-kDa protein and increased the intensity of the 75-kDa band, but did not affect the putative dimer (140-k) suggesting strong intramolecular non-disulphide protein-protein interactions resistant to high salt and non-ionic detergents used during purification or the strong denaturing conditions of SDS-boiling used during SDS-PAGE [130].

In another study, activity of lipid raft associated BACE extracted from guinea pig brain was demonstrated to be associated with a high molecular weight complex with a inconsistent size ranging from 140 to 600 kDa depending on the cell line and the technique used. From Sucrose gradient floatation studies they obtained a molecular weight larger than 100kDa, on native gel they detected BACE at around 250 kDA, on glycerol gradients BACE extracted from brain was separated at sizes larger than 600 kDa, by gel filtration from CHO cell 290 kDa and from Brain over 2000 kDa. To assess β-secretase activity within glycerol gradient fractions, this study used an internally quenched fluorogenic substrate based on the Swedish mutant APP sequence. By crude comparison of fractions from two separate gradients, they state that the mean relative fluorescent signal from higher molecular weight fractions (larger than 600 kDa) was

stronger (roughly factor 1.5) than that form the lower molecular weight fractions, although they contained ten fold less BACE protein as measure by densitometry. For this comparison, they however assumed equal affinity of the antibody to the differently sized BACE in the separate fractions. The authors conclude form these data, that the native BACE complex shows considerably higher β-secretase activity than the monomer [234].
Higher molecular weight species of BACE, approximately 120 kDa large, was also detected in human brain tissue and was resistant to high salt, nonionic detergents or reducing conditions [235]. With mere reference to the size of 120 kDa of the detected BACE species, which is a multiple of the calculated size of BACE at 60 kDa, the authors term this BACE species a dimer, although they do not strictly show, that this is the case. The BACE "dimer", was not detected by a pro-domain specific antibody suggesting that it consists of mature BACE molecules. Furthermore, BACE homodimers could only partially be separated by elution form a Q-Sepharose column at high salt conditions. BACE enriched by Ion exchange chromatography was subsequently incubated with the aspartic protease inhibitor pepstatin A-agarose beads, washed and eluted exclusively as a dimer whereas a monomer was detected in the flow through. When the same was done with purified soluble ectodomain of BACE, it was shown that it was more easily dissociated from pepstatin by the washing step, suggesting a lower affinity to the inhibitor pepstatin. Also, the ectodomain appeared exclusively as a monomer on all SDS gels.
Schmechel et. al. then went on to analyze a BACE mutant in which one of the two critical aspartates of the active site was replaced by an Alanine (D289A), such that one would expect this mutant to be inactive. Surprisingly, this mutant had similar activity as wtBACE as assayed by the production of soluble APP. To explain this, the authors suggest that in vivo, the active site of the β-secretase could be composed of two N-terminal DTGS active site motifs of two separate BACE molecules which cooperate as a dimer, so that one missing Aspartate within the monomer, as is the case in D289A could be compensated by dimerization. The authors furthermore speculate that although BACE has two active site motifs, it may have adopted the mechanism of the single lobe retroviral proteases that constitute their active site upon dimerization of two lobes only containing one half of the actives site. Also dimerization might be a means to regulate enzymatic activity [235].

## 9.2 Methods to identify a Dimer

There are several established biochemical methods to study protein-protein interactions in general: Protein Affinity Chromatography, co-immunoprecipitation, cross-linking, yeast two-hybrid system and others (for an overview see [236]). More advanced techniques to address oligomeric state and function of proteins include analytical ultracentrifugation, freeze-fracture electron microscopy chromatography, rotational correlation spectroscopy, radiation inactivation, chemical cross-linking, reconstitution titration experiments, or complementation studies [237].
To specifically proof the dimeric state of a protein, the following steps should be undertaken.
First, it should be established that BACE exists in a physiological higher molecular weight complex, by choosing an appropriate method that excludes artificial aggregation

(see section 9.3 for a discussion of BN-PAGE below). This is a technical challenge especially for membrane proteins which contain hydrophobic domains. Huse et. al had the suspicion that BACE might have a dimeric quaternary structure when they incubated BACE from 293 cells without boiling and in the absence of BME and analyzed the samples on SDS PAGE. To exclude SDS-induced aggregation, they subsequently performed sucrose velocity gradients in the presence of Triton X-100 or CHAPS and only saw minor amounts of BACE in higher molecular fractions [134]. Marlow and colleagues used gel filtration, glycerol gradients, sucrose gradient floatation as three different methods which all yielded different sizes of a HMW complex [234].

BN-PAGE was chosen for analysis of the native size of BACE, a method whose advantages in studying native membrane proteins will be discussed below and which has been successfully used to study the γ-secretase complex [214].

Second, it is interesting to show that the multi-protein complex consists of mature proteins because this makes it more likely that the putative protein complex is indeed a physiological, functional entity instead of just being the effect of artificial aggregation. Sidera et al. showed that removal of N-linked sugars by PNGase reduced the size of the putative 140kDa large Dimer to about 100kDa [130]. Schmechel and others demonstrated, that the dimeric band was not detected by the propeptide-specific antibody GM190 [235], a method that was also applied in the present study with the same result.

Third, the composition of the complex should be studied by analyzing its components. The complex should thus be purified and the purity as well as its functional integrity of the purified material confirmed, for instance by assessing enzymatic activity. In this regard, Sidera and colleagues used Ni2+ – affinity purification of BACE and assured enzymatic activity by in vitro assays using swe APP purified from HEK 293 cells [130]. Schmechel et al. applied anion exchange chromatography using a Q-Sepharose column, followed by binding to lentil-lectin sepharose, which is a specific adsorbant to glucose or mannose type sugars, and an affinity column containing the aspartic protease inhibitor pepstatin to purify a BACE dimer. However, they did not show that the purified material is still enzymatically active, thus functionally intact [235].

In the present study, BACE was purified from native membrane preparations by Ni2+ – affinity column and verified integrity of the obtained material by subsequent kinetic measurements.

However, postulating a dimer by reference to the fact that its size is a multiple of the corresponding monomer can still be mistaken because proteins of similar sizes could have been co-purified. Thus, the purified complex should be disintegrated to differentiate its components. Marlow et. al separated Monomer and Dimers on a glycerol gradient [234]. Schmechel et al. separated monomeric from dimeric BACE by gradient elution from a Q-sepharose column at high salt concentrations. After treatment with urea and high concentrations of SDS, they could partially monomerize the Dimer and separate both on 2D SDS gels. In contrast, a purified BACE-ectodomain exclusively migrated to monomeric size on all gels which is in agreement with the data obtained for BACE-NT on BN-PAGE [235].

In the present study, an alternative approach was pursued. It was determined that differently tagged BACE-FL molecules can interact with each other by detecting co-immunoprecipitated BACE on denaturing SDS gels. Furthermore, it was demonstrated

that this capacity is lost in soluble BACE-NT (Figure 17). In accordance with this, endogenous neuronal BACE has double the native size than BACE-NT on BN-PAGE, whose size in turn can however be doubled again by addition of the GPI anchor sequence.
By analogy, one can thus arrive at the conclusion that the native size differences on BN-PAGE can be explained by homodimeric interaction shown by co-immunoprecipitation and that endogenous neuronal BACE physiologically exists as a dimer. It however cannot be excluded, that BACE may not also alternatively establish stable contacts to other proteins of around 70 kDa, or that additional small molecules stably interact with the BACE homodimer.

## 9.3 BN gels to study native proteins

Analysis of the oligomeric state of membrane proteins has proven to be difficult because of their tendency to aggregate when isolated [237]. There are several reports on SDS-induced aggregation of membrane proteins which was assumed to particularly effect proteins which retain a significant level of secondary structure as was described for polytopic proteins [238].
To tackle this problem, Schagger and colleagues developed Blue Native polyacrylamide gel electrophoresis (BN-PAGE) as a method for the isolation of intact protein complexes and initially applied this technique for the study of mitochondrial proteins [220]. Meanwhile, the use of BN-PAGE has increased exponentially over the past few years and new applications have been developed [239]. BN-PAGE has been used extensively in identifying the composition of mitochondrial complexes [223, 240-248]. In recent years it was also successful in uncovering the identity of the components of the γ-secretase complex [93, 214, 249].
As a principle of electrophoresis, proteins (or complexes) need a charge to have mobility in an electric field. The charge usually comes from a chemical additive, such as sodium dodecyl sulfate (SDS), that binds to a protein and confers a uniform charge and thus electrophoretic mobility. However, SDS is such a strong detergent which not only causes dissociation of protein complexes, but also complete denaturation. Schagger et al. [220] thus introduced the Coomassie dye Serva Blue G which adds a negative charge (Schagger therefore called it “charge shift” method) to the protein complexes without dissociating them [239]. Coomassie keeps membrane proteins solubilized by tight binding due its hydrophobicity and poor solubility in water. This largely reduces the problem of artificial aggregation. Whereas in SDS-PAGE an excess of denaturing SDS is used, BN-PAGE applies only a minimum amount of neutral detergent, which furthermore only binds to the surface of the proteins unlike SDS, which unfolds and dissociates proteins. In SDS PAGE, the acrylamide concentrations used would allow all proteins to run out of the gel. The proteins however have a uniform charge/mass ratio due to excess SDS, such that the molecular mass can be inferred from the difference in distance traveled given a specific time interval. In contrast to this, in BN-PAGE, the pore-size distribution of the acrylamid-gel determines the endpoint of migration for the proteins, whereas their charge/mass ratio is variable. Determination of molecular masses of native complexes is

possible with BN-PAGE with much less protein amounts required than for analytical ultracentrifugation, velocity gradients or gel filtration [250].

Ideally however, the amount of Coomassie bound to the complex of interest should be determined to correctly deduce the real molecular mass of the complex from the observed size, since the dye adds to the observed mass [237]. However, the conclusion from the experiments presented herein rely on relative comparisons of molecular sizes that represent multiples of the size of the denatured protein. Moreover, one can refer to BACE-NT as a molecular weight standard for monomeric BACE, since it has very similar sizes under native and denaturing conditions.

Although the risk of artificial aggregation of proteins is reduced by Coomassie, membrane proteins may still aggregate nonspecifically when the detergent is replaced by the Coomassie dye [237]. In an extended study, Heuberger et al. validated BN-PAGE against analytical ultracentrifugation and found that BN-PAGE is a precise method to decipher oligomeric conformations and that furthermore the oligomeric structures observed in detergent solution reflect the real membrane-embedded states of the proteins as measured by Freeze-fracture Electronmicroscopy [237]. They also noted that aggregation can be observed as a ladder of greater molecular mass species on BN-PAGE which correlated with aggregation indicated by the inability to reach equilibrium in sedimentation equilibrium centrifugation and timedependent increases in the absorbance between 320 nm and 340 nm due to light-scattering [237].

Such a “ladder” has not been seen the experiments analyzing overexpressed BACE in cell lines and was largely suppressed by optimized native membrane prep techniques when endogenous BACE from whole brain lysates was used as probe. Moreover, not only could BACE-NT serve as a reference point for native monomeric BACE, the fact that its size could be doubled by adding the very small GPI anchor motif (SLENGGTSLSEKTVLLLVTPFLAAAWSLHP) in the absence of the TM makes it very unlikely that BACE-FL artificially aggregates due to its hydrophobic TM. It cannot be excluded, that larger oligomers of native BACE exist in viable tissue, but the data on dimeric ER-retained BACE-KKXX suggest that the BACE dimer presumably would be the initial step in any association process to a putatively larger oligomeric BACE complex.

An extension of the BN-PAGE technology that has not been exploited extensively in the investigation presented herein is the 2D electrophoresis involving BN-PAGE in the first dimension and a classical SDS-PAGE in the second dimension, which was for instance used for the purification of the γ-secretase complex. In the case of hydrophobic membrane proteins, this has particular advantages over classical isoelectric focusing (IEF). First, hydrophobic membrane proteins tend to precipitate at the basic pole during IEF. Second, all functional information regarding protein-protein interactions is lost due to the high stringency, denaturing conditions of both gel dimensions. In contrast to this, important information regarding functional protein-protein interactions is contained in the BN gels [248]. When the molecular weight of a native protein in the first dimension is different from its molecular weight in the denaturing second dimension, it is very likely that the protein is part of a complex and associated with other proteins, or multiple copies of itself [248]. However, results have to be evaluated carefully because hydrophobic membrane proteins have a tendency to form aggregates. Therefore, proving that two

proteins are in the same complex requires additional evidence. In the present study, this evidence was obtained from the Co-IP experiments.

## 9.4 Co-Immunoprecipitation to detect Dimers

As described above, Co-IP experiments (Figure 15 and Figure 17) were used to supplement the data from BN-PAGE. There are several criteria which are generally agreed on to confirm the authenticity of Co-IP experiments.

It has to be established that the antibody does not itself recognize the co-precipitated protein. The use of monoclonal antibodies generally reduces cross-reaction and it was ensured in the present study that the monoclonal antibodies did not show cross reactivity, i.e. signal were only produced if the specific HA or myc antigen was present. Also, co-precipitation was shown „both ways“ by using either antibody as precipitating antibody.

Furthermore, it has to be made sure that the interaction takes place in the cell and is not a consequence of cell lysis. In the present study, post-lysis extracts were therefore mixed to confirm that there was no false positive Co-IP signal due to artificial post-lysis aggregation.

Provided that these quality criteria are met, co-IP experiments have the following distinct advantages over other methods to show protein-protein interactions. First, they detect the interactions in the midst of all the competing proteins present in a crude lysate, such that the results have a built-in specificity control. Second, elaborate complexes can be precipitated in their native state. Third, proteins are in their natural state of posttranslational modification which might be important for the interaction.

On the other hand, a disadvantage is that co-immunoprecipitated proteins do not necessarily interact directly, since they can be part of larger complexes [236]. However, as discussed above, the difference in native size of BACE-NT and BACE-GPI imply that a hypothetical third mediating interaction partner had to be fairly small. The proteins that were reported to have an interaction with BACE (see section 5.7.3 on interaction partners above) are unlikely to account for that because of their size (PS N-terminal fragments: approximately 27 kDa [205], phospholipid scramblase 1: 37 kDa [251] Nicastrin: ~150 kDa, GGA1:78kDa [252])

## 9.5 Domain deletion analysis

The analysis of BACE-NT on BN-PAGE showed that the BACE ectodomain exists as a monomer even in the presence of excess BACE-FL. Interestingly, the BACE-NT construct used in this study mimicks shedded BACE in its sequence, thus predicting that shedded BACE might also be a monomer. BACE-shedding seems to be mediated by ADAM 10 [229] and regulated by the palmitoylation status of the C-terminus [128]. Its physiological role remains however controversial. Benjannet et al. showed a strong increase in Amyloid-β 1-40 due to the overexpression of the BACE ectodomain [128]. This finding was confirmed in the present study using APPs β accumulated over 24 hours as a selective indicator of β-secretase activity (Figure 20) suggesting that BACE-NT is active in the cell. In contrast, Hussain and co-workers did not observe any large change in APPs β or CTF production from cells expressing full length BACE if shedding was

inhibited. They suggest that inhibiting the BACE sheddase as opposed to overexpressing the BACE ectodomain is a more physiological model to study the specific effect of BACE shedding on APP processing [229].

### 9.5.1 Functionality of the BACE constructs

To verify the functionality of the constructs used in this study, it was decided to measure the production of swedish APPs-β as an indicator for BACE activity. This is advantageous because this product could specifically be detected with the neoepitope specific antibody sw192 within the media of the cells. Furthermore, APPs-β seems to be a more specific indicator of BACE-activity than amyloid-β or CTFs because it is not processed further once secreted from the cells. In contrast to this, the process by which β-CTFs are converted to β-amyloid depends on additional factors that might confound results. The in vivo experiment displayed in Figure 20 showed that all constructs were functional within a physiological environment. However, since swe APPs-β was accumulated over 24 hours in the media, no kinetic differences can be inferred from these in vivo experiments.

### 9.5.2 The role of the transmembrane domain

Significant activity of BACE-NT was detected in the in vivo experiment (Figure 20) as assessed by APPs-β which is in good agreement with other studies [127, 131, 185]. Furthermore, it was also found that BACE-pA as well as BACE-NT produced similarly large amounts of CTFs as the other constructs (Figure 20, lowest panel). This is in contrast to a finding by Yan et al. who saw no CTFs produced by a BACE ectodomain construct, not even if it was retained in the ER by a KDEL motif and confronted with excess APP by BFA treatment [136]. Yan et al. thus concluded that the TM domain is necessary for BACE to access its substrate APP. The data from the present study however showed that neither deleting the TM domain nor replacing it by an unspecific poly-alanine stretch abolished cellular activity of BACE. However, the in vitro kinetic experiments also suggest that BACE-NT has an lower enzymatic efficiency probably due to its incapacity to dimerize. Therefore it can alternatively be concluded that deleting the TM domain leads to a decreased enzymatic efficiency because it leads to artificial BACE monomers.

## 9.6 Rafts and membrane attachment of BACE

Evidence from the literature has been presented above, that APP, Amyloid-β, PS1 [154] as well as the other three components of the γ-secretase complex [253] and BACE are all found in lipid rafts, which are cholesterol enriched microdomains.

With respect to the raft-association of BACE, it is therefore interesting to discuss whether raft associated proteins were specifically enriched by the sample preparation used.

Initially DRMs on their part have been defined as membrane portions insoluble to Triton X-100 or CHAPS at 4 degree Celsius [152, 153]. In recent studies however , a wider range of detergents, among those Brij 96, Brij 98 and Lubrol, have been used to enrich rafts. There are also attempts to subclassify rafts based on their differential solubility in

different detergents. In a comparison of different detergent, Triton X-100 was shown to lead to raft aggregation following detergent extraction whereas Brij96 did not cause this problem. The properties of Lubrol in this respect have not been determined [254]. The detergent Brij 35 was furthermore shown to be more efficient than Triton X-100 in extracting rafts [255]. Riddel and colleagues found that using MBS buffer containing 1% (w/v) Lubrol WX to lyse cells resulted in the best separation on a sucrose density gradient of raft associated BACE from non-raft proteins, whereas Triton X-100 was worse [155]. Lubrol WX was also successfully used to demonstrate the association of all four components of the γ-secretase complex with rafts was also shown using Lubrol WX as a detergent [253].

The sample preparation method in the present study has been optimized to get a sharp separation of native BACE on BN-PAGE. The usage of detergent therefore was dictated by the BN-PAGE methodology, as discussed above in detail, which necessitates the usage of non-ionic detergents. Of those, Triton X-100 has produced the best results. In the present experiments, material from cells lysed in hypotonic buffer were treated with 1% (w/v) Lubrol WX and 1% (w/v) Brij35 during preparation of postnuclear supernatant (PNS) followed by ultracentrifugation to pellet Brij-Lubrol insoluble material in the presence of 5% Glycerol to prevent artificial aggregation.

As specified in material and methods, the Brij-Lubrol insoluble pellet was solubilized in 1% (w/v) Tx-100 in sodium citrate buffer at 4°C and Tx-100 insoluble material cleared by ultracentrifugation. The Brij-Lubrol insoluble and Tx-100 soluble material was consequently referred to as “membrane preparations ”. Although it was not a specific aim to enrich raft- associated proteins, the “membrane preparations” were likely to contain raft associated proteins which were cleared by some fraction insoluble in Triton X-100.

On the other hand, the Brij-Lubrol soluble material obtained as supernatant after the first ultracentrifugation step was consequently brought to a final concentration of 1% (w/v) Triton X-100, and Triton X-100 insoluble material cleared from the supernatant by ultracentrifugation. The resulting material was thus soluble in Lubrol, Brij35 and Tx-100 soluble material was subsequently referred to as “native lysate”.

Given its solubility in all three detergents used the “native lysate” was likely to be cleared off raft associated proteins. Indeed, the sample preparation used in the present study lead to a clear separation of soluble BACE-NT, which was almost exclusively found in the native lysate whereas the membrane attached BACE-GPI, reported to be found in rafts [156] was detected in the membrane preparations (Figure 22).

## 9.6.1 The effect of attaching a GPI anchor to BACE

A striking feature of the proteins in DRMs is that many of them are linked to lipids. These include both GPI anchored proteins [256], and proteins such as Src-family kinases [153].

Cordy and co-workers demonstrated that BACE can be efficiently targeted to rafts by replacing the transmembrane and cytosolic domains of BACE with a GPI-anchor sequence[156]. In the present study, it was similarly shown that adding a GPI signal to BACE-NT attaches the ectodomain to the membrane as demonstrated by the fact that it is found in the membrane preparation as opposed to BACE-NT (Figure 22). The shift in molecular size from BACE-NT (~ 70 kDa) to BACE-GPI (~ 140 kDa) displayed in Figure

21 and Figure 22 cannot be explained by size of the GPI anchor. We used the GPI anchor motif of CD59 (other names :MACIF, MIRL, HRF-20 or protectin) and added it to BACE-NT, thus prolonging it by the sequence ASLENGGTSLSE-KTVLLLVTPFLAAAWSRHP. Meri and colleagues [257] found the ω-site of the transamidase to be at the Asparagine (N77 in their numbering and underlined in the sequence). Assuming that the process of GPI-anchor attachment of BACE-GPI proceeds similar to that of CD59, the sequence of BACE-GPI would thus be elongated by four amino-acids (ASLEN). Meri et al. measured the molecular mass of the GPI anchor as Mr 2817.4 by Mass spectroscopy [257]. Adding the molecular mass of the amino-acids ASLEN, roughly estimated by a standard algorithm to approximately Mw 500 [**] thus results in a theoretical difference in molecular mass between BACE-NT and BACE-GPI of approximately 3.5 kDa. This is clearly not close to the difference in molecular size of about 70 kDa actually observed on BN-PAGE. We thus conclude that membrane anchorage of BACE-NT by the GPI anchor establishes proximity such that the dimer interfaces within the ectodomain can meet.

Furthermore it was demonstrated that in contrast to BACE-NT, BACE-GPI displays a very prominent surface staining (Figure 19) which is in agreement with the fact that the plasma membrane is very rich in sphingolipids and cholesterol and an important source of lipid rafts [153]. In contrast, the endoplasmic reticulum (ER) and intermediate compartments between the ER and the Golgi have very little sterol, and are unlikely to house DRMs. The TGN is however again rich in cholesterol and was demonstrated to contain DRMs. In accordance with this, BACE was localized to cholesterol-rich microdomains following transit from the ER to the Golgi complex [155].

Given that BACE-NT bypasses the TGN and does not maturate, it is thus most probably not found in lipid rafts whereas the majority of BACE-GPI is raft-associated. This is in agreement with the finding that BACE-NT was almost exclusively found in the detergent soluble fraction of the sample preparation procedure (Figure 22).

One could hypothesize from these data that dimerization of BACE might thus not depend on association to any type of membrane but on attachment to rafts, as cholesterol enriched microdomains of membranes, in particular. Following this thought, BACE-NT might be incapable of dimerization because it is not localized to rafts after reaching the plasma membrane but is secreted instead. Analogously, BACE-GPI would dimerize because raft association is reconstituted by adding the GPI anchor. In contrast to this line of thought however, it was also demonstrated that dimerization takes place in the ER were lipid rafts are not present in significant concentrations.

## 9.7 Kinetic Properties of monomeric and dimeric BACE

The experiments presented herein revealed that the BACE-ectodomain, widely used for measurements of enzyme kinetics and inhibitor studies is a monomer as opposed to the endogenous BACE which naturally occurs as a dimer. The significant differences in enzymatic efficiency that were identified (Figure 25 and Figure 27) suggest that one should validate results from inhibitor studies obtained with the BACE-ectodomain against full length BACE. These findings also predict that significant structural differences of the

[**] http://au.expasy.org/cgi-bin/peptide-mass.pl

active site should be found if a crystal structure of dimeric BACE-FL were obtained and compared to the existing structures of the soluble BACE ectodomain.

To present date, kinetic parameters for BACE-FL as compared to the ectodomain of BACE have only been published by Kopcho et al. [210] so far. They compared the kinetics of BACE-FL enriched in unpurified membrane-preparations of CHO cells with purified versions of BACE-NT and detected no significant kinetic differences using a Swedish-APP-like substrate. However, they did not analyze the native size of BACE-FL in their preparation and a direct comparison of both species is impossible since BACE-FL was not purified [210].

Another group reported that they observed an almost identical catalytic activity for the purified ectodomain of BACE and a full length version of the enzyme. However, no kinetic parameters were published [137]. Furthermore, these authors stored full length BACE at 4 C which given experience from our lab caused the BACE dimer to destabilize. Therefore, BACE samples were always stored immediately at -80 degrees C and we avoided multiple thaw-freeze circles. According to this experience, one could speculate that their full length BACE could have lost its native conformation.

Marlow et al. showed a separation of smaller and larger BACE variants by a glycerol gradient but the separation was not very sharp with respect to molecular weight [234]. Furthermore the comparison of the enzymatic activity within these separated fractions was very crude since simply the change of RFU over time at a single substrate concentration was measured. The actual difference in RFU which was measured was only factor 1.5. The authors however relied on the argument that in addition an approximate 10 fold difference in protein concentrations of the different fractions, as measured by WB had to be taken into account thus increasing the apparent kinetic difference.

This argument however seems only to be sound if one assumes that the antibody is equally affine to both BACE species, which can not be taken for granted. Another critical premise of Marlow et. al. which does not seem to be warranted is that the enzymatically active fraction is identical to the amount of immunoreactive BACE detected by WB, i.e. that the sample preparation did not result in any functionally inactive enzyme molecules, which is very unlikely. An equilibration according to the concentration of active sites (active site titration) followed by the determination of Michaelis-Menten kinetics, as in the present study would have been desirable.

Schmechel et al. also separated monomeric BACE from dimeric by a Q-Sepharose column and a pepstatin affinity column [235]. However they did not show that those purified BACE samples were enzymatically active [235].

In the present study, BACE-FL was purified from membrane preparations and it was ensured that the native dimer was conserved under assay conditions. Applying this criteria, it was seen that relative to the monomeric BACE-NT, the dimeric BACE-FL displays a higher affinity and turnover rate towards an APP-like substrate, while the artificial monomer shows poor kinetic parameters.

These two BACE variants differed in three aspects. First, their difference in amino-acid sequence. Second, the presence of the pro-domain in case of BACE-NT. Third their oligomeric state. Theoretically, the prodomain could alter the kinetic parameters in two ways: via an effect on the active site cleft or because BACE itself might be a competitive

substrate to APP if the report by Hussain et al on autocatalysis under in vitro conditions at pH 4.5 are true [59]. We however determined the effect of the prodomain, by cleaving it off with Furin and found it to have no significant effect on the kinetic properties observed (Figure 26) This is in good agreement with a series of papers that show that BACE is not a true zymogen, at least with respect to APP as a substrate, since prodomain containing BACE efficiently cleaves APP in vivo [128, 131] as well as in vitro [209, 212]. This leaves the differences in primary or quaternary structure as explanations for the kinetic differences observed.

A limitation of the studies presented above as well as the present study therefore is that they can not differentiate between kinetic differences observed due to the sequence differences or the difference in quaternary structure. To properly test this hypothesis, one would thus have to separate purified BACE-FL in its monomeric and dimeric native configuration. Marlow tried this but only presented a very crude assay for enzymatic activity that does not allow for a quantitative comparison. Schmechel et. al did not prove enzymatic functionality of their monomeric and dimeric BACE preparations.

In the present experiments, a BACE-FL monomer was however not observed on a BN-PAGE nor were monomers detected in the eluate from the purification column.

An alternative approach to overcome the limitations of the study would have been to artificially disrupt the BACE dimer by a detergent. This method however takes the risk that the native conformation is destroyed and enzymatic function is severely perturbed. The BN-PAGE technique used in the present study prevented usage of charged detergents. Trials with NP40 and SDS, followed by dialysis to remove the charged detergents, did only produce a “smear” across different molecular weights on a BN-PAGE but no sharp monomeric bands, such that this approach was not pursued any further.

In summary, it could still theoretically be possible that the differences in kinetic properties between dimeric BACE-FL and monomeric BACE-NT observed in the present study are explainable by the different amino acid sequences as opposed to the difference in the quaternary structure of the two species of BACE. Given the data about their extremely different quaternary structure however, one assumes that a significant part of the kinetic differences observed were due to the impact of the different oligomeric states of BACE on its enzymatic activity. This leads to the interesting hypothesis that BACE activity could be modulated by dimerization. Furthermore, it will be interesting to study the effect of dimerization on the enzymatic efficiency of BACE with respect to the other known substrates of BACE, which might prove to be more physiological than APP.

## 9.8 Physiological function of Dimers in general

In light of evolution theory, it is very interesting to hypothesize about the functional role of protein assembling to complex quaternary structures.

First, dimerization of proteins could be advantageous because of a gain in stability. Indeed, the interactions between the subunits in dimeric proteins are amongst the strongest and most extensive in nature. By means of hydrophobic interaction, hydrogen and dissulfide bonds, as well as salt bridges, dimer interactions are very long-lived.

These features distinguish dimer interactions from other protein-protein contacts, which in comparison, are often weaker temporary contacts [258].
Second, dimerization could also serve in regulating the trafficking of the proteins. Such motifs regulating the quality control of the ER have been identified and will be discussed below. Also, dimerization could be important in coding information and passing it on in signal transduction processes. In this way, dimerization appears to be a general concept for membrane receptors such as G protein-coupled receptors where dimerization results in second messenger production [259].
Third, dimerization might be essential as a means to improve and regulate enzymatic function. Indeed, oligomerization of enzymes to multi-enzyme-complexes is favored because it greatly improves the maximum catalytic efficiency [260]. This parameter is limited by the speed of diffusion processes that determine the maximum frequency with which an enzyme interacts with its substrate. In multi-enzyme complexes, the distances that a reaction product (which is the substrate of the subsequent enzymatic reaction) has to travel between the enzymatic components is minimized thus increasing the maximum efficiency of the total enzymatic reaction. Furthermore, in some instances, water is excluded from the complex, such that hydrating and dehydrating of the substrate does not have to take place between every reaction. Also “channeling” the substrate through an enzymatic complex prevents it from being consumed in uncontrolled side-reactions. Finally, there is the great advantage that a multi-enzyme-complex can be subjected to a uniform control mechanism which operates through interacting conformational changes in multi-protein complexes [260].
A remarkable example of such regulated multi-enzyme complexes is the pyrimidinebiosynthetic pathway which in E. coli is catalyzed by a half dozen individual enzymes, whereas in mammalian cells those components are covalently linked into two multi-catalytic proteins [260]. A number of metabolic pathways are known in which sequential enzymes interact with each other, both physically and functionally. These include nucleotide synthesis, Krebs urea cycle, Krebs TCA cycle, glycolysis, the pentose phosphate shunt as well as synthesis of RNA [260]. In this sense, dimerization serves as the basis for enzymatic cooperativity.

## 9.9 Physiological function of the BACE dimer in particular

### 9.9.1 Stability

Whereas other non-viral aspartic proteases, like Pepsin, Gastricin, Renin and Cathepsin D exist as soluble monomers, Cathepsin E is the only known aspartic protease that exists as a homodimer consisting of two fully catalytically active monomers. [261]. Dimerization of Cathepsin E, occurs by intermolecular disulfide-linkage at an dissulfide bond close to the N-terminus that is not present in the other aspartic proteases [262]. Mutating this cysteine to an alanine, resulted in a full length Cathepsin E monomer that displayed correct intracellular localization and carbohydrate modification [263]. It showed almost identical enzymatic efficiency as tested by a chromogenic substrate and was equally inhibited by pepstatin, an inhibitor of aspartyl proteases. However, the artificial monomer showed a 30 fold shorter half-life under 55° C, and a worse pH

resistance than the dimeric wt Cathepsin E, suggesting that dimerization confers stability to the enzyme whereas it does not modulate enzymatic efficiency [262, 263]. In contrast to Cathepsin E, Sidera et. al established for BACE, that the dimeric band at 140 kDa which they detected could not be reduced by DTT nor β-mercaptoethanol, suggesting that the BACE dimer is not stabilized by dissulfide bonds [130].
In agreement with this, BACE was subjected to 10% Mercaptoethanol and did not detect a breakdown of the dimeric band on BN-PAGE (Figure 22, last lane). This is in keeping with data presented above which showed that the three dissulfide bonds in BACE are all intramolecular linkages which can not be used for intermolecular interactions [133] but are important for correct folding and enzymatic activity [113].
It would be interesting to compare the stability of dimeric BACE-FL to that of BACE-FL monomers. As stated above, BACE-FL monomer was not observed on a BN-PAGE nor were BACE monomers eluated from the purification column. However, one could try to devise a purification scheme that is capable of separating BACE monomers form BACE dimers. An alternative strategy would be to identify the critical residues within the dimer interact to generate an artificial monomeric BACE-FL.

## 9.9.2 Dimerization and Raft association

Many surface receptors, such as Fc receptors, T- and B-cell receptors, dimerize or oligomerize after ligand binding, and this has been shown to increase association with lipid rafts [264, 265]. In analogy, dimerization might be important for regulating raft association of BACE. Interestingly, APP also dimerizes and an artificially stabilized APP dimer results in a 7-fold increase in Amyloid-β production [266]. Although the authors favor the idea that this might be due to impaired clearance of Amyloid-β, it could also be due to improved raft association of APP which was found in rafts [154]. Thus, apart from improving the enzymatic efficiency of BACE as shown in the present study, dimerization of BACE might also favor the access to its substrate APP by improving raft-association of BACE [159].

## 9.9.3 Cooperative active sites

### 9.9.3.1 Cooperation of active sites in the BACE Dimer

As discussed above, a conclusion from the present study would be that homodimerization of BACE optimizes the enzymatic efficiency with respect to APP as a substrate.
An extension of this idea was presented by Schmechel et al. who stated that the critical aspartates of two BACE molecules might cooperatively form an active site by dimerization in analogy to single lobe retroviral aspartic proteases [267]. Retroviral proteases are symmetrical homodimers, with each dimer structurally related to the larger class of single-chain aspartic peptidases. Dimerization is essential for catalytic activity as the substrate binding site and the active site are formed from residues of each monomer [268].
Schmechel et al. put forward the hypothesis that the active sites in the BACE dimer could be formed “between” two BACE molecules in a BACE dimer, rather than “within” each

monomer separately, that is, instead of possessing an independent active site consisting of two aspartates, each BACE monomer could contribute one of its aspartates to an active site formed between the BACE monomers.
They suggest this hypothesis to explain the finding, that the BACE mutant D289A, lacking one of the critical aspartates, was nevertheless similarly active as wt BACE.
However there is a line of papers which do not replicate this finding with respect to the activity of an aspartate mutant of BACE.
In one of the initial papers, which identified BACE as the β-secretase, Hussain et. al. mutated both catalytical aspartyl residues in BACE to asparagine and saw that APPs-β production was abolished in comparison to wt BACE. They suggested based on this finding that BACE is an aspartic protease [111]. The inactivity of BACE D289N was subsequently confirmed by Huse et. al. who did not observe any increase in Amyloid-β production when they overexpressed this mutant as compared with wt BACE [203].
Similarly, it was shown that mutating the complementary aspartyl residue D93 to an Alanine (D93A), abolishes C99 and Amyloid-β production [126, 128]. The same result was reported by Hattori et. al who tested both D93A and D289A [204]. The BACE D93A mutant also did not cleave APP nor the alternative substrate PSGL1 in an assay using alkaline phosphatase (AP) fusion proteins (APP-AP and PSGL1-AP) [201], nor did a double mutation D93/289A in the same assay [150]. Furthermore a D93N variant was not proteolytically active towards an APP-invertase reporter protein in a yeast-growth assay [269].
It is unclear, how the contrasting results reported by Schmechel et. al. could be explained. It is conceivable that endogenous BACE was upregulated in the D289A expressing cells, which was not controlled for by these authors. In this respect, a purification of D289A dimers followed by kinetic in vitro measurement in comparison to wt BACE dimers would be method to exclude this confounder. If indeed D289A were active in such an in vitro assay, one would expect that this activity could be abolished in the monomeric analog BACE D289A-NT. Furthermore, complementary experiments with the D93A mutant should be performed.
In fact, lysates from cells expressing D93A, D289A and both variants together were studied in the enzymatic assay and no cleavage of the fluorescent substrate was detected as controlled with BACE-FL (data not shown). Similarly, de Strooper expressed combinations of those mutations in cells and did not measure any activity (personal communication).
One has to conclude from this that the hypothesis by Schmechel et. al. stating that the active sites of BACE monomers can cooperate in a BACE dimer is not supported by the data presented above.

### 9.9.4 Interference with the dimer interface as a therapeutic strategy

As alluded to above, the wide substrate pocket of BACE [179] as well as the strong structural similarities [65] to BACE2 raise severe technical difficulties for the development of potent and specific inhibitors directed against the active site of BACE. Given the devastating nature of AD and its increasing incidence with prolonged human life-spans, it is of course of paramount interest to inhibit the rate-limiting step of Amyloid-β generation.

Thus it is worthwhile thinking about an alternative and potentially complementary therapeutic strategies to inhibit β-secretase activity.
Given that BACE is a dimer according to the data presented herein, inspiration from applied research on the HIV protease can be sought. As presented above, the HIV protease is activated by dimerization of two inactive monomers. In recent years, researchers have thus looked for methods to interfere with dimerization and thereby inhibit activity of the HIV protease. Similarly, the dimeric interface of the HIV reverse transcriptase and integrase, whose action is also dependent on oligomeric structure, have been assessed as targets for therapeutic intervention [270]. Several low-molecular weight and cross-linked interfacial peptides were generated which interfere with the highly conserved dimeric interface and inhibit HIV protease activity at nanomolar concentrations [268]. Although there is no clinical candidate for HIV therapy so far, realizing this dimeric interface interference approach [271], the technical idea has been widely extended to other targets directly relevant in medicine, such as the Herpes simplex Virus [272, 273] or the pathogen causing malaria [274].
In order to extend this approach to BACE, one however has to analyze the conditions that have to be met for an attractive target for such an approach. The HIV Protease for instance is very suitable because of the interdigitating nature of its dimerization interface, the limited number of crucial residues responsible for stable dimer formation, the fact that monomers are not extremely tightly bound and of course most importantly the fact that the monomers are inactive [268]. In contrast to this, the residues in the ectodomain of BACE that are critical for the dimer interface are yet to be identified in detail.

### 9.9.4.1 Prediction of the dimer interface of BACE

Given that several 3D structures of BACE are available, computational methods to predict the Dimer interface might provide crucial data to restrict the search space for a future mutation analysis.
In this regard, there has been longstanding interest in identifying the binding forces between proteins in multimeric complexes. Early analysis concentrated on aspects of stoichiometry and stereochemistry and gained an understanding of the fundamental importance of symmetry. Protein-protein interactions, hydrophobic interactions, hydrogen bonds, salt bridges and disulfide bonds have been studies with respect to their impact on dimeric stability and specificity of the interaction. In an extensive review on dimeric structures, Jones et. al have identified the relative probability of amino-acid residues to be in the dimeric interface rather than on the surface of the protein. They also performed statistical analyses of structural similarities [258].
On the basis of these and other studies, considerable advances have been made recently by a multi-disciplinary approach to build a “comprehensive dictionary of proteins” which will “allow us to assemble proteins as words into meaningful sentences [275].” One of these techniques is “computational docking” which tries to predict biologically relevant quaternary conformations from crystallographic data of the isolated proteins. These “docking methods” are based on observed properties of the statistical composition of interacting surfaces in terms of residue types (polarity, charge, etc.) and on the structure of the surfaces. Modern implementations of those in neural networks reach an accuracy in predicting resolved structures of ~70% [276]. Smith and colleagues published an

interesting review [277] on novel methods for physical docking and also indicate web pages, where those algorithms can be tested [††].

One of these programs, termed DCOMPLEX, predicts the binding affinity of protein complexes [278]. It provides an accurate prediction of binding free energy of protein–peptide and protein–protein complexes with a correlation coefficient of 0.87 with respect to the actual observed data form a large databank of dimeric interactions.

Querying this program [‡‡] with the structure of the BACE ectodomain resolved by Hong et al. [181], resulted in a the binding free energy is -7.019728 Kcal/mol for the ectodomain interacting with itself which is a respective value as compared to the database of dimeric interactions used which resulted in calculated values ranging form -4.7 to -22.65 Kcal/mol.

It is also interesting to note that the structures of inhibitor-bound BACE ectodomain, (entry "1FKN" in the Protein Data Bank (PDB) [179]) and "1MH4" [181] respectively) displayed dimeric conformation in the asymmetric unit. The structure of unbound β-Secretase Catalytic Domain (entry: 1SGZ [279]) even contains 4 identical chains in their asymmetric unit. In this respect, the structures solved for BACE are not decisive, because there were also structures of BACE resolved which have only a single chain of BACE bound to the inhibitor as asymmetric unit (entry 1W50 and 1W51 [182] as well as Entry 1XS7 [280].

Those three "monomeric" structures were fed to the Docking Algorithm ClusPro [281, 282 §§]. This algorithm uses rigid-body docking and a discrimination algorithm that rapidly filters docked conformations with respect to their electrostatics properties and ranks them according to their clustering properties. The matrix below depicts which PDB entries were used for the docking simulation (Figure 28). The resulting three-dimensional docked conformations were subsequently analyzed with DeepView / Swiss-Pdb Viewer v.3.70 (© GlaxoSmithKline), as freely available on the web [***]. Side groups that are within a radius of 6 Å adjacent to the docked protein chain were selected to visualize the predicted dimer interface.

[††] Servers http://www.bmm.icnet.uk/~smithgr/db.html#servers , Programs http://www.bmm.icnet.uk/~smithgr/soft.html

[‡‡] available at the site http://phyyz4.med.buffalo.edu/czhang/complex.html

[§§] available on the web page http://nrc.bu.edu/cluster/

[***] http://kr.expasy.org/spdbv/

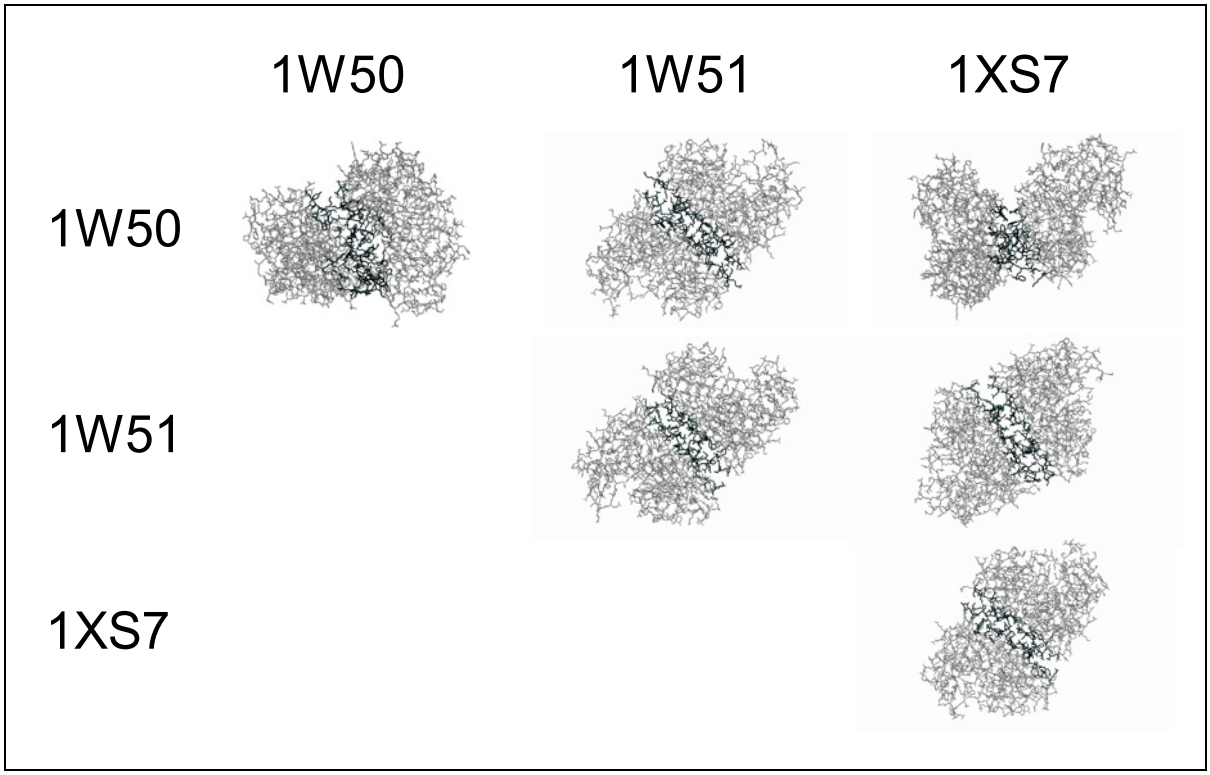


**Figure 28: Matrix of Docking Simulations performed with ClusPro**

Shown are representational pictures of the three-dimensional "docked dimers" created by DeepView / Swiss-Pdb Viewer v.3.70 (© GlaxoSmithKline). The matrix indicates which combination of crystallographic structures (PDB entries 1W50, 1W51 and 1xS7 respectively) were subjected to ClusPro. Side groups within 6 Å, representing the dimer interface are seen is colored black.

Interestingly, there were six "motifs" within the BACE sequence (LOCUS: AF190725- The Entrez Nucleotides database [†††]) that were within the dimer interface of 5 out of 6 of the docking simulations performed (Figure 29).

**Figure 29: Residues predicted by ClusPro to be in the dimer interface**

MAQALPWLLLWMGAGVLPAHGTQHGIRLPLRSGLGGAPLGLRLPRETDEEPEEPGRRGSFVEMVDNLRGKSGQ
GYYVEMTVGSPPQTLNILVDTGSSNFAVGAAPHPFLHRYYQRQLSSTYRDLRKGVYVPYTQGKWEGELGTDLV
SIPHGPNVTV**RAN**IAAITESDKFFINGSNWEGILGLA**YAE**IARP**DDSLE**PFF**DSLVKQTHVPN**LFSLQLCGAG
FPLNQSEVLASVGGSMIIGGIDHSLYTGSLWYT**PIRRE**WYYEVIIVRVEINGQDLKMDCKEYNYDKSIVDSGT
TNLRLPKKVFEAAVKSIKAASSTEKFPDGFWLGEQLVCWQAGTTPWNIFPVISLYL**MGEVTN**QSFRITILPQQ
YLRPVEDVATSQDDCYKFAISQSSTGTVMGAVIMEGFYVVFD**RARKR**IGFAVSACHVHDEFRTAAVEGPFVTL
DM***ED***C***GYN***IPQTDESTLMTIAYVMAAICALFMLPLCLMVCQWRCLRCLRQQHDDFADDISLLK

Residues predicted to be in the dimer interface are inidcated as follows: residues found 1x (grey), 2x (***italic***) , 3x (**BOLD**) , and 5x (**BOLD**) out of the 6 docking simulations performed are formatted in the style indicated in the brackets.

[†††] http://www.ncbi.nlm.nih.gov/entrez/query.fcgi?db=Nucleotide&itool=toolbar

It will be very interesting to test these predictions by mutating the respective residues and controlling whether BACE is monomerized as a result.
The crucial question however remains whether the reduction of enzymatic efficiency obtained by creating artificial BACE monomers would suffice to prevent accumulation of Amyloid-β and clinical symptoms, since the data shows that although BACE-FL is about 30 fold more catalytically active than BACE-NT as calculated at 10 µM (Figure 25 and Table 27), BACE-NT displays considerable enzymatic activity.
However, monomerizing BACE by an interfacial peptide might also exert a beneficial effect via other mechanisms.
If the hypothesis of Ehehalt et. al. [159] is valid, which states that dimerization of BACE improves association to lipid rafts, interference with the dimeric interface of BACE could decrease raft association of BACE and thereby access of BACE to APP. Given that the incidence of AD rises late in life (increase from 2.8 per 1,000 person years in the 65-69 year age group to 56.1 per 1,000 person years in the older than 90 year age group [283]), one might speculate that it might suffice to prolong the onset of AD for about 10 years in order to dramatically reduce the incidence of AD. Therefore a small decrease in BACE activity might already be effective.
Furthermore, since correct folding to quaternary structure often is a prerequisite for an oligomeric protein to pass the quality control in the ER, monomerizing BACE could also lead to the sequestration and degradation of BACE thus reducing the amount of active BACE within the cell. In support of this idea is the finding of Yan et. al, that ER retained BACE-NT-KDEL does not effectively cleave APP [136]. Assuming that BACE-NT-KDEL is monomeric, which would have to be confirmed experimentally, these data could indicate that monomeric BACE retained in the ER is much less active. Similarly BACE-FL, when artificially monomerized by interfacial peptides and thus retained in the ER, could be effectively inhibited in its enzymatic activity.
Taken together, one could thus conceive of three potential effects of interfacial inhibitors on BACE: the reduction of enzymatic efficiency, impaired raft association resulting in decreased access to APP, as well as reduced half-life due to sequestration in the ER. Although classical inhibitors of the active site have certainly a high potential to be effective in the future, those alternative theoretical interventions, could serve as a valuable alternative for the prevention and treatment of Alzheimer´s disease. Computational methods to predict the dimer interface, shown to be within the ectodomain by the present study, put crucial constraints on future experiments which will evalutate these therapeutic ideas.

# 10 Conclusions

The analysis of BACE under native conditions on BN-PAGE and in Co-immunoprecipitation experiments revealed that BACE physiologically has a dimeric quaternary structure in murine brain and in different cell lines. Domain deletion experiments subsequently revealed that the dimeric interface lies within the ectodomain of BACE but that for dimerization to occur, membrane attachment is an additional prerequisite. ER-retention of BACE showed that dimerization occurs as early as in the ER. Measurements of enzyme kinetics furthermore demonstrated that the monomeric BACE ectodomain less enzymatically efficient as compared with dimeric native full length BACE. Since the monomeric BACE ectodomain is so widely used for kinetic studies, this has implications on future inhibitor screens. In particular, the data presented herein suggests that results obtained with the artificial monomeric BACE ectodomain should be validated with dimeric full length BACE preparations. In addition, the observed differences in enzymatic efficiency will prompt further investigations in to a putative regulative function of BACE dimerization with respect to the in vivo cleavage of the known BACE substrates. Pinpointing the exact structure of the dimeric interface of BACE, predicted to be in the ectodomain by the present study, would be desirable to examine whether Amyloid-β production could be therapeutically decreased by interference with the dimeric interface of BACE. The feasibility of such an alternative therapeutic strategy to treat Alzheimer´s disease has been discussed.

# 11 Acknowledgements

I am much obliged to Prof. Haass and Dr. Michael Willem for their theoretical guidance and friendly support as well as their invaluable help on everyday challenges. I thank Michael for the amicable atmosphere he created in the lab and for many hours of discussion. I am grateful for intellectual input from Stefan Lichtenthaler and Christoph Kaether and practical support from Hartmut Kaiser and Glenn Lurman. I am also very much indebted to C, A, V, R, S, J for their support.

# 12 Bibliography


1. UpToDate, I. U., Inc. founded by Burton D. Rose, MD & Joseph M. Rush, MD. UpToDate Online 13.1. (2005).
2. Alzheimer, A. Über einen eigenartigen, schweren Erkrankungsprozess der Hirnrinde. Neurol Zbl 25, 1134 (1906).
3. Alzheimer, A. Über eine eigenartige Erkrankung der Hirnrinde. Allg Z Psychiatrie Psychisch-Gerichtl Med 64, 146-148 (1907a).
4. Alzheimer, A. Über eine eigenartige Erkrankung der Hirnrinde. Zbl Nervenheilkd Psychiatr 30 (Neue Folge 18 bd), 177–179 (1907b).
5. Alzheimer, A. Über eigenartige Krankheitsfälle des späteren Alters. Zbl Ges Neurol Psych 4, 356-385 (1911).
6. Moller, H. J. & Graeber, M. B. The case described by Alois Alzheimer in 1911. Historical and conceptual perspectives based on the clinical record and neurohistological sections. Eur Arch Psychiatry Clin Neurosci 248, 111-22 (1998).
7. Graeber, M. B., Kosel, S., Grasbon-Frodl, E., Moller, H. J. & Mehraein, P. Histopathology and APOE genotype of the first Alzheimer disease patient, Auguste D. Neurogenetics 1, 223-8 (1998).
8. IV, D.-. Diagnostic and Statistical Manual of Mental Disorders DSM-IV-TR.
9. Cotran, R. S., Kumar V, Collins T. Robbins pathologic basis of disease. (1999).
10. Yankner, B. A. Mechanisms of neuronal degeneration in Alzheimer's disease. Neuron 16, 921-32 (1996).
11. Crowther, R. A. & Goedert, M. Abnormal tau-containing filaments in neurodegenerative diseases. J Struct Biol 130, 271-9 (2000).
12. Masters, C. L. et al. Amyloid plaque core protein in Alzheimer disease and Down syndrome. Proc Natl Acad Sci U S A 82, 4245-9 (1985).
13. Ikeda, S., Yanagisawa, N., Allsop, D. & Glenner, G. G. Early senile plaques in Alzheimer's disease demonstrated by histochemistry, immunocytochemistry, and electron microscopy. Hum Pathol 21, 1221-6 (1990).
14. Kang, J. et al. The precursor of Alzheimer's disease amyloid A4 protein resembles a cell-surface receptor. Nature 325, 733-6 (1987).
15. Sisodia, S. S. & St George-Hyslop, P. H. gamma-Secretase, Notch, Abeta and Alzheimer's disease: where do the presenilins fit in? Nat Rev Neurosci 3, 281-90 (2002).
16. wKang, J. & Muller-Hill, B. The sequence of the two extra exons in rat preA4. Nucleic Acids Res 17, 2130 (1989).
17. Selkoe, D. J. Alzheimer's disease: genes, proteins, and therapy. Physiol Rev 81, 741-66 (2001).
18. Haass, C., Koo, E. H., Mellon, A., Hung, A. Y. & Selkoe, D. J. Targeting of cell-surface beta-amyloid precursor protein to lysosomes: alternative processing into amyloid-bearing fragments. Nature 357, 500-3 (1992).
19. Koo, E. H. & Squazzo, S. L. Evidence that production and release of amyloid beta-protein involves the endocytic pathway. J Biol Chem 269, 17386-9 (1994).
20. Koo, E. H., Squazzo, S. L., Selkoe, D. J. & Koo, C. H. Trafficking of cell-surface amyloid beta-protein precursor. I. Secretion, endocytosis and recycling as detected by labeled monoclonal antibody. J Cell Sci 109 (Pt 5), 991-8 (1996).
21. Lammich, S. et al. Constitutive and regulated alpha-secretase cleavage of Alzheimer's amyloid precursor protein by a disintegrin metalloprotease. Proc Natl Acad Sci U S A 96, 3922-7 (1999).
22. Lichtenthaler, S. F. & Haass, C. Amyloid at the cutting edge: activation of alpha-secretase prevents amyloidogenesis in an Alzheimer disease mouse model. J Clin Invest 113, 1384-7 (2004).
23. Buxbaum, J. D. et al. Evidence that tumor necrosis factor alpha converting enzyme is involved in regulated alpha-secretase cleavage of the Alzheimer amyloid protein precursor. J Biol Chem 273, 27765-7 (1998).
24. Slack, B. E., Ma, L. K. & Seah, C. C. Constitutive shedding of the amyloid precursor protein ectodomain is up-regulated by tumour necrosis factor-alpha converting enzyme. Biochem J 357, 787-94 (2001).
25. Haass, C. et al. Amyloid beta-peptide is produced by cultured cells during normal metabolism. Nature 359, 322-5 (1992).
26. Kaether, C. & Haass, C. A lipid boundary separates APP and secretases and limits amyloid beta-peptide generation. J Cell Biol 167, 809-12 (2004).
27. Gotz, J., Chen, F., van Dorpe, J. & Nitsch, R. M. Formation of neurofibrillary tangles in P301l tau transgenic mice induced by Abeta 42 fibrils. Science 293, 1491-5 (2001).
28. Mudher, A. & Lovestone, S. Alzheimer's disease-do tauists and baptists finally shake hands? Trends Neurosci 25, 22-6 (2002).
29. Hardy, J. & Selkoe, D. J. The amyloid hypothesis of Alzheimer's disease: progress and problems on the road to therapeutics. Science 297, 353-6 (2002).
30. Selkoe, D. J. Alzheimer's disease is a synaptic failure. Science 298, 789-91 (2002).
31. Selkoe, D. J. Deciphering the genesis and fate of amyloid beta-protein yields novel therapies for Alzheimer disease. J Clin Invest 110, 1375-81 (2002).
32. Walsh, D. M. & Selkoe, D. J. Deciphering the molecular basis of memory failure in Alzheimer's disease. Neuron 44, 181-93 (2004).
33. Schenk, D. Alzheimer's disease. A partner for presenilin. Nature 407, 34-5 (2000).
34. Schenk, D., Games, D. & Seubert, P. Potential treatment opportunities for Alzheimer's disease through inhibition of secretases and Abeta immunization. J Mol Neurosci 17, 259-67 (2001).
35. Oddo, S., Billings, L., Kesslak, J. P., Cribbs, D. H. & LaFerla, F. M. Abeta immunotherapy leads to clearance of early, but not late, hyperphosphorylated tau aggregates via the proteasome. Neuron 43, 321-32 (2004).
36. Lewis, J. et al. Enhanced neurofibrillary degeneration in transgenic mice expressing mutant tau and APP. Science 293, 1487-91 (2001).
37. Gotz, J., Schild, A., Hoerndli, F. & Pennanen, L. Amyloid-induced neurofibrillary tangle formation in Alzheimer's disease: insight from transgenic mouse and tissue-culture models. Int J Dev Neurosci 22, 453-65 (2004).
38. Hebert, L. E. et al. Age-specific incidence of Alzheimer's disease in a community population. Jama 273, 1354-9 (1995).
39. Evans, D. A. et al. Prevalence of Alzheimer's disease in a community population of older persons. Higher than previously reported. Jama 262, 2551-6 (1989).
40. Silverman, J. M., Smith, C. J., Marin, D. B., Mohs, R. C. & Propper, C. B. Familial patterns of risk in very late-onset Alzheimer disease. Arch Gen Psychiatry 60, 190-7 (2003).
41. Tan, Z. S. et al. Plasma total cholesterol level as a risk factor for Alzheimer disease: the Framingham Study. Arch Intern Med 163, 1053-7 (2003).
42. Kalmijn, S. et al. Dietary intake of fatty acids and fish in relation to cognitive performance at middle age. Neurology 62, 275-80 (2004).
43. Engelhart, M. J. et al. Diet and risk of dementia: Does fat matter? The Rotterdam Study. Neurology 59, 1915-21 (2002).
44. Citron, M. et al. Mutation of the beta-amyloid precursor protein in familial Alzheimer's disease increases beta-protein production. Nature 360, 672-4 (1992).
45. Citron, M. et al. Excessive production of amyloid beta-protein by peripheral cells of symptomatic and presymptomatic patients carrying the Swedish familial Alzheimer disease mutation. Proc Natl Acad Sci U S A 91, 11993-7 (1994).
46. Slooter, A. J. et al. The impact of APOE on myocardial infarction, stroke, and dementia: the Rotterdam Study. Neurology 62, 1196-8 (2004).
47. Esch, F. S. et al. Cleavage of amyloid beta peptide during constitutive processing of its precursor. Science 248, 1122-4 (1990).
48. Anderson, J. P. et al. Exact cleavage site of Alzheimer amyloid precursor in neuronal PC-12 cells. Neurosci Lett 128, 126-8 (1991).
49. Kojro, E., Gimpl, G., Lammich, S., Marz, W. & Fahrenholz, F. Low cholesterol stimulates the nonamyloidogenic pathway by its effect on the alpha -secretase ADAM 10. Proc Natl Acad Sci U S A 98, 5815-20 (2001).
50. Hooper, N. M. & Turner, A. J. The search for alpha-secretase and its potential as a therapeutic approach to Alzheimer s disease. Curr Med Chem 9, 1107-19 (2002).
51. Fahrenholz, F., Gilbert, S., Kojro, E., Lammich, S. & Postina, R. Alpha-secretase activity of the disintegrin metalloprotease ADAM 10. Influences of domain structure. Ann N Y Acad Sci 920, 215-22 (2000).
52. Postina, R. et al. A disintegrin-metalloproteinase prevents amyloid plaque formation and hippocampal defects in an Alzheimer disease mouse model. J. Clin. Invest. 113, 1456-1464 (2004).
53. Saunders, A. J. et al. BACE Maps to Chromosome 11 and a BACE Homolog, BACE2, Reside in the Obligate Down Syndrome Region of Chromosome 21 . Science 286, 1255a- (1999).
54. Vassar, R. et al. Beta-secretase cleavage of Alzheimer's amyloid precursor protein by the transmembrane aspartic protease BACE. Science 286, 735-41 (1999).
55. Yan, R. et al. Membrane-anchored aspartyl protease with Alzheimer's disease beta-secretase activity. Nature 402, 533-7 (1999).
56. Acquati, F. et al. The gene encoding DRAP (BACE2), a glycosylated transmembrane protein of the aspartic protease family, maps to the down critical region. FEBS Lett 468, 59-64 (2000).
57. Solans, A., Estivill, X. & de La Luna, S. A new aspartyl protease on 21q22.3, BACE2, is highly similar to Alzheimer's amyloid precursor protein beta-secretase. Cytogenet Cell Genet 89, 177-84 (2000).
58. Kim, D. Y., Ingano, L. A. & Kovacs, D. M. Nectin-1alpha, an immunoglobulin-like receptor involved in the formation of synapses, is a substrate for presenilin/gamma-secretase-like cleavage. J Biol Chem 277, 49976-81 (2002).
59. Hussain, I., Christie, G., Schneider, K., Moore, S. & Dingwall, C. Prodomain processing of Asp1 (BACE2) is autocatalytic. J Biol Chem 276, 23322-8 (2001).
60. Yan, R., Munzner, J. B., Shuck, M. E. & Bienkowski, M. J. BACE2 functions as an alternative alpha-secretase in cells. J Biol Chem 276, 34019-27 (2001).
61. Bennett, B. D. et al. Expression analysis of BACE2 in brain and peripheral tissues. J Biol Chem 275, 20647-51 (2000).
62. Hussain, I. et al. ASP1 (BACE2) cleaves the amyloid precursor protein at the beta-secretase site. Mol Cell Neurosci 16, 609-19 (2000).
63. Farzan, M., Schnitzler, C. E., Vasilieva, N., Leung, D. & Choe, H. BACE2, a beta -secretase homolog, cleaves at the beta site and within the amyloid-beta region of the amyloid-beta precursor protein. Proc Natl Acad Sci U S A 97, 9712-7 (2000).
64. Fluhrer, R. et al. A non-amyloidogenic function of BACE-2 in the secretory pathway. J Neurochem 81, 1011-20 (2002).
65. Chou, K. C. Insights from modeling the tertiary structure of human BACE2. J Proteome Res 3, 1069-72 (2004).
66. Sherrington, R. et al. Cloning of a gene bearing missense mutations in early-onset familial Alzheimer's disease. Nature 375, 754-60 (1995).
67. Levy-Lahad, E. et al. Candidate gene for the chromosome 1 familial Alzheimer's disease locus. Science 269, 973-7 (1995).
68. Feng, R. et al. Deficient neurogenesis in forebrain-specific presenilin-1 knockout mice is associated with reduced clearance of hippocampal memory traces. Neuron 32, 911-26 (2001).
69. Yu, H. et al. APP processing and synaptic plasticity in presenilin-1 conditional knockout mice. Neuron 31, 713-26 (2001).
70. De Strooper, B. et al. A presenilin-1-dependent gamma-secretase-like protease mediates release of Notch intracellular domain. Nature 398, 518-22 (1999).
71. De Strooper, B. et al. Deficiency of presenilin-1 inhibits the normal cleavage of amyloid precursor protein. Nature 391, 387-90 (1998).

72. Wolfe, M. S. et al. Two transmembrane aspartates in presenilin-1 required for presenilin endoproteolysis and gamma-secretase activity. Nature 398, 513-7 (1999).
73. Weihofen, A. & Martoglio, B. Intramembrane-cleaving proteases: controlled liberation of proteins and bioactive peptides. Trends Cell Biol 13, 71-8 (2003).
74. Wolfe, M. S. Presenilin and gamma-secretase: structure meets function. J Neurochem 76, 1615-20 (2001).
75. Wolfe, M. S. & Haass, C. The Role of presenilins in gamma-secretase activity. J Biol Chem 276, 5413-6 (2001).
76. Thinakaran, G. et al. Endoproteolysis of presenilin 1 and accumulation of processed derivatives in vivo. Neuron 17, 181-90 (1996).
77. Ratovitski, T. et al. Endoproteolytic processing and stabilization of wild-type and mutant presenilin. J Biol Chem 272, 24536-41 (1997).
78. Thinakaran, G. et al. Evidence that levels of presenilins (PS1 and PS2) are coordinately regulated by competition for limiting cellular factors. J Biol Chem 272, 28415-22 (1997).
79. Steiner, H. et al. Expression of Alzheimer's disease-associated presenilin-1 is controlled by proteolytic degradation and complex formation. J Biol Chem 273, 32322-31 (1998).
80. Esler, W. P. & Wolfe, M. S. A portrait of Alzheimer secretases--new features and familiar faces. Science 293, 1449-54 (2001).
81. Haass, C. & Steiner, H. Alzheimer disease gamma-secretase: a complex story of GxGD-type presenilin proteases. Trends Cell Biol 12, 556-62 (2002).
82. Wolfe, M. S. et al. Peptidomimetic probes and molecular modeling suggest that Alzheimer's gamma-secretase is an intramembrane-cleaving aspartyl protease. Biochemistry 38, 4720-7 (1999).
83. Martoglio, B. & Golde, T. E. Intramembrane-cleaving aspartic proteases and disease: presenilins, signal peptide peptidase and their homologs. Hum Mol Genet 12 Spec No 2, R201-6 (2003).
84. Lichtenthaler, S. F. et al. The intramembrane cleavage site of the amyloid precursor protein depends on the length of its transmembrane domain. Proc Natl Acad Sci U S A 99, 1365-70 (2002).
85. Steiner, H. et al. Glycine 384 is required for presenilin-1 function and is conserved in bacterial polytopic aspartyl proteases. Nat Cell Biol 2, 848-51 (2000).
86. Capell, A. et al. The proteolytic fragments of the Alzheimer's disease-associated presenilin-1 form heterodimers and occur as a 100-150-kDa molecular mass complex. J Biol Chem 273, 3205-11 (1998).
87. Li, Y. M. et al. Presenilin 1 is linked with gamma-secretase activity in the detergent solubilized state. Proc Natl Acad Sci U S A 97, 6138-43 (2000).
88. Yu, G. et al. Nicastrin modulates presenilin-mediated notch/glp-1 signal transduction and betaAPP processing. Nature 407, 48-54 (2000).
89. Goutte, C., Tsunozaki, M., Hale, V. A. & Priess, J. R. APH-1 is a multipass membrane protein essential for the Notch signaling pathway in Caenorhabditis elegans embryos. Proc Natl Acad Sci U S A 99, 775-9 (2002).
90. Francis, R. et al. aph-1 and pen-2 are required for Notch pathway signaling, gamma-secretase cleavage of betaAPP, and presenilin protein accumulation. Dev Cell 3, 85-97 (2002).
91. Lee, S. F. et al. Mammalian APH-1 interacts with presenilin and nicastrin and is required for intramembrane proteolysis of amyloid-beta precursor protein and Notch. J Biol Chem 277, 45013-9 (2002).
92. Steiner, H. et al. PEN-2 is an integral component of the gamma-secretase complex required for coordinated expression of presenilin and nicastrin. J Biol Chem 277, 39062-5 (2002).
93. Edbauer, D. et al. Reconstitution of gamma-secretase activity. Nat Cell Biol 5, 486-8 (2003).
94. Kimberly, W. T. et al. Gamma-secretase is a membrane protein complex comprised of presenilin, nicastrin, Aph-1, and Pen-2. Proc Natl Acad Sci U S A 100, 6382-7 (2003).
95. Takasugi, N. et al. The role of presenilin cofactors in the gamma-secretase complex. Nature 422, 438-41 (2003).
96. Shirotani, K., Edbauer, D., Kostka, M., Steiner, H. & Haass, C. Immature nicastrin stabilizes APH-1 independent of PEN-2 and presenilin: identification of nicastrin mutants that selectively interact with APH-1. J Neurochem 89, 1520-7 (2004).
97. LaVoie, M. J. et al. Assembly of the gamma-secretase complex involves early formation of an intermediate subcomplex of Aph-1 and nicastrin. J Biol Chem 278, 37213-22 (2003).
98. Iwatsubo, T. The gamma-secretase complex: machinery for intramembrane proteolysis. Curr Opin Neurobiol 14, 379-83 (2004).
99. Kopan, R. & Goate, A. A common enzyme connects notch signaling and Alzheimer's disease. Genes Dev 14, 2799-806 (2000).
100. Fortini, M. E. Gamma-secretase-mediated proteolysis in cell-surface-receptor signalling. Nat Rev Mol Cell Biol 3, 673-84 (2002).
101. Artavanis-Tsakonas, S., Rand, M. D. & Lake, R. J. Notch signaling: cell fate control and signal integration in development. Science 284, 770-6 (1999).
102. Ebinu, J. O. & Yankner, B. A. A RIP tide in neuronal signal transduction. Neuron 34, 499-502 (2002).
103. Ni, C. Y., Murphy, M. P., Golde, T. E. & Carpenter, G. gamma -Secretase cleavage and nuclear localization of ErbB-4 receptor tyrosine kinase. Science 294, 2179-81 (2001).
104. Lee, H. J. et al. Presenilin-dependent gamma-secretase-like intramembrane cleavage of ErbB4. J Biol Chem 277, 6318-23 (2002).
105. Cao, X. & Sudhof, T. C. A transcriptionally [correction of transcriptively] active complex of APP with Fe65 and histone acetyltransferase Tip60. Science 293, 115-20 (2001).
106. Kimberly, W. T., Zheng, J. B., Guenette, S. Y. & Selkoe, D. J. The intracellular domain of the beta-amyloid precursor protein is stabilized by Fe65 and translocates to the nucleus in a notch-like manner. J Biol Chem 276, 40288-92 (2001).
107. Cupers, P., Orlans, I., Craessaerts, K., Annaert, W. & De Strooper, B. The amyloid precursor protein (APP)-cytoplasmic fragment generated by gamma-secretase is rapidly degraded but distributes partially in a nuclear fraction of neurones in culture. J Neurochem 78, 1168-78 (2001).
108. Edbauer, D., Willem, M., Lammich, S., Steiner, H. & Haass, C. Insulin-degrading enzyme rapidly removes the beta-amyloid precursor protein intracellular domain (AICD). J Biol Chem 277, 13389-93 (2002).
109. Walter, J., Kaether, C., Steiner, H. & Haass, C. The cell biology of Alzheimer's disease: uncovering the secrets of secretases. Curr Opin Neurobiol 11, 585-90 (2001).
110. Sinha, S. et al. Purification and cloning of amyloid precursor protein beta-secretase from human brain. Nature 402, 537-40 (1999).
111. Hussain, I. et al. Identification of a novel aspartic protease (Asp 2) as beta-secretase. Mol Cell Neurosci 14, 419-27 (1999).
112. Citron, M. Beta-secretase as a target for the treatment of Alzheimer's disease. J Neurosci Res 70, 373-9 (2002).
113. Fischer, F., Molinari, M., Bodendorf, U. & Paganetti, P. The disulphide bonds in the catalytic domain of BACE are critical but not essential for amyloid precursor protein processing activity. J Neurochem 80, 1079-88 (2002).
114. Cai, H. et al. BACE1 is the major beta-secretase for generation of Abeta peptides by neurons. Nat Neurosci 4, 233-4 (2001).
115. Luo, Y. et al. Mice deficient in BACE1, the Alzheimer's beta-secretase, have normal phenotype and abolished beta-amyloid generation. Nat Neurosci 4, 231-2 (2001).
116. Roberds, S. L. et al. BACE knockout mice are healthy despite lacking the primary beta-secretase activity in brain: implications for Alzheimer's disease therapeutics. Hum Mol Genet 10, 1317-24 (2001).
117. Luo, Y. et al. BACE1 (beta-secretase) knockout mice do not acquire compensatory gene expression changes or develop neural lesions over time. Neurobiol Dis 14, 81-8 (2003).
118. Pastorino, L. et al. BACE (beta-secretase) modulates the processing of APLP2 in vivo. Mol Cell Neurosci 25, 642-9 (2004).
119. Harrison, S. M. et al. BACE1 (beta-secretase) transgenic and knockout mice: identification of neurochemical deficits and behavioral changes. Mol Cell Neurosci 24, 646-55 (2003).
120. Ohno, M. et al. BACE1 Deficiency Rescues Memory Deficits and Cholinergic Dysfunction in a Mouse Model of Alzheimer's Disease. Neuron 41, 27-33 (2004).
121. Bodendorf, U. et al. Expression of human beta-secretase in the mouse brain increases the steady-state level of beta-amyloid. J Neurochem 80, 799-806 (2002).
122. Mohajeri, M. H., Saini, K. D. & Nitsch, R. M. Transgenic BACE expression in mouse neurons accelerates amyloid plaque pathology. J Neural Transm 111, 413-25 (2004).
123. Chiocco, M. J. et al. Altered Amyloid-{beta} Metabolism and Deposition in Genomic-based {beta}-Secretase Transgenic Mice. J Biol Chem 279, 52535-52542 (2004).
124. Willem, M. et al. beta-Site amyloid precursor protein cleaving enzyme 1 increases amyloid deposition in brain parenchyma but reduces cerebrovascular amyloid angiopathy in aging BACE x APP[V717I] double-transgenic mice. Am J Pathol 165, 1621-31 (2004).
125. Lee, E. B. et al. BACE overexpression alters the subcellular processing of APP and inhibits A{beta} deposition in vivo. J Cell Biol 168, 291-302 (2005).
126. Bennett, B. D. et al. A furin-like convertase mediates propeptide cleavage of BACE, the Alzheimer's beta -secretase. J Biol Chem 275, 37712-7 (2000).
127. Capell, A. et al. Maturation and pro-peptide cleavage of beta-secretase. J Biol Chem 275, 30849-54 (2000).
128. Benjannet, S. et al. Post-translational processing of beta-secretase (beta-amyloid-converting enzyme) and its ectodomain shedding. The pro- and transmembrane/cytosolic domains affect its cellular activity and amyloid-beta production. J Biol Chem 276, 10879-87 (2001).
129. Pinnix, I. et al. Convertases other than furin cleave beta-secretase to its mature form. Faseb J 15, 1810-2 (2001).
130. Sidera, C., Liu, C. & Austen, B. M. Pro-domain removal in ASP-2 and the cleavage of the amyloid precursor are influenced by pH. BMC Biochem 3, 25 (2002).
131. Creemers, J. W. et al. Processing of beta-secretase by furin and other members of the proprotein convertase family. J Biol Chem 276, 4211-7 (2001).
132. Chou, K. C. & Howe, W. J. Prediction of the tertiary structure of the beta-secretase zymogen. Biochem Biophys Res Commun 292, 702-8 (2002).
133. Haniu, M. et al. Characterization of Alzheimer's beta -secretase protein BACE. A pepsin family member with unusual properties. J Biol Chem 275, 21099-106 (2000).
134. Huse, J. T., Pijak, D. S., Leslie, G. J., Lee, V. M. & Doms, R. W. Maturation and endosomal targeting of beta-site amyloid precursor protein-cleaving enzyme. The Alzheimer's disease beta-secretase. J Biol Chem 275, 33729-37 (2000).
135. Huse, J. T. & Doms, R. W. Neurotoxic traffic: uncovering the mechanics of amyloid production in Alzheimer's disease. Traffic 2, 75-81 (2001).
136. Yan, R., Han, P., Miao, H., Greengard, P. & Xu, H. The transmembrane domain of the Alzheimer's beta-secretase (BACE1) determines its late Golgi localization and access to beta -amyloid precursor protein (APP) substrate. J Biol Chem 276, 36788-96 (2001).
137. Gruninger-Leitch, F., Schlatter, D., Kung, E., Nelbock, P. & Dobeli, H. Substrate and inhibitor profile of BACE (beta-secretase) and comparison with other mammalian aspartic proteases. J Biol Chem 277, 4687-93 (2002).

138. Kuentzel, S. L., Ali, S. M., Altman, R. A., Greenberg, B. D. & Raub, T. J. The Alzheimer beta-amyloid protein precursor/protease nexin-II is cleaved by secretase in a trans-Golgi secretory compartment in human neuroglioma cells. Biochem J 295 (Pt 2), 367-78 (1993).
139. Huse, J. T. et al. Beta-secretase processing in the trans-Golgi network preferentially generates truncated amyloid species that accumulate in Alzheimer's disease brain. J Biol Chem 277, 16278-84 (2002).
140. Chyung, A. S., Greenberg, B. D., Cook, D. G., Doms, R. W. & Lee, V. M. Novel beta-secretase cleavage of beta-amyloid precursor protein in the endoplasmic reticulum/intermediate compartment of NT2N cells. J Cell Biol 138, 671-80 (1997).
141. Cook, D. G. et al. Alzheimer's A beta(1-42) is generated in the endoplasmic reticulum/intermediate compartment of NT2N cells. Nat Med 3, 1021-3 (1997).
142. Westmeyer, G. G. et al. Dimerization of BACE. J Biol Chem (2004).
143. Kinoshita, A. et al. Demonstration by FRET of BACE interaction with the amyloid precursor protein at the cell surface and in early endosomes. J Cell Sci 116, 3339-46 (2003).
144. Walter, J. et al. Phosphorylation regulates intracellular trafficking of beta-secretase. J Biol Chem 276, 14634-41 (2001).
145. Shiba, T. et al. Insights into the phosphoregulation of beta-secretase sorting signal by the VHS domain of GGA1. Traffic 5, 437-48 (2004).
146. Pastorino, L., Ikin, A. F., Nairn, A. C., Pursnani, A. & Buxbaum, J. D. The carboxyl-terminus of BACE contains a sorting signal that regulates BACE trafficking but not the formation of total A(beta). Mol Cell Neurosci 19, 175-85 (2002).
147. He, X. et al. Biochemical and structural characterization of the interaction of memapsin 2 (beta-secretase) cytosolic domain with the VHS domain of GGA proteins. Biochemistry 42, 12174-80 (2003).
148. He, X., Chang, W. P., Koelsch, G. & Tang, J. Memapsin 2 (beta-secretase) cytosolic domain binds to the VHS domains of GGA1 and GGA2: implications on the endocytosis mechanism of memapsin 2. FEBS Lett 524, 183-7 (2002).
149. Wahle, T. et al. GGA proteins regulate retrograde transport of BACE1 from endosomes to the trans-Golgi network. Mol Cell Neurosci 29, 453-61 (2005).
150. von Arnim, C. A. et al. Demonstration of BACE (beta-secretase) phosphorylation and its interaction with GGA1 in cells by fluorescence-lifetime imaging microscopy. J Cell Sci 117, 5437-45 (2004).
151. Capell, A. et al. Apical sorting of beta-secretase limits amyloid beta-peptide production. J Biol Chem 277, 5637-43 (2002).
152. Fiedler, K., Kobayashi, T., Kurzchalia, T. V. & Simons, K. Glycosphingolipid-enriched, detergent-insoluble complexes in protein sorting in epithelial cells. Biochemistry 32, 6365-73 (1993).
153. Brown, D. A. & London, E. Structure of detergent-resistant membrane domains: does phase separation occur in biological membranes? Biochem Biophys Res Commun 240, 1-7 (1997).
154. Dingwall, C. Spotlight on BACE: the secretases as targets for treatment in Alzheimer disease. J Clin Invest 108, 1243-6 (2001).
155. Riddell, D. R., Christie, G., Hussain, I. & Dingwall, C. Compartmentalization of beta-secretase (Asp2) into low-buoyant density, noncaveolar lipid rafts. Curr Biol 11, 1288-93 (2001).
156. Cordy, J. M., Hussain, I., Dingwall, C., Hooper, N. M. & Turner, A. J. Exclusively targeting beta-secretase to lipid rafts by GPI-anchor addition up-regulates beta-site processing of the amyloid precursor protein. Proc Natl Acad Sci U S A 100, 11735-40 (2003).
157. Mayor, S. & Riezman, H. Sorting GPI-anchored proteins. Nat Rev Mol Cell Biol 5, 110-20 (2004).
158. Lodish, B., Zipursky, Matsudeira, Baltimore, Darnell. Molecular Cell Biology 4th ed. (1999).
159. Ehehalt, R., Keller, P., Haass, C., Thiele, C. & Simons, K. Amyloidogenic processing of the Alzheimer beta-amyloid precursor protein depends on lipid rafts. J Cell Biol 160, 113-23 (2003).
160. Bigl, M. et al. Expression of beta-secretase mRNA in transgenic Tg2576 mouse brain with Alzheimer plaque pathology. Neurosci Lett 292, 107-10 (2000).
161. Lushchekina, E. A. et al. Expression of beta-Secretase mRNA in the brain of rats with immunohistochemical destruction of basal forebrain cholinergic system. Bull Exp Biol Med 134, 236-40 (2002).
162. Marcinkiewicz, M. & Seidah, N. G. Coordinated expression of beta-amyloid precursor protein and the putative beta-secretase BACE and alpha-secretase ADAM10 in mouse and human brain. J Neurochem 75, 2133-43 (2000).
163. Rossner, S., Apelt, J., Schliebs, R., Perez-Polo, J. R. & Bigl, V. Neuronal and glial beta-secretase (BACE) protein expression in transgenic Tg2576 mice with amyloid plaque pathology. J Neurosci Res 64, 437-46 (2001).
164. Fukumoto, H., Cheung, B. S., Hyman, B. T. & Irizarry, M. C. Beta-secretase protein and activity are increased in the neocortex in Alzheimer disease. Arch Neurol 59, 1381-9 (2002).
165. Holsinger, R. M., McLean, C. A., Beyreuther, K., Masters, C. L. & Evin, G. Increased expression of the amyloid precursor beta-secretase in Alzheimer's disease. Ann Neurol 51, 783-6 (2002).
166. Tyler, S. J., Dawbarn, D., Wilcock, G. K. & Allen, S. J. alpha- and beta-secretase: profound changes in Alzheimer's disease. Biochem Biophys Res Commun 299, 373-6 (2002).
167. Sennvik, K., Bogdanovic, N., Volkmann, I., Fastbom, J. & Benedikz, E. Beta-secretase-cleaved amyloid precursor protein in Alzheimer brain: a morphologic study. J Cell Mol Med 8, 127-34 (2004).
168. Yang, L. B. et al. Elevated beta-secretase expression and enzymatic activity detected in sporadic Alzheimer disease. Nat Med 9, 3-4 (2003).
169. Li, R. et al. Amyloid beta peptide load is correlated with increased beta-secretase activity in sporadic Alzheimer's disease patients. Proc Natl Acad Sci U S A 101, 3632-7 (2004).
170. Fukumoto, H. et al. Beta-secretase activity increases with aging in human, monkey, and mouse brain. Am J Pathol 164, 719-25 (2004).
171. Gatta, L. B., Albertini, A., Ravid, R. & Finazzi, D. Levels of beta-secretase BACE and alpha-secretase ADAM10 mRNAs in Alzheimer hippocampus. Neuroreport 13, 2031-3 (2002).
172. Preece, P. et al. Beta-secretase (BACE) and GSK-3 mRNA levels in Alzheimer's disease. Brain Res Mol Brain Res 116, 155-8 (2003).
173. Yasojima, K., McGeer, E. G. & McGeer, P. L. Relationship between beta amyloid peptide generating molecules and neprilysin in Alzheimer disease and normal brain. Brain Res 919, 115-21 (2001).
174. Gau, J. T. et al. Stable beta-secretase activity and presynaptic cholinergic markers during progressive central nervous system amyloidogenesis in Tg2576 mice. Am J Pathol 160, 731-8 (2002).
175. Lange-Dohna, C. et al. Cloning and expression of the rat BACE1 promoter. J Neurosci Res 73, 73-80 (2003).
176. Sambamurti, K., Kinsey, R., Maloney, B., Ge, Y. W. & Lahiri, D. K. Gene structure and organization of the human beta-secretase (BACE) promoter. Faseb J 18, 1034-6 (2004).
177. Christensen, M. A. et al. Transcriptional regulation of BACE1, the beta-amyloid precursor protein beta-secretase, by Sp1. Mol Cell Biol 24, 865-74 (2004).
178. Lammich, S., Schobel, S., Zimmer, A. K., Lichtenthaler, S. F. & Haass, C. Expression of the Alzheimer protease BACE1 is suppressed via its 5'-untranslated region. EMBO Rep 5, 620-5 (2004).
179. Hong, L. et al. Structure of the protease domain of memapsin 2 (beta-secretase) complexed with inhibitor. Science 290, 150-3 (2000).
180. Sauder, J. M., Arthur, J. W. & Dunbrack, R. L., Jr. Modeling of substrate specificity of the Alzheimer's disease amyloid precursor protein beta-secretase. J Mol Biol 300, 241-8 (2000).
181. Hong, L. et al. Crystal structure of memapsin 2 (beta-secretase) in complex with an inhibitor OM00-3. Biochemistry 41, 10963-7 (2002).
182. Patel, S., Vuillard, L., Cleasby, A., Murray, C. W. & Yon, J. Apo and inhibitor complex structures of BACE (beta-secretase). J Mol Biol 343, 407-16 (2004).
183. Wang, W. et al. Crystallization of glycosylated human BACE protease domain expressed in Trichoplusia ni. Biochim Biophys Acta 1698, 255-9 (2004).
184. Haass, C. et al. The Swedish mutation causes early-onset Alzheimer's disease by beta-secretase cleavage within the secretory pathway. Nat Med 1, 1291-6 (1995).
185. Lin, X. et al. Human aspartic protease memapsin 2 cleaves the beta-secretase site of beta-amyloid precursor protein. Proc Natl Acad Sci U S A 97, 1456-60 (2000).
186. Turner, R. T., 3rd et al. Subsite specificity of memapsin 2 (beta-secretase): implications for inhibitor design. Biochemistry 40, 10001-6 (2001).
187. Fluhrer, R. et al. Identification of a beta-secretase activity, which truncates amyloid beta-peptide after its presenilin-dependent generation. J Biol Chem 278, 5531-8 (2003).
188. Gouras, G. K. et al. Generation and regulation of beta-amyloid peptide variants by neurons. J Neurochem 71, 1920-5 (1998).
189. Lee, E. B., Skovronsky, D. M., Abtahian, F., Doms, R. W. & Lee, V. M. Secretion and intracellular generation of truncated Abeta in BACE expressing human neurons. J Biol Chem (2002).
190. Qahwash, I., He, W., Tomasselli, A., Kletzien, R. F. & Yan, R. Processing amyloid precursor protein at the beta-site requires proper orientation to be accessed by BACE1. J Biol Chem 279, 39010-6 (2004).
191. Liu, K., Doms, R. W. & Lee, V. M. Glu11 site cleavage and N-terminally truncated A beta production upon BACE overexpression. Biochemistry 41, 3128-36 (2002).
192. McGowan, E. et al. Amyloid phenotype characterization of transgenic mice overexpressing both mutant amyloid precursor protein and mutant presenilin 1 transgenes. Neurobiol Dis 6, 231-44 (1999).
193. Vandermeeren, M. et al. The functional gamma-secretase inhibitor prevents production of amyloid beta 1-34 in human and murine cell lines. Neurosci Lett 315, 145-8 (2001).
194. Fluhrer, R. et al. Identification of a beta-secretase activity, which truncates amyloid beta-peptide after its presenilin dependent generation. J Biol Chem (2002).
195. Shi, X. P. et al. Beta-secretase cleavage at amino acid residue 34 in the amyloid beta peptide is dependent upon gamma-secretase activity. J Biol Chem 278, 21286-94 (2003).
196. Schechter, I. & Berger, A. On the size of the active site in proteases. I. Papain. Biochem Biophys Res Commun 27, 157-62 (1967).
197. Tomasselli, A. G. et al. Employing a superior BACE1 cleavage sequence to probe cellular APP processing. J Neurochem 84, 1006-17 (2003).
198. Turner, R. T., 3rd, Hong, L., Koelsch, G., Ghosh, A. K. & Tang, J. Structural locations and functional roles of new subsites S5, S6, and S7 in memapsin 2 (beta-secretase). Biochemistry 44, 105-12 (2005).
199. Kitazume, S. et al. Alzheimer's beta-secretase, beta-site amyloid precursor protein-cleaving enzyme, is responsible for cleavage secretion of a Golgi-resident sialyltransferase. Proc Natl Acad Sci U S A 98, 13554-9 (2001).
200. Kitazume, S., Saido, T. C. & Hashimoto, Y. Alzheimer's beta-secretase cleaves a glycosyltransferase as a physiological substrate. Glycoconj J 20, 59-62 (2004).

201. Lichtenthaler, S. F. et al. The cell adhesion protein P-selectin glycoprotein ligand-1 is a substrate for the aspartyl protease BACE1. J Biol Chem 278, 48713-9 (2003).
202. Li, Q. & Sudhof, T. C. Cleavage of amyloid-beta precursor protein and amyloid-beta precursor-like protein by BACE 1. J Biol Chem 279, 10542-50 (2004).
203. Huse, J. T. et al. Endoproteolysis of beta-secretase (beta-site amyloid precursor protein-cleaving enzyme) within its catalytic domain. A potential mechanism for regulation. J Biol Chem 278, 17141-9 (2003).
204. Hattori, C. et al. BACE1 interacts with nicastrin. Biochem Biophys Res Commun 293, 1228-32 (2002).
205. Hebert, S. S. et al. Presenilin-1 interacts directly with the beta-site amyloid protein precursor cleaving enzyme (BACE1). Neurobiol Dis 13, 238-45 (2003).
206. Huang, X. P. et al. Internalization of exogenously added memapsin 2 (beta-secretase) ectodomain by cells is mediated by amyloid precursor protein. J Biol Chem 279, 37886-94 (2004).
207. Kametaka, S. et al. Identification of phospholipid scramblase 1 as a novel interacting molecule with beta -secretase (beta -site amyloid precursor protein (APP) cleaving enzyme (BACE)). J Biol Chem 278, 15239-45 (2003).
208. Wickham, L., Benjannet, S., Marcinkiewicz, E., Chretien, M. & Seidah, N. G. beta-amyloid protein converting enzyme 1 and brain-specific type II membrane protein BRI: binding partners processed by furin. J Neurochem 92, 93-102 (2005).
209. Ermolieff, J., Loy, J. A., Koelsch, G. & Tang, J. Proteolytic activation of recombinant pro-memapsin 2 (Pro-beta-secretase) studied with new fluorogenic substrates. Biochemistry 39, 16263 (2000).
210. Kopcho, L. M. et al. Comparative studies of active site-ligand interactions among various recombinant constructs of human beta-amyloid precursor protein cleaving enzyme. Arch Biochem Biophys 410, 307-16 (2003).
211. Mallender, W. D. et al. Characterization of recombinant, soluble beta-secretase from an insect cell expression system. Mol Pharmacol 59, 619-26 (2001).
212. Shi, X. P. et al. The pro domain of beta-secretase does not confer strict zymogen-like properties but does assist proper folding of the protease domain. J Biol Chem 276, 10366-73 (2001).
213. Toulokhonova, L., Metzler, W. J., Witmer, M. R., Copeland, R. A. & Marcinkeviciene, J. Kinetic studies on beta-site amyloid precursor protein-cleaving enzyme (BACE): Confirmation of an Iso-mechanism. J Biol Chem (2002).
214. Edbauer, D., Winkler, E., Haass, C. & Steiner, H. Presenilin and nicastrin regulate each other and determine amyloid beta-peptide production via complex formation. Proc Natl Acad Sci U S A 99, 8666-71 (2002).
215. Townsley, F. M. & Pelham, H. R. The KKXX signal mediates retrieval of membrane proteins from the Golgi to the ER in yeast. Eur J Cell Biol 64, 211-6 (1994).
216. MANIATIS, S. Molecular Cloning, A Laboratory Handbook. Cold Spring Harbor Laboratory Press, second edition (1989).
217. Kruse, P. P., MK. Tissue culture: methods and applications. (1973).
218. Andra, K. et al. Expression of APP in transgenic mice: a comparison of neuron-specific promoters. Neurobiol Aging 17, 183-90 (1996).
219. Maniatis, G. M. Erythropoiesis: a model for differentiation. Prog Clin Biol Res 102 pt A, 13-24 (1982).
220. Schagger, H. & von Jagow, G. Blue native electrophoresis for isolation of membrane protein complexes in enzymatically active form. Anal Biochem 199, 223-31 (1991).
221. Schagger, H. Native electrophoresis for isolation of mitochondrial oxidative phosphorylation protein complexes. Methods Enzymol 260, 190-202 (1995).
222. Schagger, H. et al. Electrophoretic separation of multiprotein complexes from blood platelets and cell lines: technique for the analysis of diseases with defects in oxidative phosphorylation. Electrophoresis 17, 709-14 (1996).
223. Schagger, H. Blue-native gels to isolate protein complexes from mitochondria. Methods Cell Biol 65, 231-44 (2001).
224. Milgram, S. L. & Mains, R. E. Differential effects of temperature blockade on the proteolytic processing of three secretory granule-associated proteins. J Cell Sci 107 (Pt 3), 737-45 (1994).
225. Nasciutti, L. E., Picart, R., Rosenbaum, E., Tixier-Vidal, A. & Tougard, C. Effect of reduced temperatures and brefeldin A on prolactin secretion and on subcellular distribution of the secretory product and membrane antigens in GH3 pituitary cells. Biol Cell 75, 25-35 (1992).
226. Sanderson, C. M., McQueen, N. L. & Nayak, D. P. Sendai virus assembly: M protein binds to viral glycoproteins in transit through the secretory pathway. J Virol 67, 651-63 (1993).
227. Knight, C. G. Active-site titration of peptidases. Methods Enzymol 248, 85-101 (1995).
228. Holsinger, R. M., McLean, C. A., Collins, S. J., Masters, C. L. & Evin, G. Increased beta-Secretase activity in cerebrospinal fluid of Alzheimer's disease subjects. Ann Neurol 55, 898-9 (2004).
229. Hussain, I. et al. Characterization of the ectodomain shedding of the beta-site amyloid precursor protein-cleaving enzyme 1 (BACE1). J Biol Chem 278, 36264-8 (2003).
230. Misumi, Y. et al. Novel blockade by brefeldin A of intracellular transport of secretory proteins in cultured rat hepatocytes. J Biol Chem 261, 11398-403 (1986).
231. Itin, C., Schindler, R. & Hauri, H. P. Targeting of protein ERGIC-53 to the ER/ERGIC/cis-Golgi recycling pathway. J Cell Biol 131, 57-67 (1995).
232. Molinari, M., Galli, C., Piccaluga, V., Pieren, M. & Paganetti, P. Sequential assistance of molecular chaperones and transient formation of covalent complexes during protein degradation from the ER. J Cell Biol 158, 247-57 (2002).
233. Molinari, M., Calanca, V., Galli, C., Lucca, P. & Paganetti, P. Role of EDEM in the release of misfolded glycoproteins from the calnexin cycle. Science 299, 1397-400 (2003).
234. Marlow, L., Cain, M., Pappolla, M. A. & Sambamurti, K. Beta-secretase processing of the Alzheimer's amyloid protein precursor (APP). J Mol Neurosci 20, 233-9 (2003).
235. Schmechel, A. et al. Human BACE forms dimers and colocalizes with APP. J Biol Chem 279, 39710-7 (2004).
236. Phizicky, E. M. & Fields, S. Protein-protein interactions: methods for detection and analysis. Microbiol Rev 59, 94-123 (1995).
237. Heuberger, E. H., Veenhoff, L. M., Duurkens, R. H., Friesen, R. H. & Poolman, B. Oligomeric state of membrane transport proteins analyzed with blue native electrophoresis and analytical ultracentrifugation. J Mol Biol 317, 591-600 (2002).
238. Sagne, C., Isambert, M. F., Henry, J. P. & Gasnier, B. SDS-resistant aggregation of membrane proteins: application to the purification of the vesicular monoamine transporter. Biochem J 316 (Pt 3), 825-31 (1996).
239. Nijtmans, L. G., Henderson, N. S. & Holt, I. J. Blue Native electrophoresis to study mitochondrial and other protein complexes. Methods 26, 327-34 (2002).
240. Reif, S., Voos, W. & Rassow, J. Intramitochondrial dimerization of citrate synthase characterized by blue native electrophoresis. Anal Biochem 288, 97-9 (2001).
241. Jung, C., Higgins, C. M. & Xu, Z. Measuring the quantity and activity of mitochondrial electron transport chain complexes in tissues of central nervous system using blue native polyacrylamide gel electrophoresis. Anal Biochem 286, 214-23 (2000).
242. Rodriguez, P., Ruiz, M. T., Price, G. B. & Zannis-Hadjopoulos, M. NAP-2 is part of multi-protein complexes in HeLa cells. J Cell Biochem 93, 398-408 (2004).
243. Camacho-Carvajal, M. M., Wollscheid, B., Aebersold, R., Steimle, V. & Schamel, W. W. Two-dimensional Blue native/SDS gel electrophoresis of multi-protein complexes from whole cellular lysates: a proteomics approach. Mol Cell Proteomics 3, 176-82 (2004).
244. Claeys, D., Geering, K. & Meyer, B. J. Two-dimensional Blue Native/sodium dodecyl sulfate gel electrophoresis for analysis of multimeric proteins in platelets. Electrophoresis (2005).
245. Molnar, A. M., Alves, A. A., Pereira-da-Silva, L., Macedo, D. V. & Dabbeni-Sala, F. Evaluation by blue native polyacrylamide electrophoresis colorimetric staining of the effects of physical exercise on the activities of mitochondrial complexes in rat muscle. Braz J Med Biol Res 37, 939-47 (2004).
246. Chery, C. C., De Cremer, K., Dumont, E., Cornelis, R. & Moens, L. Vanadium speciation in serum by means of blue native gel electrophoresis. Electrophoresis 23, 3284-8 (2002).
247. Devreese, B., Vanrobaeys, F., Smet, J., Van Beeumen, J. & Van Coster, R. Mass spectrometric identification of mitochondrial oxidative phosphorylation subunits separated by two-dimensional blue-native polyacrylamide gel electrophoresis. Electrophoresis 23, 2525-33 (2002).
248. Brookes, P. S. et al. High throughput two-dimensional blue-native electrophoresis: a tool for functional proteomics of mitochondria and signaling complexes. Proteomics 2, 969-77 (2002).
249. Culvenor, J. G. et al. Characterization of presenilin complexes from mouse and human brain using Blue Native gel electrophoresis reveals high expression in embryonic brain and minimal change in complex mobility with pathogenic presenilin mutations. Eur J Biochem 271, 375-85 (2004).
250. Schagger, H., Cramer, W. A. & von Jagow, G. Analysis of molecular masses and oligomeric states of protein complexes by blue native electrophoresis and isolation of membrane protein complexes by two-dimensional native electrophoresis. Anal Biochem 217, 220-30 (1994).
251. Balasubramanian, K. & Schroit, A. J. Aminophospholipid asymmetry: A matter of life and death. Annu Rev Physiol 65, 701-34 (2003).
252. Boman, A. L., Zhang, C., Zhu, X. & Kahn, R. A. A family of ADP-ribosylation factor effectors that can alter membrane transport through the trans-Golgi. Mol Biol Cell 11, 1241-55 (2000).
253. Vetrivel, K. S. et al. Association of gamma-secretase with lipid rafts in post-Golgi and endosome membranes. J Biol Chem 279, 44945-54 (2004).
254. Chamberlain, L. H. Detergents as tools for the purification and classification of lipid rafts. FEBS Lett 559, 1-5 (2004).
255. Kim, K. B., Kim, S. I., Choo, H. J., Kim, J. H. & Ko, Y. G. Two-dimensional electrophoretic analysis reveals that lipid rafts are intact at physiological temperature. Proteomics 4, 3527-35 (2004).
256. Brown, D. A. & Rose, J. K. Sorting of GPI-anchored proteins to glycolipid-enriched membrane subdomains during transport to the apical cell surface. 68, 533 (1992).
257. Meri, S., Lehto, T., Sutton, C. W., Tyynela, J. & Baumann, M. Structural composition and functional characterization of soluble CD59: heterogeneity of the oligosaccharide and glycophosphoinositol (GPI) anchor revealed by laser-desorption mass spectrometric analysis. Biochem J 316 (Pt 3), 923-35 (1996).
258. Jones, S. & Thornton, J. M. Protein-protein interactions: a review of protein dimer structures. Prog Biophys Mol Biol 63, 31-65 (1995).
259. Angers, S., Salahpour, A. & Bouvier, M. Dimerization: an emerging concept for G protein-coupled receptor ontogeny and function. Annu Rev Pharmacol Toxicol 42, 409-35 (2002).
260. Pardee, A. B. & Reddy, G. P. Beginnings of feedback inhibition, allostery, and multi-protein complexes. Gene 321, 17-23 (2003).
261. Dunn, B. M. Structure and mechanism of the pepsin-like family of aspartic peptidases. Chem Rev 102, 4431-58 (2002).
262. Fowler, S. D., Kay, J., Dunn, B. M. & Tatnell, P. J. Monomeric human cathepsin E. FEBS Lett 366, 72-4 (1995).
263. Tsukuba, T. et al. Biochemical properties of the monomeric mutant of human cathepsin E expressed in Chinese hamster ovary cells: comparison with dimeric forms of the natural and recombinant cathepsin E. J Biochem (Tokyo) 119, 126-34 (1996).
264. Cheng, P. C. et al. Floating the raft hypothesis: the roles of lipid rafts in B cell antigen receptor function. Semin Immunol 13, 107-14 (2001).

265. Harder, T. Lipid raft domains and protein networks in T-cell receptor signal transduction. Curr Opin Immunol 16, 353-9 (2004).
266. Scheuermann, S. et al. Homodimerization of amyloid precursor protein and its implication in the amyloidogenic pathway of Alzheimer's disease. J Biol Chem 276, 33923-9 (2001).
267. Schmechel, A. et al. Alzheimer beta-amyloid homodimers facilitate A beta fibrillization and the generation of conformational antibodies. J Biol Chem 278, 35317-24 (2003).
268. Bowman, M. J. & Chmielewski, J. Novel strategies for targeting the dimerization interface of HIV protease with cross-linked interfacial peptides. Biopolymers 66, 126-33 (2002).
269. Luthi, U. et al. Human beta-secretase activity in yeast detected by a novel cellular growth selection system. Biochim Biophys Acta 1620, 167-78 (2003).
270. Sluis-Cremer, N. & Tachedjian, G. Modulation of the oligomeric structures of HIV-1 retroviral enzymes by synthetic peptides and small molecules. Eur J Biochem 269, 5103-11 (2002).
271. Rodriguez-Barrios, F. & Gago, F. HIV protease inhibition: limited recent progress and advances in understanding current pitfalls. Curr Top Med Chem 4, 991-1007 (2004).
272. Liuzzi, M. et al. A potent peptidomimetic inhibitor of HSV ribonucleotide reductase with antiviral activity in vivo. Nature 372, 695-8 (1994).
273. Digard, P. et al. Specific inhibition of herpes simplex virus DNA polymerase by helical peptides corresponding to the subunit interface. Proc Natl Acad Sci U S A 92, 1456-60 (1995).
274. Singh, S. K., Maithal, K., Balaram, H. & Balaram, P. Synthetic peptides as inactivators of multimeric enzymes: inhibition of Plasmodium falciparum triosephosphate isomerase by interface peptides. FEBS Lett 501, 19-23 (2001).
275. Sali, A., Glaeser, R., Earnest, T. & Baumeister, W. From words to literature in structural proteomics. Nature 422, 216-25 (2003).
276. Valencia, A. & Pazos, F. Computational methods for the prediction of protein interactions. Curr Opin Struct Biol 12, 368-73 (2002).
277. Smith, G. R. & Sternberg, M. J. Prediction of protein-protein interactions by docking methods. Curr Opin Struct Biol 12, 28-35 (2002).
278. Liu, S., Zhang, C., Zhou, H. & Zhou, Y. A physical reference state unifies the structure-derived potential of mean force for protein folding and binding. Proteins 56, 93-101 (2004).
279. Hong, L. & Tang, J. Flap position of free memapsin 2 (beta-secretase), a model for flap opening in aspartic protease catalysis. Biochemistry 43, 4689-95 (2004).
280. Ghosh, A. K. et al. Structure-based design of cycloamide-urethane-derived novel inhibitors of human brain memapsin 2 (beta-secretase). Bioorg Med Chem Lett 15, 15-20 (2005).
281. Comeau, S. R., Gatchell, D. W., Vajda, S. & Camacho, C. J. ClusPro: a fully automated algorithm for protein-protein docking. Nucleic Acids Res 32, W96-9 (2004).
282. Comeau, S. R., Gatchell, D. W., Vajda, S. & Camacho, C. J. ClusPro: an automated docking and discrimination method for the prediction of protein complexes. Bioinformatics 20, 45-50 (2004).
283. Kukull, W. A. et al. Dementia and Alzheimer disease incidence: a prospective cohort study. Arch Neurol 59, 1737-46 (2002).

# 13 Lebenslauf

## ANGABEN ZUR PERSON


| | |
|---|---|
| Name: | Westmeyer, Gil Gregor |
| Geburtstag: | 3.12.1976 |
| Geburtsort: | Essen |
| Anschrift: | Herzog-Heinrich-Str.35<br>80336 München |
| e-mail: | gil.westmeyer@web.de |
| Familienstand: | ledig |


## SCHULBILDUNG

| | |
|---|---|
| 09/87 - 06/96 | **Helmholtz-Gymnasium** in Essen |
| | **Marlborough College**, England (09/93 – 03/94) |
| 13.6. 1996 | **Abitur** Helmholtz-Gymnasium |

## ZIVILDIENST

| | |
|---|---|
| 08/96 – 02/97 | Familien– und Krankenpflege e.V., Essen |
| 02/97 – 08/97 | Krankenhaus Hyussenstiftung, Essen |

## UNIVERSITÄRE AUSBILDUNG

| | |
|---|---|
| 04/98 - 03/05 | **Medizinstudium** an der LMU München<br>- spezielles Interesse: Neurowissenschaften |
| 04/98 – 07/00 | **Studium der Philosophie** - Hochschule für Philosophie<br>- Schwerpunkt: Philosophie des Geistes, Künstliche Intelligenz und Bioethik |
| 20.7. 2000 | **Bakkalaureat in Philosophie** |
| 2.12.2004 | **Ärztliche Prüfung** |

## PRAKTISCHE AUSBILDUNG

| | |
|---|---|
| 09/98 – 11/98 | Institut für medizinische **Psychologie** (Prof. E. Pöppel)<br>- neuropsychologische Grundlagenforschung: zeitliche Aspekte der Motorik |
| 09/00 | **Max-Planck-Institut für Neurobiologie** (Prof. S. Stamm)<br>**Max-Planck-Institut für Biochemie** („Martinsrieder Praktikum“)<br>- biochemische und biophysikalische Arbeitsmethoden: alt. neuronales Splicen |
| 10/03-02/04 | Praktische Ausbildung in der **Neurologie des Klinkums-Grosshadern (LMU)** – Prof. Brandt |
| 02/04-03/04 | Praktische Ausbildung in der **Neurochirugie des Klinkums Grosshadern (LMU)** – Prof. Thonn |
| 03/04 | Clinical Core Clerkship in Internal Medicine<br>**Harvard Medical School, Brigham and Women`s Hospital** |
| 07/04 | Subinternship in Internal Medicine (4th year of Med-School)<br>**Harvard Medical School, Mount Auburn Hospital** |
| 08/04 | Forschungspraktikum in Kognitiver Neurowissenschaft<br>**Martinos Center of Biomedical Imaging – MGH – Harvard Medical School**<br>fMRI- psycholinguistics in schizophrenia |
| 05/05 - | Department of Brain and Cognitive Sciences – Jasanoff Lab<br>**Massachusetts Institute of Technology** |

## SPRACHEN

| | |
|---|---|
| Englisch | verhandlungssicher |
| Französisch | gute Kenntnisse |
| Portugiesisch | erweiterte Grundkenntnisse |

## STIPENDIEN

Studienstiftung des Deutschen Volkes

Munich-Harvard Alliance for Medical Education

The Raymond and Beverly Sackler Foundation

Stiftung Familie Klee

## WISSENSCHAFTLICHE VERÖFFENTLICHUNGEN

Mikhail G. Shapiro, Tatjana Atanasijevic, Henryk Faas, Gil G. Westmeyer, & Alan Jasanoff
**Dynamic imaging with MRI contrast agents: quantitative considerations**
*J. Mag. Res. Imag.* in press

Gil G. Westmeyer, Michael Willem, Stefan F. Lichtenthaler, Glenn Lurman, Gerd Multhaup, Irmgard Assfalg-Machleidt, Karina Reiss, Paul Saftig, and Christian Haass
**Dimerization of β-Site β-Amyloid Precursor Protein-cleaving Enzyme**
*J. Biol. Chem.*, Dec 2004; 279: 53205 - 53212 ; 10.1074/jbc.M410378200.

Stefan F. Lichtenthaler, Diana-ines Dominguez, Gil G. Westmeyer, Karina Reiss, Christian Haass, Paul Saftig, Bart De Strooper, and Brian Seed
**The Cell Adhesion Protein P-selectin Glycoprotein Ligand-1 Is a Substrate for the Aspartyl Protease BACE1**
J. Biol. Chem., Dec 2003; 278: 48713 - 48719 ; 10.1074/jbc.M303861200.

Regina Fluhrer, Gerd Multhaup, Andrea Schlicksupp, Masayasu Okochi, Masatoshi Takeda, Sven Lammich, Michael Willem, Gil Westmeyer, Wolfram Bode, Jochen Walter, and Christian Haass
**Identification of a β-Secretase Activity, Which Truncates Amyloid β-Peptide after Its Presenilin-dependent Generation**
*J. Biol. Chem.*, Feb 2003; 278: 5531 - 5538 ; 10.1074/jbc.M211485200.

Fluhrer, R.; Capell, A.; Westmeyer, G.; Willem, M.; Hartung, B.; Condron, M. M.; Teplow, D. B.; Haass, C.; Walter, J. (2002)
**A non-amyloidogenic function of BACE-2 in the secretory pathway.**
*J Neurochem. ,* Jun 2002*,* 81: 1011-20

## Erklärung

Hiermit erkläre ich, dass ich diese Dissertation selbständig und nur mit den angegebenen Hilfsmitteln angefertigt habe.

Cambridge, den 12.9.2006

Gil Gregor Westmeyer